

**Selected sections from**  
***Luminescence Analysis in Analytical Chemistry*, J. D. Winefordner, T. C. O'Haver, and S. Schulman, Wiley-Interscience, New York, 1972.**

**Chapter 3: Instrumentation and Methodology**

**A. General Luminescence Instrumentation**

- o 1. Instrumental layout and requirements. Pages 140 141
- o 2. Sources of Excitation. Pages 142 143
  - + a. Incandescent sources. Pages 143 144 145
  - + b. Arc lamps. Pages 145 148 149 150
  - + c. Flash lamps Pages 150 151 152 153
- o 3. Monochromators. Pages 153
  - + a. Dispersion. Page 154
  - + b. Spectral Bandpass. Page 155
  - + c. Resolution. Page 155
  - + d. Theoretical Resolution and Resolving Power. Pages 155 156 157
  - + e. Slit illumination and entrance optics. Pages 157 158
  - + f. Light losses. Page 159
  - + h. Radiant flux emerging from spectrometric system. Pages 159 160 161
  - + i. Stray radiation. Pages 161 162
  - + j. Prism monochromators. Pages 162 163 164
  - + k. Grating monochromators. Pages 164 165 166 167
  - + l. Filters. Page 167
- o 4. Photodetectors. Page 167
  - + a. General aspects of photoemissive detectors. Pages 168 169 170 171 172 173
  - + b. Characteristics of single-stage phototubes. Page 173
  - + b. Characteristics of multiplier phototubes (photomultipliers). Pages 173 174 175 176 177 178
- o 5. Amplifier-readout systems. Pages 178
  - + a. General aspects of photoemissive detectors. Pages 179 182
  - + d. Photon-counting systems. Pages 182 183
  - + f. Stroboscopic systems. Pages 183 184
  - + f. Readout systems. Pages 184 185
- o 6. Glossary of symbols. Pages 185 186 187

**C. Molecular Luminescence Instrumentation**

- o 1. Sampling devices. Pages 200 201 202
- o 2. Sample cooling methods. Pages 202 203
- o 3. Modulation methods. Pages 203 204 205 206
- o 4. Commercial instruments. Pages 206 207 208
- o 5. Glossary of symbols. Pages 208

**D. Signal-to-noise ratio theory**

- o 1. General aspects.
  - + a. Noise. Pages 209 210
  - + b. Electrical bandwidth. Pages 210 211
  - + c. Effect of electrical bandwidth on noise. Pages 211 212
  - + d. Significance of response time. Pages 212 213
  - + e. Noise sources in spectrometric instrumentation. Pages 213 214
  - + f. Addition of noise sources. Pages 214 215
  - + g. Signal-to-noise ratio and the optimization of experimental conditions. Page 215
  - + h. Effect of random noise on analytical precision and detection limits. Pages 215 216 217

**Appendix 3. General expressions for the measured luminescence signal for a spectrometric system.**

- o A. The optical system under consideration. Pages 324 325 326
- o B. Radiant flux emerging from exit slit of spectrometer set at a fixed wavelength. Pages 326 327
- o C. Total radiant energy emerging from exit slit of spectrometer when wavelength scanning the spectral line or band. Pages 327 328 329

**Appendix 4. Principles and operation of non-photoemissive detectors.**

- o A. Photovoltaic or barrier-layer cells. Pages 330 331
- o B. Photoconductive cells. Pages 331 332 333
- o C. Thermal detectors. Pages 333 334
- o D. Chemical detectors. Pages 334 335
- o E. Quantum counters. Pages 335 336
- o F. Photodiodes and photodetectors. Pages 336

**Appendix 5. Signal processing instruments.**

- o A. Single-section low-pass filter. Page 337
- o B. DC integrator. Page 337
- o C. Higher-order filters. Page 337
- o D. DC systems. Page 338
- o E. Boxcar integrator. Pages 338 339
- o F. Multichannel signal averager. Page 339
- o G. Summary. Page 339

**Appendix 6. Principles of single-photon counting. Pages 340 341**

**Appendix 7. Special spectral techniques.**

- o A. Fourier transform spectroscopy. Pages 342 343 344
- o B. Hadamard spectroscopy. Page 344
- o C. Other systems. Page 345

## INSTRUMENTATION AND METHODOLOGY

### A. GENERAL LUMINESCENCE INSTRUMENTATION

#### 1. INSTRUMENTAL LAYOUT AND REQUIREMENTS<sup>1,2</sup>

The basic instrumental components of atomic and molecular luminescence instrumentation are not unlike those used in other ultraviolet and visible methods, but the arrangement of these components is unique. Figure III-A-1 illustrates the general instrumental layout for all types of photoluminescence studies. The chemical system to be investigated (i.e., the sample) is contained in a sample cell. This may be an actual glass or quartz container, as in

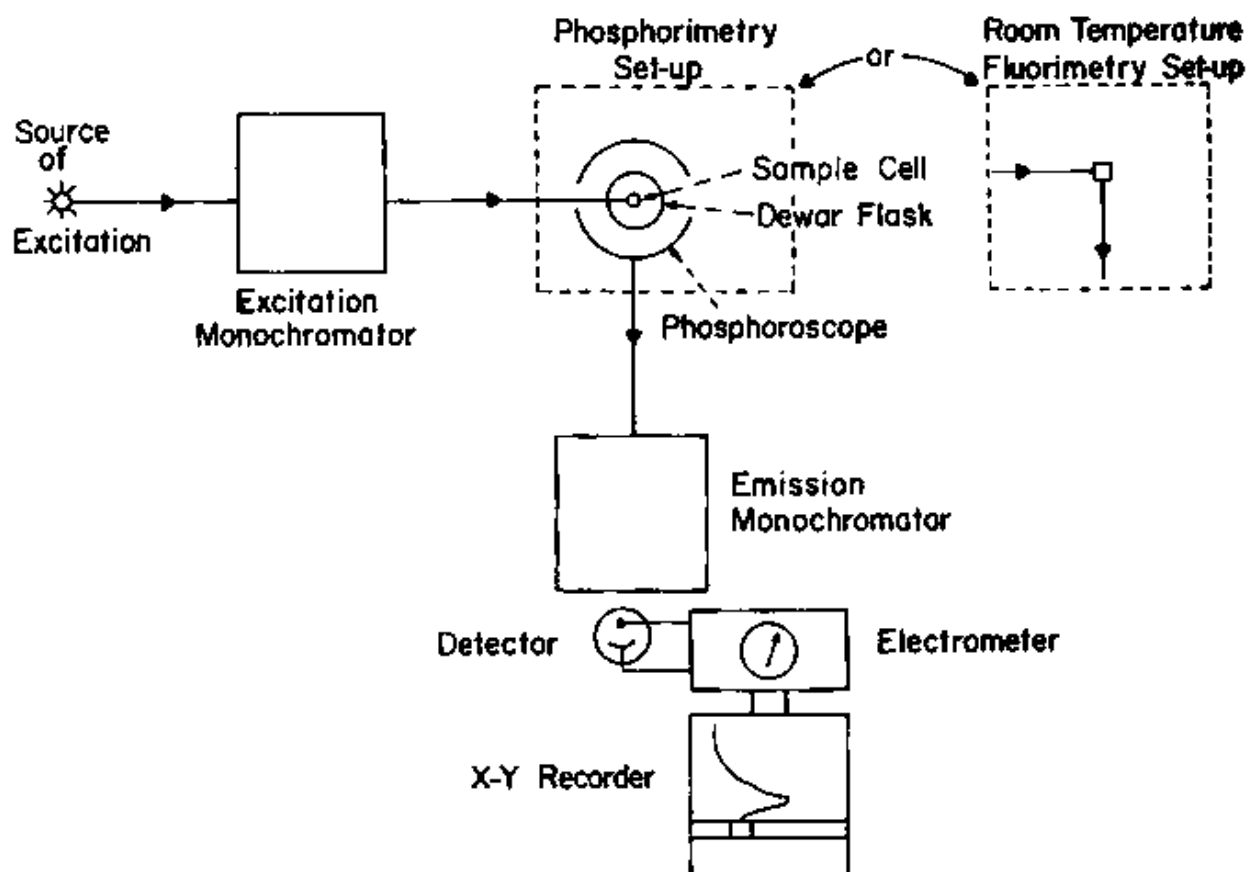


**Fig. III-A-1.** General instrumental layout for photoluminescence spectrometry. Note variation in sample compartment for phosphorimetry and room temperature luminescence spectrometry.

molecular luminescence spectrometry, or a flame cell, as in atomic fluorescence flame spectrometry. The sample is excited by ultraviolet or visible light from the source excitation, which is usually an arc or discharge lamp. The desired excitation wavelength region may be selected by means of the excitation monochromator if desired (this is seldom necessary or even desirable in atomic fluorescence experiments). The luminescence radiation is emitted by the sample in all directions; a portion of it is sampled by the detection system at some angle, traditionally  $90^\circ$ , from the axis of excitation. The detection system consists of the emission monochromator, which selects the wavelength region of luminescence emission to be measured; the photodetector, which converts the luminescence radiant flux to an electrical signal; and the amplifier-readout system, which amplifies and processes the electrical signal as required and displays it in a convenient fashion. Often one or more light choppers may be placed in the light path in order to separate the desired luminescence radiation from undesirable light emission from the sample. Simpler instruments use optical filters in place of monochromators and are called *filter fluorometers*. The more versatile system of Figure III-A-1 would be called a *spectrofluorometer* or *spectrophotofluorometer*, the prefix "spectro-" indicating that at least one monochromator is used. Such an instrument adapted for the measurement of phosphorescence would be called a *spectrophosphorimeter*. A more general term for all luminescence spectrometers might be *spectroluminometer*. The additional term "photo-" occasionally inserted into names of such instrumentation usually implies photoelectric detection of light intensity (rather than visual or photographic, now seldom used in luminescence studies). The spectroluminometer has the advantage over a filter instrument of being able to measure the spectral distribution of luminescence emission (the *emission spectrum*) and the variation in emission spectral radiance with excitation wavelength (the *excitation spectrum*).

The instrumental system is required to have reasonably *high spectral resolution*, *sensitivity*, and *signal-to-noise ratio* over the desired wavelength regions of excitation and emission. In addition, a certain degree of *convenience* and *speed* in obtaining data is desirable.

*Spectral resolution* is a measure of the ability of the instrument to isolate small wavelength regions of the excitation or emission radiation and to separate closely spaced lines or bands in the excitation or emission spectra. It is primarily a function of the design and adjustment of the monochromator(s). *Sensitivity* is a measure of the magnitude of the electrical output of the instrument which results from a given concentration of analyte in the sample, under a given set of experimental conditions. It is a function of almost every experimental variable in the instrumental system (e.g., the spectral radiance of the source emission; the design and adjustment of the monochromator(s); the nature and condition of the sample—i.e., temperature, matrix components

(interferents); concentration and chemical form of analyte; photodetector sensitivity; and amplification (gain) of the readout system). More specifically, the *linear analytical sensitivity* of the entire system is defined as the slope of the analytical curve,\* which is the plot of instrument response (e.g., electrical output, recorder deflection) versus analyte concentration. It is desirable that the analytical curve be linear (i.e., that the analytical sensitivity be independent of analyte concentration), but this is not always the case — especially at high analyte concentrations.

The *signal-to-noise ratio* is the ratio of the instrumental response (the signal) resulting from the presence of analyte in the sample to undesirable variations in that signal (noise). The noise may be in the form of a random fluctuation or an unpredictable drift in instrument response, and it is a function of many instrumental variables. Most of the noise in luminescence spectrometry is contributed by the source, the sample and sample cell, the photodetector, and (occasionally) the amplifier-readout system. The signal-to-noise ratio is important because it influences the precision with which the instrumental response may be measured and determines the minimum concentration of a particular analyte that may be detected under a given set of conditions (the *detection limit*).†

Additional factors influencing the design of luminescence instrumentation include the *convenience* and *speed* with which the instrument may be used to determine analytical curves, excitation and emission spectra, luminescence decay times, and the effect of sample temperature, polarization of excitation or emission radiation and other variables on luminescence radiances, spectra, and decay times.

## 2. SOURCES OF EXCITATION<sup>9</sup>

Sources of radiant energy may be classified according to the spectral distribution of the radiation emitted. *Continuum sources* are characterized by a broad spectral distribution covering a relatively large range of wavelengths (generally without sharp lines or bands). An ordinary tungsten filament light bulb is an example; it emits a continuum in the visible and infrared spectra. *Line sources* are characterized by spectra consisting of a number of relatively sharp lines or bands. An example is a low pressure mercury vapor lamp. The distinction between line and continuum sources is not always clear, however. In fact, one of the most common excitation sources used in luminescence spectrometry emits a characteristic line spectrum superimposed on a broad background continuum. The high pressure xenon and mercury arc lamps are of this type.

\* Also called working curve and calibration curve.

† Also called limit of detection and minimum detectable concentration.

There are essentially two systems of units commonly used to express the intensity of light sources—the *radiometric* system, an absolute system based on the actual energy radiated by a source; and the *photometric* system, a relative system based on the apparent intensity of a source as viewed by the “average” human eye. The radiometric system is the more useful quantitatively and is used in this book.

The basic quantity is the *radiant flux*, which is the total energy radiated per unit time. Radiant flux is most commonly expressed in watts. In dealing with practical light sources, modification of these units is customary. In order to account for the finite radiating areas of real sources, intensities are expressed in watts square centimeter of radiating surface. Furthermore, a light source may not radiate equally in all directions because of the geometry of the device; or reflectors may be used to concentrate the light in a particular direction. Consequently, the intensity in a given direction may be more important for practical applications than the total light output, and intensities are often expressed as the power radiated into a unit solid angle, that solid angle being oriented in a specified direction. A unit solid angle, called a *steradian* (sr), is the solid angle subtended at the center of a sphere by the area on the surface equal to the square of the radius of the sphere. Because the area of a sphere of radius  $r$  is  $4\pi r^2$ , there are  $4\pi$  steradians per sphere.

Source intensity expressed in watts per square centimeter per steradian is termed the *radiance* of the source. The intensity of a line in the spectrum of a line source is often expressed this way. Because the line is actually of finite spectral width, the intensity given in this way has been effectively integrated over all wavelengths in the line profile. For continuum sources, on the other hand, the total integrated intensity is usually less important than the intensity per unit wavelength interval at a particular wavelength. Consequently, intensities of continuum sources are most often expressed in watts per square centimeter per steradian per nanometer, which is called the *spectral radiance*.

#### a. INCANDESCENT SOURCES<sup>3</sup>

Probably the simplest type of light source, and the only one giving a smooth continuum spectrum without lines, is an *incandescent source*, such as a tungsten filament lamp. Although commonly used in visible and infrared absorption spectrophotometers, incandescent sources are not sufficiently intense, particularly in the ultraviolet region, to be useful in luminescence spectrometry. Nevertheless, the principles of black body emission are important.

An incandescent source emits radiation by virtue of its temperature, rather than by specific transitions between quantized energy levels characteristic of the particular incandescent substance. The radiation emitted is broad continuum whose spectral distribution is a function of the temperature of the

emitter. The specific material of which the source is made may affect the overall intensity of the radiation, but has little effect on its spectral distribution. The spectral radiance as a function of wavelength is given by the *Planck black body distribution equation*:

$$B_{B\lambda} = \frac{5.8967\lambda^{-5} \epsilon_{\lambda}}{\exp(14388/\lambda T) - 1} \quad (\text{III-A-1})$$

where  $B_{B\lambda}$  = spectral radiance, watt  $\text{cm}^{-2}$   $\text{sr}^{-1}$   $\text{nm}^{-1}$

$\lambda$  = wavelength, nm

$T$  = temperature, °K

$\epsilon_{\lambda}$  = spectral emissivity, typically 0.4 for tungsten at 3000°K, no units.

In Figure III-A-2,  $B_{B\lambda}$  is plotted against  $\lambda$  for several different temperatures, according to equation III-A-1. The importance of this equation lies less in the applications of incandescent sources in luminescence spectrometry, which are few, than in the continuum background emission component of high pressure arc lamps, which closely approaches the characteristic spectral distribution of high temperature black bodies. For instance, the continuum emission of a 500-watt xenon arc lamp corresponds closely to that of a 7000°K black body with an emissivity of 0.06.

The operating temperatures of the filament in an incandescent lamp depends on the power input. A typical 500-watt tungsten lamp operates at only about 3000°K and has an emissivity of 0.4. The intensity emitted by this lamp has a maximum at about 1000 nm and drops to one-hundredth of that value at about 300 and 5000 nm. Thus the tungsten lamp finds its greatest use in the visible and near infrared regions.

The intensity drops off very rapidly in the ultraviolet region. (In addition, the glass envelopes usually absorb strongly below 280 nm, but the intensity at that point is so low anyway that the use of quartz envelopes is of little practical value). The spectral radiance of a 500-Watt lamp at 300 nm is about  $10^{-4}$  watt  $\text{cm}^{-2}$   $\text{sr}^{-1}$   $\text{nm}^{-1}$ , more than two orders of magnitude below that from a typical high pressure xenon arc lamp.

Incandescent lamps are important as sources in spectrometric applications because of their *excellent stability*, rather than because of their *spectral radiance*, which is low compared to continuum arc sources such as the high pressure xenon arc. Long and short term stabilities of the order of 0.01% can be obtained by powering the lamp from a programmable power supply controlled by a feedback signal obtained from a photocell monitoring the lamp output.<sup>4</sup> This order of stability is impossible to obtain with gas discharge and arc lamps.

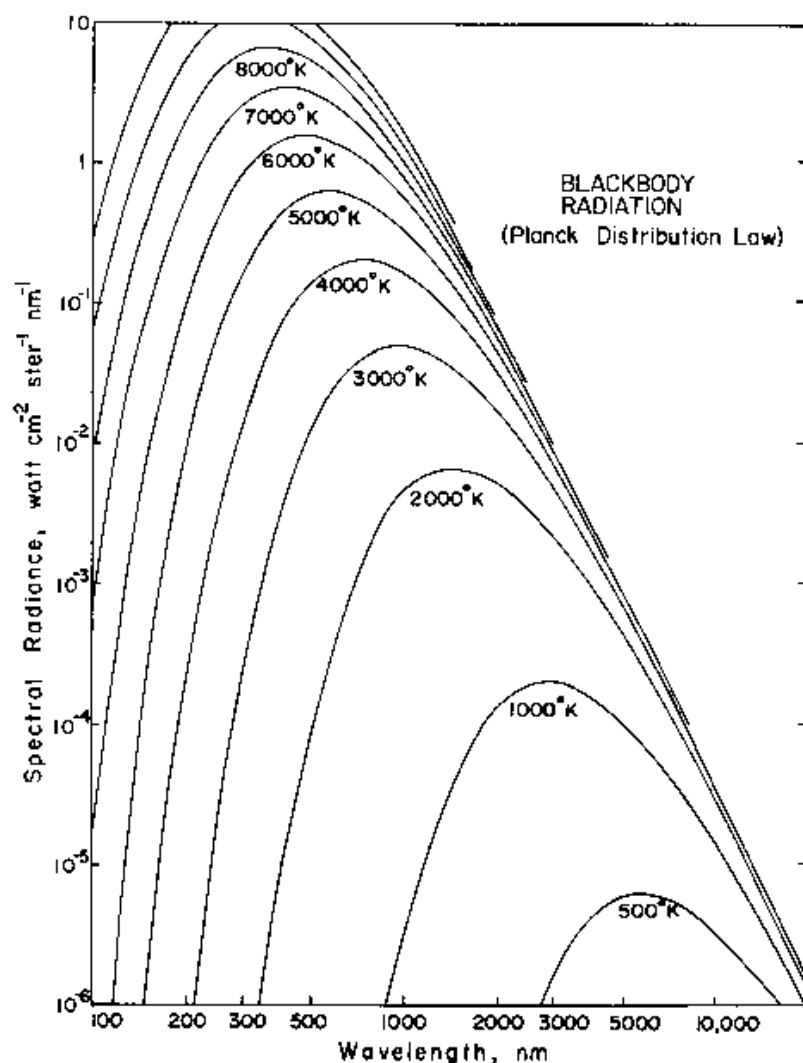


Fig. III-A-2. Spectral distribution of black body radiation at several temperatures.

#### b. ARC LAMPS<sup>3</sup>

Most commercial molecular luminescence spectrometers use high pressure xenon, mercury, or mercury-xenon arc lamps as excitation sources because of their relatively high intensity, wide spectral range, and low cost. Arc lamps of this type are quite intense in the wavelength region from 200 nm through the near infrared.

An arc lamp consists of an enclosed arc discharge between two electrodes in a gas or metal vapor atmosphere. The metal vapor types are limited to the more volatile metals such as mercury, cadmium, zinc, gallium, indium, and thallium, and are capable of producing very intense line spectra of those elements. Gas-type arc lamps are constructed with hydrogen, nitrogen, and the rare gases.



A high pressure mercury arc lamp is a very intense source of ultraviolet radiation. Its spectral output consists of a number of very intense mercury lines superimposed on a continuum background. A typical mercury arc spectrum appears in Figure III-A-3. Although more intense in the ultraviolet than an equivalent xenon arc lamp, the mercury arc lamp is far less smooth in spectral distribution and is therefore less suitable for instruments designed to record excitation spectra.

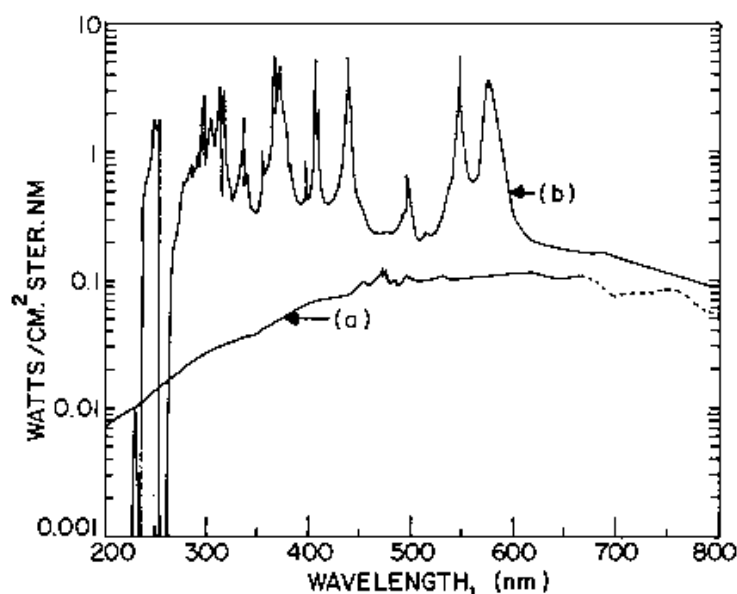


**Fig. III-A-3.** Spectral distribution of two typical sources: curve *a*, PEK75 xenon arc lamp (with permission of PEK, Sunnyvale, Calif.); curve *b*, Osram HBO100 mercury arc lamp (with permission of Osram, Berlin).

The most widely used excitation source in molecular luminescence instrumentation is the high pressure xenon arc lamp.<sup>5-6</sup> This type of lamp is constructed of two tungsten electrodes in a small quartz envelope. Most types have arc gaps of a few millimeters and are referred to as *short* or *compact arcs*. Xenon gas pressures under typical operating conditions range from 10 to 30 atm (see Figure III-A-3). Except for a few low intensity xenon lines around 450 nm, the spectral distribution in the visible and ultraviolet regions corresponds closely to that of a 600°K black body with an emissivity of 0.06.<sup>7</sup> A serious deviation from a black body distribution occurs in the near-infrared region, where there is a system of very strong lines between 800 and 1000 nm. Because most excitation spectra are obtained between 200 and 450 nm, the xenon lamp will not cause the appearance of false peaks. The ratio of line to continuum intensity depends on the current density in the arc. The spectral radiance of the continuum increases with approximately the 1.6 power of the current density, whereas the radiance of the

line emission increases almost linearly. Thus a purer continuum is obtained at higher current densities.

Commercial xenon arc lamps are available in a wide range of input power ratings from a few watts to thousands of watts. The increased input power of the higher power lamps is due mainly to the increased total arc current, rather than arc voltage or arc current density. For lamps in the 100 to 5000-watt range, total arc currents range from 5 to more than 1000 A, but the arc voltage increases only slightly with lamp power and generally remains between 15 and 30 volts. This variation is owing primarily to the increased arc length, which varies typically from 1 to 9 mm. In general, the arc width also increases with arc power, so that the arc current density is not necessarily much greater in the high power lamps. The color temperature is nearly independent of lamp power. The increased *total light output of high power lamps is primarily due to the increased arc area*. However, the average spectral irradiance does increase somewhat with lamp power, because the spectral emissivity increases to some extent. The total radiative efficiency of a xenon arc lamp is typically 30 to 50%. The losses are primarily thermal and are the result of ions and electrons in the arc colliding with the envelope walls and giving up their kinetic energy. The heat is then carried from the walls by air convection or radiated as long wavelength infrared radiation. For a given current density, the energy loss by thermal conduction is expected to be proportional to the wall area. Thus a large-diameter, short-arc lamp would tend to have a higher total radiative efficiency than a long, small-diameter lamp of the same internal volume.

Compared with a 100-watt tungsten lamp, a 100-watt xenon arc has a lower radiative efficiency and therefore generates more heat, but its spectral radiance in the visible and ultraviolet is much higher because its color temperature is much more nearly optimum for this region. Calculating on the basis of the respective color temperatures and spectral emissivities, it is found that the spectral radiance of the xenon arc at 500 nm would be about  $0.1 \text{ watt cm}^{-2} \text{ sr}^{-1} \text{ nm}^{-1}$  compared with about  $0.005 \text{ watt cm}^{-2} \text{ sr}^{-1} \text{ nm}^{-1}$  for the tungsten lamp. In the ultraviolet, the difference is even more striking.\*

\* It is important to realize the distinction between emissivity and radiative efficiency when dealing with arc sources whose spectral distributions approximate those of a black body. The arc is not, of course, a real incandescent source, and trying to fit the arc into the black body scheme is somewhat artificial. The black body nomenclature serves merely as a basis of comparison of sources. The temperature is chosen for the best fit to the spectral distribution of the arc radiation, and then the emissivity is adjusted to reconcile the spectral radiance. A significant characteristic of a xenon arc is that the color temperature of the arc plasma (i.e., the black body temperature with the same spectral distribution) is close to 6500°K regardless of the input power, quite unlike a true incandescent filament lamp. The increased input power and light output of highpowered tubes is due more to the increased arc width than to increased color temperature, as mentioned previously.

Xenon arc lamps are almost always operated on DC for greatest stability and longest life. As with other high pressure DC arcs, polarity is important; and the lamp should be operated vertically with the anode (heaviest electrode) up. The starting voltage required is between 20 and 30 kV, considerably greater than that required for mercury arc lamps, because of the higher pressure in the xenon lamp before ignition. The pressure of xenon gas at room temperature before the lamp is started is relatively high (ca. 5 atm), whereas the vapor pressure of mercury at that temperature is very low (ca.  $10^{-5}$  atm). The high voltage may be applied across the arc, to an auxiliary electrode, or to a wire placed close to the bulb. Immediately after ignition, the light output is about 80% of the final value, which is reached in a few minutes. Warm-up time is considerably less than that for mercury arcs.

Although the xenon arc, like the mercury arc, is convection stabilized, it is less sensitive to cooling conditions because there is no danger of xenon condensation. Forced air cooling is possible if care is taken to maintain a reasonably laminar air flow. Natural convection cooling is usually sufficient for all but the highest powered lamps.

The useful life of a xenon arc lamp is limited by the intensity loss due to deposition of electrode material on the bulb. Quoted values range from 200 to more than 1000 hours. Operation of lamps at powers in excess of the rated values increases the rate of electrode evaporation and decreases useful life. More starts and shorter average burning times also shorten life. Operation of a xenon lamp beyond its useful lifetime is not recommended, because absorption of radiated energy by the walls may generate excessive heat and cause the lamp to explode. As a rule, the average useful life of xenon arc lamps is somewhat longer than that of mercury arc lamps.

Arc lamps filled with a mixture of approximately 80% mercury and 20% xenon are often used. Such lamps have the ultraviolet lines of mercury and the infrared lines of xenon, as well as a strong continuous background. The electrical properties are similar to those of mercury arc lamps. The ultraviolet radiation of mercury-xenon lamps is considerably more intense than that of xenon lamps of the same power, but it is much less uniform in spectral distribution.

### C. FLASH LAMPS<sup>8,9</sup>

In some applications, a very intense, short-duration pulse of exciting light may be desirable. This can be obtained from an arc lamp by applying a short high current pulse to the lamp, usually by discharging a high voltage capacitor through the lamp. Xenon arc lamps designed for this sort of service are called xenon flash lamps. They are used as sources of high intensity light pulses in the visible and ultraviolet region. Such lamps have been shown to have considerable analytical utility in luminescence spectrometry. They are

particularly useful for the measurement of short luminescence decay times. In addition to xenon, other gases such as nitrogen and hydrogen may be used. Nitrogen flash lamps have been used to measure fluorescence decay times of the order of several nanoseconds.

A simple flash tube driving circuit is shown in Figure III-A-4. The DC power supply charges the energy storage capacitor  $C$  through resistance  $R$  to

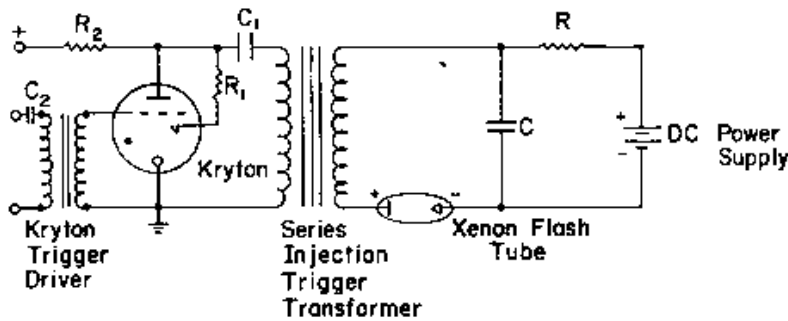


**Fig. III-A-4.** Simple flash tube circuit identical to the circuit in TM-12 Trigger Module, Technical Data, EG & G, Inc., Electronics Division, Boston, Mass. 02215 (with permission of EG & G, Inc.).

a voltage  $V$ , the operating voltage. This voltage must be below the self-flash voltage of the lamp, so that the lamp will operate only when triggered. The lamp is triggered by the application of a high voltage trigger pulse, which causes the fill gas in the tube to ionize. The energy stored in the capacitor  $C$  is then rapidly discharged through the lamp, producing an intense flash of light. The energy input (joule) to the lamp per flash is equal to the energy stored in the capacitor and is given by

$$J = \frac{1}{2} CV^2 \quad (\text{III-A-2})$$

where  $J$  is the input energy (joules),  $C$  is the value of the storage capacitor ( $\mu\text{F}$ ),\* and  $V$  is the operating voltage (kV). The value of  $C$  is typically between 0.1 and 500  $\mu\text{F}$ , and  $V$  is usually between 0.5 and 3.0 kV. The maximum allowable value of  $J$  is limited by lamp construction and is specified by the manufacturer of the lamp.

The duration (sec) of the light flash  $t_f$  is approximately equal to the duration of the current pulse through the lamp

$$t_f = \frac{1}{2} R_f C \quad (\text{III-A-3})$$

\* 1 microfarad ( $\mu\text{F}$ ) =  $10^{-6}$  farad.

where  $R_f$  is the effective arc resistance during the flash and is approximately directly proportional to the arc gap length and inversely proportional to the  $\frac{2}{3}$  power of the operating voltage  $V$ . Thus the shortest, most intense flashes are produced from short gap tubes operated from relatively high  $V$  and low  $C$ . The value of  $R_f$  is given by the manufacturer of the lamp for a specified set of operating conditions.

The *peak input power* (watt) per flash is given approximately by

$$P_i = \frac{J}{t_f} \quad (\text{III-A-4})$$

More important is the *peak light output* power per flash, which is  $P_i$  times the radiative efficiency, typically 25 to 50% for xenon flash tubes. The radiative efficiency is also a function of operating parameters, particularly  $V$ . For xenon tubes the peak output power per flash turns out to be roughly proportional to  $C^{2/3}V^3$ .

The *average input electrical power*  $\bar{P}_i$ , in watts, is

$$\bar{P}_i = Jf \quad (\text{III-A-5})$$

where  $f$  is the flash repetition frequency (Hz). A maximum value of  $\bar{P}_i$  is also recommended by the manufacturer. The higher powered types may have to be forced-air cooled.

The average current drawn from the DC power supply is given by

$$i = VCf \quad (\text{III-A-6})$$

where the terms have the same definitions as previously. The value of the charging resistor  $R$  in Figure III-A-4 should be chosen so that

$$R = \frac{1}{5fC} \quad (\text{III-A-7})$$

Its power rating should be greater than  $\bar{P}_i$ . The value of  $f$  should never exceed about  $0.1 t_f^{-1}$  to prevent continuous ionization of the lamp.

As an example of the application of the foregoing equations, consider the operation of a small commercial xenon flash lamp with maximum ratings of 5 joules per flash, 2-kV operating voltage, 10-watt average input power, and a quoted arc resistance of 5 ohms at 1 joule. Suppose that, in order to increase useful lamp life, the lamp is to be operated at 1.0 kV and 1 joule per flash, somewhat below the maximum ratings. The maximum allowable repetition frequency is that at which  $\bar{P}_i$  is 10 watts and is equal to 10 Hz according to equation III-A-5. Equation III-A-2 gives the value of  $C$  as  $2 \mu\text{F}$ . The peak input power per flash  $P_i$  is  $2 \times 10^5$  watts (equation III-A-4) and the peak output power  $P_o$  will probably be about  $5 \times 10^4$  watts (assuming

25% efficiency). The flash duration is  $5 \mu\text{sec}$  (equation III-A-3). Equation III-A-7 gives the value of the charging resistor  $R$  as  $10 \text{ k}\Omega$ . The average current drawn from the power supply is  $20 \text{ mA}$  by equation III-A-6.

The spectral distribution of flash lamps depends mainly on the nature and pressure of the fill gas. Xenon flash tubes with quartz envelopes have an effective color temperature of about  $7000^\circ\text{K}$ , similar to DC xenon arcs; but the emissivity is considerably greater and often approaches unity near the peak of the flash.

When a xenon flash tube is operated below its maximum peak input power per flash, not all the gas is ionized and the arc may take on a narrow, filamentary appearance. The position of the arc tends to shift from flash to flash, causing irregularities in the measured light output. If the energy input is increased so that all the xenon ionizes, the arc is stabilized. For this reason, it is usually not advisable to operate a flash tube very far below its maximum input. Certain tubes are specifically designed for stable, low energy operation.

### 3. MONOCHROMATORS<sup>10-12</sup>

In most modern commercial spectroluminometers, two monochromators are used, one for emission and one for excitation. Usually the two are identical in design.

A generalized diagram of the dispersive and optical portion of a monochromator is supplied in Figure III-A-5. Radiation from the sample is col-

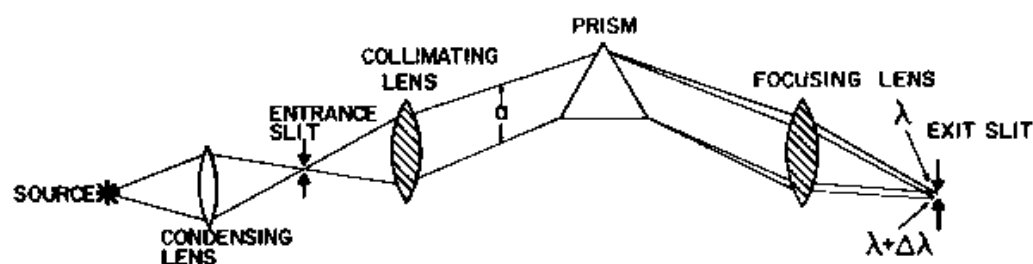


Fig. III-A-5. Generalized diagram of dispersive and optical portion of a monochromator.

lected by the condensing lens and focused onto the entrance slit, which defines the shape of the images at the focal plane. Radiation emerging from the entrance slit is collimated onto the dispersing element, a prism or grating, where it is separated into its spectral components. This radiation is focused onto the exit slit, which isolates a small region of the spectrum. In real instruments, the collimating and focusing elements may be lenses or mirrors; or, their functions are often combined into one element, but the schematic diagram shown will satisfy the requirements of the following general treat-

ment of *dispersion*, *resolution*, and *spectral bandpass*. The focal lengths of the collimating and focusing elements are almost always equal in practice, and this is assumed in the following discussion.

#### a. DISPERSION

An important characteristic of a spectrometer is its *dispersion*, or its ability to separate different wavelengths of radiation so that they emerge from the dispersion element at different angles and come to a focus at different positions in the focal plane. The *angular dispersion*  $D$  is given by  $d\theta/d\lambda$  where  $d\theta$  is the angular separation of two dispersed beams separated by a wavelength difference of  $d\lambda$ . The value of  $D$  depends on the construction of the dispersing element (prism or grating). The *linear dispersion* is the separation between different wavelengths in the focal plane, and is given by  $dx/d\lambda$ , where  $dx$  (cm) is the linear distance between two wavelengths separated by  $d\lambda$  (nm). The relation between angular and linear dispersion is easily determined by geometry. If  $F$  is the focal length of the lens which focuses a dispersed beam of light with angular dispersion  $d\theta/d\lambda$ , the linear dispersion at the focal plane will be

$$\frac{dx}{d\lambda} = F \frac{d\theta}{d\lambda} = FD \quad (\text{III-A-8})$$

A more useful measure of dispersion, and one which is most often specified by spectrometer manufacturers, is the *reciprocal linear dispersion*  $R_d$ , defined by

$$R_d = \frac{d\lambda}{dx} = \frac{1}{DF} \quad (\text{III-A-9})$$

The reciprocal linear dispersion is often expressed in Angstrom units per millimeter or nanometers per centimeter. Typical values of  $R_d$  for monochromators in a luminescence spectrometer range from 1 to 10 nm mm<sup>-1</sup>.

#### b. SPECTRAL BANDPASS

The ability of a monochromator to produce a monochromatic beam of radiation from a polychromatic light source is expressed in terms of its *spectral bandpass*  $s$ , which is the range of wavelengths of radiation emerging from the exit slit when polychromatic radiation is incident upon the entrance slit. More precisely, the spectral bandpass is defined in terms of the *slit function* of the monochromator, which is the plot of intensity emerging from the exit slit versus wavelength when the monochromator is scanned through a monochromatic line from a line source evenly illuminating the entrance slit (see Appendix 3). The slit function will be a trapezoid or triangle whose

half width (width at half-maximum) expressed in wavelength units is defined as the spectral bandpass  $s$ ,

$$s = R_d W \quad (\text{III-A-10})$$

where we have  $R_d$  ( $\text{nm cm}^{-1}$ ) and the width  $W$  (cm) of the entrance or exit slit, if they are equal, or of the larger of the two slits, if they are unequal. The base width  $\Delta\lambda$  of the slit function is given by

$$\Delta\lambda = R_d(W_s + W_e) \quad (\text{III-A-11})$$

where  $W_s$  and  $W_e$  are the entrance and exit slit widths, respectively. If  $W_s = W_e = W$ ,

$$\Delta\lambda = 2R_d W \quad (\text{III-A-12})$$

and the slit function is triangular. This is the most usual case.

### c. RESOLUTION

The *resolution*  $\Delta\lambda_R$  of a spectrometer may be defined as the minimum wavelength separation between two monochromatic spectral lines that are just separated. The exact definition depends on the criterion for separation. For essentially *complete* separation, the slit functions of the two lines may join but may not overlap at their adjacent bases. In this case, the resolution is the same as the basewidth of one slit function

$$\Delta\lambda_R = R_d(W_s + W_e) \quad (\text{III-A-13})$$

and

$$\Delta\lambda_R = 2R_d W = 2s \quad \text{if} \quad W_s = W_e = W \quad (\text{III-A-14})$$

neglecting diffraction and optical imperfections.

### d. THEORETICAL RESOLUTION AND RESOLVING POWER

It might be thought, on the basis of the expression for linear dispersion given in equation III-A-8, that two adjacent spectral lines, no matter how close, could be resolved simply by increasing the focal length sufficiently. This would be so only if: (a) the slit widths could be made indefinitely small\* and (b) the entrance slits were imaged in the focal plane as a geometrical image of the slit. In reality, of course, a finite slit width must always be used to allow a measurable amount of light to pass through. Even if an infinitely narrow slit could be used, however, the resolution would be limited by *Fraunhofer diffraction* of the collimated beam by the effective aperture of the instrument. The effective aperture is the width of the collimated beam, or, in other words, the width of whatever aperture defines or limits the width of

\* As  $W \rightarrow 0$ , the parallelism of the slit jaws would also have to be maintained.



the collimated beam (designated by the distance  $a$  in Figure III-A-5). The diffraction of the collimated beam by the edges of the effective aperture causes the entrance slit to be imaged at the focal plane as a diffraction pattern rather than as a geometrical image. The result is that, as the slit widths are decreased, the observed slit function approaches a Fraunhofer diffraction pattern of finite width instead of an infinitely narrow line. The half width  $X$  of the central intensity maximum of the diffracting pattern is given by elementary diffraction theory.

$$X = \frac{\lambda F}{a} \quad (\text{III-A-15})$$

Thus, as the slit widths approach zero, the spectral bandpass approaches a minimum value  $s_{\text{min}}$  given by

$$s_{\text{min}} = R_d X = \frac{R_d \lambda F}{a} \quad (\text{III-A-16})$$

By comparison with equation III-A-10, we see that in the common case\*  $W_s = W_e = W$ , the effect of diffraction is to limit the *effective* slit width to a minimum value  $W_{\text{min}}$  as the mechanical slit width approaches zero.

$$W_m = \frac{\lambda F}{a} \quad (\text{III-A-17})$$

In addition to the diffraction effect, optical imperfections such as *spherical aberration*, *coma*, and *astigmatism* may cause the experimentally observed spectral bandpass to approach a value slightly higher than that calculated by equation III-A-16 as the slit widths approach zero. This additional aberration-limited spectral bandpass term  $s_a$  must also be included in  $s_{\text{min}}$ . Thus equation III-A-16 should be replaced by

$$s_{\text{min}} = \frac{R_d \lambda F}{a} + s_a \quad (\text{III-A-18})$$

It is not unreasonable to expect the slit width, diffraction, and aberration terms to add approximately linearly, and so the actual spectral bandpass for equal entrance and exit slits may be written as

$$s \cong R_d W + s_{\text{min}} \cong R_d W + \frac{R_d \lambda F}{a} + s_a \quad (\text{III-A-19})$$

For purposes of calculation, all the length terms in this equation must be converted to units comparable with those of  $R_d$ ;  $s_a$  must be determined

\* Most monochromators have bilateral slits, but the slits may differ slightly (i.e.,  $W_s \neq W_e$ ). This is especially noticeable as  $W_s$  and  $W_e$  approach  $W_{\text{min}}$ .

experimentally. An experimental plot of  $s$  versus  $W$  is a useful test of a monochromator. The spectral bandpass  $s$  is equal to the half width of the slit function obtained by scanning the monochromator through an isolated monochromatic line from a line source of very narrow true line width. The slope of the plot on linear coordinates is  $R_d$ , and the vertical intercept is  $R_d \lambda F/a + s_a$ . Because the diffraction term can be calculated, the optical quality can be assessed by the smallness of  $s_a$ . In such measurements, the entrance slit must be very evenly illuminated in order to obtain slit functions of good triangular shape.

The actual resolution expected from a monochromator should be calculated on the basis of equation III-A-19. For essentially *complete* resolution, two lines must be separated by  $2s$  if the exit and entrance slit widths are equal. Somewhat less than complete resolution can sometimes be tolerated, however. In any case,  $\Delta\lambda$  must always be greater than  $s$ .

The *resolving power*  $R$  of a spectrometer is defined by

$$R = \frac{\bar{\lambda}}{\Delta\lambda_R} \quad (\text{III-A-20})$$

where  $\Delta\lambda_R$  is the wavelength difference (nm) between two monochromatic spectral lines which can just barely be distinguished as separate lines and  $\bar{\lambda}$  is the mean wavelength of the two lines (nm). A value of  $10^4$  is not unusual for a medium-resolution monochromator.

The *theoretical resolving power*  $R_{\text{theor}}$  is the diffraction-limited resolving power for zero slit widths and no optical imperfections. Using the "Rayleigh criterion" of resolution,  $R_{\text{theor}}$  is given by

$$R_{\text{theor}} = \frac{\bar{\lambda}}{\lambda R_d} = \frac{a}{R_d F} \quad (\text{III-A-21})$$

The extent to which  $R$  of a real spectrometer approaches  $R_{\text{theor}}$  is also considered as an indication of quality.

#### e. SLIT ILLUMINATION AND ENTRANCE OPTICS

The radiant flux of a spectrum at the focal plane of a spectrometer depends not only on the source radiance but also on the way in which the entrance slit is illuminated. Obviously, the highest possible radiant flux at the slit face is desirable in luminescence work to obtain high sensitivities. However, of all the light that passes through the entrance slit, only that part which is collected by the collimator lens is effective in producing the image at the focal plane. In other words, radiation falling outside the solid angle subtended at the entrance slit by the collimator lens will be wasted (and may, in fact, contribute to undesirable stray light in the instrument). Sometimes a condensing lens (mirror) is placed between the source and the entrance slit

to collect and focus the light on the slit. The maximum radiant flux at the focal plane with a given source is obtained when the collimator is filled with light, regardless of the arrangement of the condensing lens. If the luminous area of the source is large enough to subtend a solid angle at the slit equal to that subtended by the collimator lens, then the collimator lens will be completely illuminated and a condensing lens will be of no help. This is often true of the emission monochromator in luminescence spectrometers.

If, on the other hand, the source area is too small to fully illuminate the collimator, then using a condensing lens to form an image of the source on the entrance slit will increase the image brightness at the focal plane. This is often true of the excitation monochromator. The lens should be placed so that it subtends a solid angle at the entrance slit equal to that subtended by the collimator lens. In this way, the collimator will be filled with light. The image of the source on the slit should just fill the slit.

It might be thought that the image brightness could be increased by using a condensing lens of large diameter and short focal length to form a small, high intensity image of the source on the entrance slit. This would indeed increase the radiant flux per unit area falling on the slit; but the solid angle at the slit would be proportionately decreased, and the spectral flux of the light emerging from the slit onto the collimator would remain unchanged.\*

If the dimensions of the luminous area of the source are suitable dimensions for a slit, the entrance slit can be replaced by the source itself, thus simplifying the instrument and eliminating losses in the condensing lens. This is occasionally done in excitation monochromators when high pressure arc lamps are used as sources. A disadvantage, however, is that the effective slit width is not adjustable. Furthermore, arc wander causes unpredictable shifts in the monochromator calibration. In most cases, the use of a condensing lens and separate entrance slit is preferable.

#### f. SPEED

The *speed* of a spectrometer is an indication of the ability of the collimator lens to collect light emerging from the entrance slit. It is expressed by the "*f* number":

$$f = \frac{F_c}{D_c} \quad (\text{III-A-22})$$

\* Because object area  $\times$  solid angle = image area  $\times$  image solid angle, an increase in image area compared to object area must be achieved with a decrease in image solid angle compared with object solid angle. The maximum radiant flux passing through the entrance slit and the maximum resolution results if the entrance slit is fully illuminated with source radiation. An array of lens and mirrors will only increase the radiant flux if more than *one* solid angle of radiation from the source fills the monochromator collimator.

where  $F_c$  and  $D_c$  are the focal length and diameter of the collimator lens (or mirror), respectively. In general, the term *speed* may be applied to any lens; the smaller the focal-length-to-diameter ratio ( $f$  number), the faster the lens, and the greater the light gathering ability. The solid angle, in steradians, of light collected by a lens from a point source is

$$\Omega = \frac{A_l}{F_c^2} \quad (\text{III-A-23})$$

where  $A_l$  is the area of the lens ( $\text{cm}^2$ ) and  $F_c$  is its focal length (cm). Thus fast lenses (i.e., lenses with large diameters and short focal lengths) pick up a large solid angle of radiation.

#### g. LIGHT LOSSES

In a real spectrometer, the total flux of radiation at the focal plane is always less than that collected by the collimator lens, owing to unavoidable light losses in the instrument. The light transmitting ability of a spectrometer at a particular wavelength  $\lambda$  is indicated by its *transmission factor*  $T_f$ , which is the ratio of the monochromatic light flux of wavelength  $\lambda$  emerging from the exit slit (or incident on the focal plane) to that collected by the collimator lens. The primary causes of light losses in spectrometers are reflection, absorption, and scattering by the various optical components (e.g., prisms, lenses, gratings, and mirrors) in the instrument. It is obviously desirable to use lens and prism materials of high transmittance and mirrors of high reflectivity in the desired wavelength range. Furthermore, reflection losses at the surfaces of prisms and lenses can be reduced in a limited wavelength range by the use of special low reflectance coatings. Gratings should be blazed in the desired wavelength range. Finally, light losses can be reduced by reducing the total number of optical components in the light path. This can be done by combining the functions of two or more components into one (e.g., using a concave grating as both a dispersing element and a focusing element). In some designs, such as the Fery prism monochromator and the concave grating mountings, the only optical components in the light path is the dispersing element itself.

#### h. RADIANT FLUX EMERGING FROM SPECTROMETRIC SYSTEM<sup>2</sup>

All calculations involving the response of a spectrometric system to a "light source," as well as any predictions that can be made concerning the effect and optimization of the slit widths and other optical parameters, require that an expression be obtained for the light flux emerging from the exit slit of a monochromator as a function of the source radiance (line source) or source spectral radiance (continuum source) and monochromator optical

variables. The radiance flux expressions for the excitation and emission monochromators in luminescence spectrometers are similar; the "source" radiance or spectral radiance refers to the excitation source radiance (or spectral radiance) and sample luminescence radiance (or spectral radiance), respectively.

To derive an expression for the radiant flux emerging from the exit slit, the following definitions are needed:

$B_N^\circ$  = radiance of a line source, watt  $\text{cm}^{-2} \text{sr}^{-1}$

$B_{C\lambda}^\circ$  = spectral radiance of continuum source, watt  $\text{cm}^{-2} \text{sr}^{-1} \text{nm}^{-1}$

$W$  = Illuminated width of slit, cm

$H$  = Illuminated height of slit, cm

$T_f$  = transmission factor of optical system, no units

$\Omega$  = solid angle of light collected by collimator, sr

$s$  = spectral bandpass of monochromator, nm

$\Phi$  = total flux emerging from exit slit, watt

$K_o$  = optics factor =  $HT_f\Omega$ , cm sr

Assuming that the exit and entrance slits are equal in  $W$  and  $H$  and that all light losses are included in  $T_f$ , then for a "line source"

$$\Phi = B_N^\circ WHT_f\Omega = B_N^\circ K_o W \quad (\text{III-A-24})$$

and for a "continuum source"

$$\Phi = B_{C\lambda}^\circ WHT_f\Omega s = B_{C\lambda}^\circ K_o s W \quad (\text{III-A-25})$$

Neglecting diffraction,  $s = R_d W$ ; thus for a continuum source

$$\Phi = B_{C\lambda}^\circ W^2 HT_f\Omega R_d = B_{C\lambda}^\circ K_o R_d W^2 \quad (\text{III-A-26})$$

For a source of light containing both line and continuum components, the line-to-continuum ratio is inversely proportional to the slit width. This is of particular importance in luminescence spectrometry. In molecular fluorescence work, we must often attempt to measure relatively broad band emission spectrum of the sample in the presence of scattered light from the excitation source, often a mercury or mercury-xenon lamp. The relative contribution of the intense mercury lines can be reduced by using relatively large emission monochromator slit widths. In atomic fluorescence spectrometry with a continuum excitation source, the ratio of the desired fluorescence line emission to the continuum background due to scattering of the excitation radiation by flame particles and droplets is increased by using relatively narrow slits.

It is sometimes helpful to record an observed excitation or emission spectrum at several values of excitation and/or emission monochromator slit widths in order to determine which features of the spectrum are due to line emission (radiant fluxes directly proportional to slit width) and which are due to essentially continuum emission (radiant fluxes proportional to square of slit width).

It is of interest that the best balance between radiant flux\* and resolution is obtained if the entrance and exit slits of a monochromator are equal.<sup>2</sup>

#### i. STRAY RADIATION

Stray radiation is particularly undesirable in luminescence instrumentation because of the very low luminescence intensities that must often be measured and because the very intense light from the excitation source may tend to "leak" into the emission monochromator, even in the absence of real luminescence of the sample.

Stray radiation in spectrometers may result from the following causes:

1. Leakage of room light into the instrument through unshielded slits or through light leaks in the instrument's case.
2. Reflection and scattering of radiation from walls, optics, mountings, slits, and baffles.
3. Reflection and scattering on optical surfaces.
4. Scattering of light within prisms and lenses.
5. Scattering of light by dust particles.
6. Unused orders in grating spectra.
7. Fluorescence of optical materials.

In monochromators, stray light causes contamination of the selected spectral bandwidth with light of other wavelengths. This undesirable effect may be minimized by proper design of the instrument and by the use of carefully selected optical materials. The amount of stray light in a monochromator is usually quoted by the manufacturer as a certain percentage of the total flux of desired radiation emerging from the exit slit. Typical values range from 0.1 to 1.0% for small commercial monochromators. Stray light in an existing instrument can often be reduced by painting the interior of the instrument flat black, by inserting baffles to obstruct unwanted rays, by carefully shielding slits from room light, and by using windows in front of the slits to seal out dust and corrosive fumes. The problem of stray radiation is

\* Refer to Appendix 3 for a more detailed discussion of optical factors affecting the measured radiant flux and the measured instrumental signal.

most severe if the light intensity at the wavelength of interest is much less than that in neighboring regions. This situation occurs, for instance, when a monochromator is employed to select a wavelength in the ultraviolet region from a xenon arc lamp, which radiates most intensely in the visible. A filter that transmits only the wavelength region of interest may be placed in the light path to reduce interference by the unwanted radiation. A related problem arises when observing a weak atomic line close to a very strong one, as might occur in an atomic fluorescence experiment. Stray light from the strong line may seriously interfere with the weak line and may make resolution of the two lines impossible, even if the resolving power of the instrument is sufficient to separate the two lines if they were equally intense.

Probably the most satisfactory, and unfortunately most expensive, way of reducing interference from stray radiation is the use of the *double monochromator*, which is essentially a system of two monochromators connected in series, the exit slit of the first being the entrance slit of the second. With two identical monochromators, the dispersion and resolution are approximately doubled, and stray radiation is greatly reduced. For example, if the intensity of the stray radiation in each monochromator is 0.1% of that of the primary beam, then the double monochromator would reduce this to 0.0001% (i.e., 0.1% of 0.1%). A slight disadvantage, however, is that the transmission factor of the double monochromator would be about half that of either half by itself. A more serious difficulty is the necessity of keeping the wavelength settings of both monochromators exactly the same at all times during the scanning of a spectrum. This is generally accomplished by mounting both dispersing elements on the same rotating platform or shaft. In some double monochromators, different dispersing elements are used in each half; usually the first is a prism and the second a grating. It is also possible to get some of the effect of two dispersing elements by passing the light through a single dispersing element twice. This arrangement may be considerably less expensive than a true double monochromator, but it is also less effective in reducing scattered light.

At least one commercial luminescence spectrometer uses two double monochromators.

#### j. PRISM MONOCHROMATORS

Dispersion by a prism depends on the change of refractive index  $n$  of the prism material with wavelength. The angular dispersion  $D$  is given by

$$D \equiv \frac{\partial \Theta}{\partial \lambda} = \frac{\partial n}{\partial \lambda} \frac{\partial \Theta}{\partial n} \quad (\text{III-A-27})$$

where  $\Theta$  is the deviation angle, that is, the angle through which an incident light beam is deviated in passing through the prism (Figure III-A-6a). The

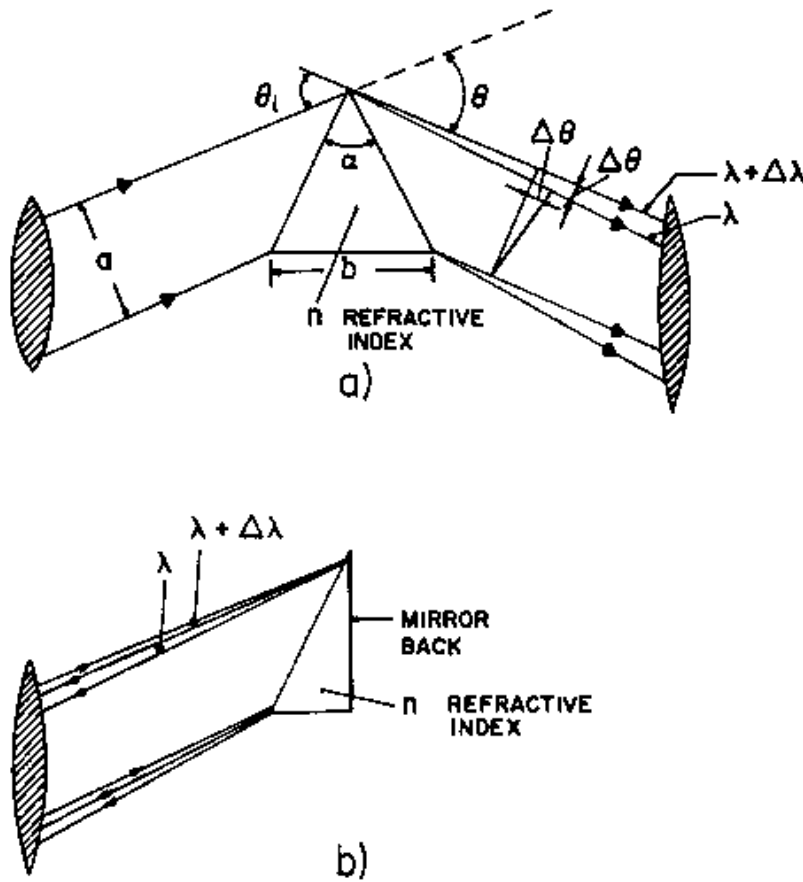


**Fig. III-A-6.** Dispersion of radiation by two typical prisms: (a) Cornu type, (b) Littrow type. (For simplicity, angles and distances do not appear in (b), but note that the Littrow mounting is simply a folded Cornu mounting.)

first term in this equation is the *optical dispersion* of the prism material, and it depends only on the *wavelength* and the *nature* of the prism material and is independent of the geometry of the prism or its mounting. The second term  $\partial\Theta/\partial n$  is the so-called *geometrical factor* and is a function of the geometry and mounting of the prism. In general, the prism mounting is arranged so that the ray internal to the prism is parallel to the prism base, this being the most symmetrical arrangement. In this case, the deviation angle  $\Theta$  is a minimum, and astigmatism and reflective losses are minimized. The geometrical factor is then given by

$$\frac{\partial\Theta}{\partial n} = \frac{2 \sin \alpha/2}{[1 - n^2 \sin^2 (\alpha/2)]^{1/2}} = \frac{2 \tan \Theta_i}{n} = \frac{b}{a} \quad (\text{III-A-28})$$

where  $\alpha$  is the apex angle of the prism,  $\Theta_i$  is the incidence angle at the first prism face,  $b$  is the thickness of the prism base, and  $a$  is the effective aperture as defined previously, assuming that the whole prism face is illuminated (usually true). By far the most common apex angle  $\alpha$  is  $60^\circ$ , and



the geometrical factor for this angle at minimum deviation is about 1.5. More common than a full  $60^\circ$  equilateral prism is the  $30 \times 60 \times 90^\circ$  Littrow prism with a reflective (aluminized) long side, shown in Figure III-A-6b. The reflection back through the prism gives the effect of a full  $60^\circ$  prism with a smaller amount of quartz. In addition, the birefringence of the quartz is canceled.

The theoretical resolving power of a prism may be shown to be

$$R_{\text{theor}} = b \frac{\partial n}{\partial \lambda} \quad (\text{III-A-29})$$

Thus large prisms of high optical dispersion are desirable. Quartz prisms are used in the ultraviolet region, but glass is preferred in the visible because  $\partial n/\partial \lambda$  is higher than quartz.

#### k. GRATING MONOCHROMATORS

All modern commercial luminescence spectrometers now have grating monochromators, principally because of their superior dispersion, resolution, and speed and because the dispersion of a grating is nearly independent of wavelength over a considerable range. The dispersion properties of a grating can be obtained from the basic grating equation. This equation, which is derived in elementary optics textbooks, states that maxima in the intensity of the diffracted light occur for those wavelengths  $\lambda$  for which

$$m\lambda = \Delta(\sin \Theta_i - \sin \Theta_d) \quad (\text{III-A-30})$$

where  $m$  is a positive or negative integer called the *order*,  $\Delta$  is the spacing between the grooves or rulings,  $\Theta_i$  is the incidence angle, and  $\Theta_d$  is the angle of diffraction, as in Figure III-A-7a. The angular dispersion of a grating is obtained by differentiating  $\Theta_d$  with respect to  $\lambda$  in the previous equation:

$$\frac{d\Theta_d}{d\lambda} = \frac{m}{\Delta \cos \Theta_d} = \frac{m\delta}{\cos \Theta_d} \quad (\text{III-A-31})$$

where  $\delta$  is the number of lines (grooves) per centimeter ( $=1/\Delta$ ). The reciprocal linear dispersion of a grating monochromator of focal length  $F$  is

$$R_d = \frac{10^5 \cos \Theta_d}{\delta F m} \quad (\text{III-A-32})$$

where  $F$  is in meters and  $R_d$  is in nanometers per centimeter. In most monochromators,  $\cos \Theta_d$  is nearly unity and does not change much over the wavelength range of the instrument. Thus  $R_d$  is nearly independent of wavelength. This fact greatly simplifies the calibration of grating monochromators. According to this equation, the highest dispersion (lowest  $R_d$ ) is obtained

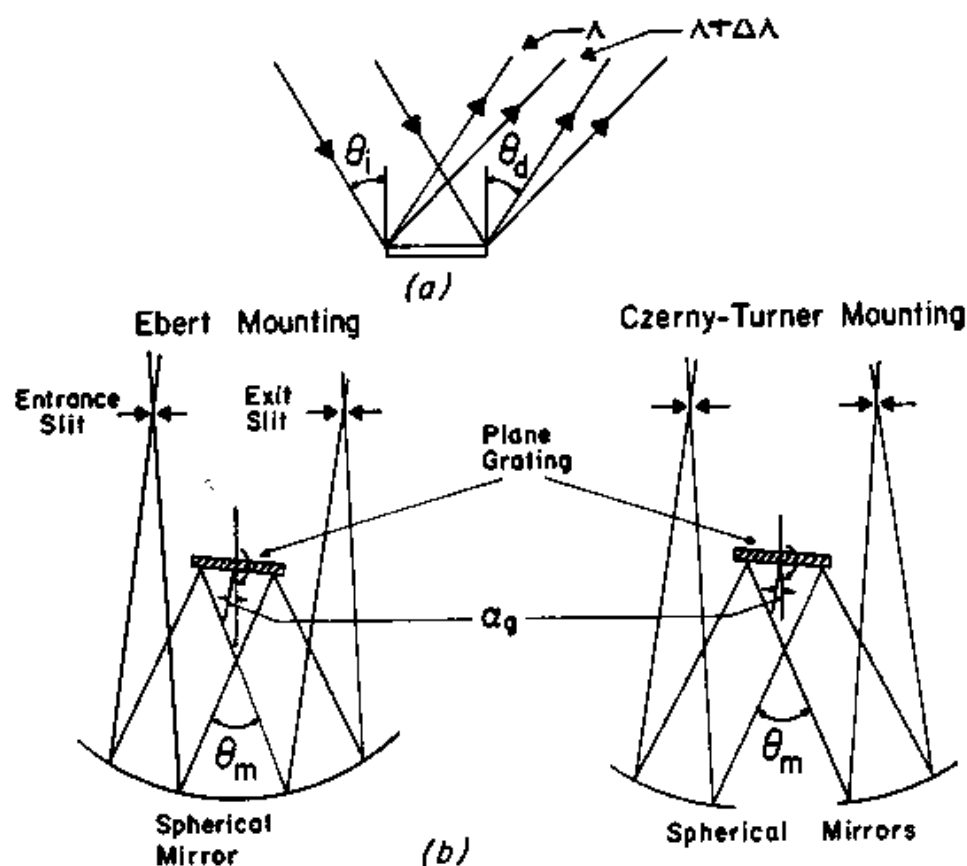


Fig. III-A-7. (a) Diffraction of radiation by a grating, and (b) rotation of a grating to vary wavelengths.

in monochromators of long focal length using finely ruled grating in a high order. Monochromators in luminescence spectrometers typically have focal lengths between 0.25 and 1.0 m and use gratings of 600 to 1200 lines  $\text{mm}^{-1}$  in the first order.

Reflection gratings may be plane or concave, the concave type being used mainly in photographic spectrographs. Most commercial luminescence spectrometers use plane reflection gratings in either the Ebert or the Czerny-Turner mountings (see Figure III-A-7b). In these mountings, the grating is rotated to change wavelengths while the angle between the incident and diffracted rays remains constant ( $\Theta_m$  in Figure III-A-7). It is convenient to modify equation III-A-30 for this case. Defining  $\alpha_g$  as the angle between the grating normal and the monochromator center line:

$$m\lambda = \left[ 2\Delta \sin\left(\frac{\Theta_m}{2}\right) \right] \sin \alpha_g \quad (\text{III-A-33})$$

The factor in brackets is a constant for a given instrument and grating. For convenience in wavelength readout, a specially ground cam or "sine

bar" mechanism is included in commercial monochromators to convert the linear rotation of the wavelength counter or dial to the sine rotation required by the equation, thus providing a linear wavelength scale. A "cosecant bar" can be used to provide a linear wavenumber (reciprocal wavelength) scale.

Note that according to equations II-A-30 and II-A-33, all grating monochromator wavelength dials read out in  $m\lambda$ , not simply  $\lambda$ ; this must be considered if grating orders other than the first are used. For instance, the 546.074-nm green mercury line would be picked up in the second order at a dial reading of  $2(546.074)$  or 1092.348 nm. On the other hand, the dial setting for a wavelength  $\lambda$  in the first order is also the proper setting for all wavelengths  $\lambda/m$  in correspondingly higher orders. This order overlap problem is particularly severe in spectrofluorimetry with a mercury arc excitation source, and the experimenter must understand quite well the operation of grating orders in order to avoid erroneous interpretation of data. For example, a fluorescence band at 507.4 nm could be interfered with by scattering of the intense 253.7-nm line from a mercury arc lamp, because this line would appear in the second order near a dial reading of 507.4 nm.

These problems of order overlap and ambiguity are the most serious disadvantages of grating spectrometers, but there are ways to avoid or reduce these difficulties. For instance, a filter may be placed in the monochromator light path to absorb unwanted wavelength regions, or a prism may be combined with the grating as an "order separator." The waste of precious light intensity in unwanted orders may be reduced by the use of "blazed" gratings,\* whose rulings are shaped to throw most of the diffracted intensity into a particular  $m\lambda$  region. In blazed gratings, the reflective flats are ruled at an angle  $\beta$ , the *blaze angle*, to the grating surface. The greatest diffracted intensities occur at those values of  $\Theta_d$  most closely corresponding to the angle of specular reflection from the surface; this occurs when  $(\Theta_i - \beta)$  equals  $(\beta - \Theta_d)$  in Figure III-A-7a. For an Ebert or Czerny-Turner monochromator, this condition is met when  $\alpha_g = \beta$ ; that is, at the value of  $m\lambda$  satisfying

$$m\lambda = 2\Delta \sin \frac{\Theta_m}{2} \sin \beta \quad (\text{III-A-34})$$

It is again important to note that this equation tells us that gratings are blazed for a given  $m\lambda$ , not for a particular order or wavelength alone. A grating blazed at 500 nm in the first order also exhibits an intensity maximum at 250 nm in the second order. Thus second-order interference at 500 nm from ultraviolet radiation near 250 nm is *not* reduced by the use of a grating blazed at 500 nm in the first order.

\* Blazed gratings are called echelette gratings.

The symmetrical path of light through Ebert and Czerny-Turner monochromators largely cancels out the adverse effects of spherical aberration, coma, and astigmatism. In addition, there is no chromatic aberration in any system with all-reflective optics. However, residual astigmatism does cause the spectral lines to be curved along their lengths; this effect can impair resolution if long, narrow straight slits are used. Special slits correspondingly curved along their lengths are used in some high resolution monochromators to correct this effect, but they are costly. Curved slits are seldom necessary in luminescence instrumentation, particularly if small slit heights are used ( $H \leq 5$  mm).

#### 1. FILTERS<sup>2,13-15</sup>

Filters may be used as substitutes for monochromators, as in filter fluorometers, or to decrease the stray light in spectrofluorometers. Filter fluorometers have the advantages of simplicity, low cost, and very high light gathering ability, but they are obviously less selective and cannot record spectra. Filters are often used in conjunction with grating monochromators to prevent interference from undesired orders or other stray light.

A large variety of glass and gelatine filters are currently manufactured by several firms (e.g., Corning Glass Works, Corning, N.Y.). Sill<sup>13</sup> has given a convenient summary of the transmission spectra of a large number of filters, both single and in combination. Both low-pass and high-pass filters are available. High quality band pass filters may be made by combining a low-pass and with a high-pass filter. Concentrated solutions of many substances may serve as very effective high-pass filters.<sup>2</sup>

Interference filters<sup>15</sup> may also be useful in some cases. These have narrower pass bands than do absorption filters but are more expensive.

#### 4. PHOTODETECTORS<sup>16-20</sup>

Most commercial luminescence spectrometers use multiplier phototubes for the measurement of luminescence intensity, although some also use other types of photodetectors to monitor the intensity of the source for ratio fluorescence measurements or for the measurement of corrected spectra or absolute quantum efficiencies. The principal requirements for measurement of luminescence radiation are high *sensitivity* and *signal-to-noise ratio* over the required spectral range, *high linearity* of response, *low dark current*, and *fast response time*. The *radiant sensitivity* of a detector  $\gamma$  is defined as the ratio of the output current (A) to the radiant flux on the cathode (watt). Ideally, the detector sensitivity should be independent of wavelength if undistorted luminescence spectra are to be measured. Unfortunately the last requirement is impossible to attain in the most sensitive detectors

## a. GENERAL ASPECTS OF PHOTOEMISSIVE DETECTORS.\*

The multiplier phototube is one type of photoemissive detector. The principle of operation of photoemissive detectors may be illustrated by the single-stage vacuum photodiode shown schematically in Figure III-A-8. This

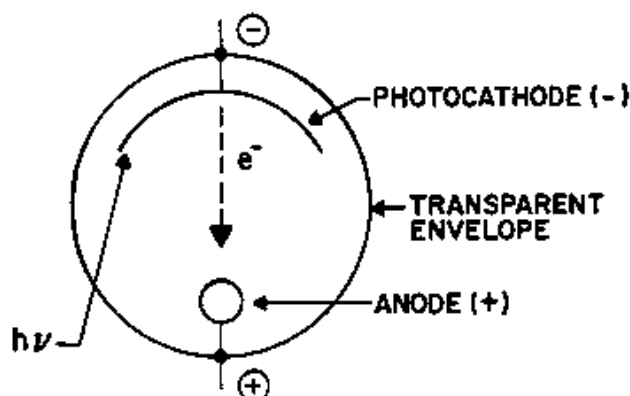


Fig. III-A-8. Schematic representation of a single-stage photoemissive (photo-diode) detector.

device consists of two metal electrodes sealed in a glass or silica envelope and held at a potential difference of about 100 volts by means of an external battery or power supply. The negative electrode (photocathode) is coated with a photoemissive substance, usually a mixture of metals and metal oxides, of low work function. When light falls upon the photocathode, those photons of energy  $h\nu$  greater than the work function  $\Phi_a$  of the cathode material eject photoelectrons, which are attracted to and collected by the positive anode. The resulting current flowing in the external circuit is directly proportional to the rate of photoelectron emission, which is proportional in turn to the incident light radiant flux. Such a detector is stable, linear, and very fast, but unfortunately the sensitivity is comparatively low and is dependent on the wavelength. A photoemissive detector can not respond to light whose photons have an energy below the work function. This occurs at wavelengths above the *threshold wavelength*  $\lambda_{th}$  given by

$$\lambda_{th} = \frac{hc}{\Phi_a} = \frac{12400}{\Phi_a} \text{ \AA} \quad (\text{III-A-35})$$

where  $\Phi_a$  is the cathode work function (eV).

Even below  $\lambda_{th}$  not all the photoelectrons may have enough kinetic energy ( $h\nu - \Phi_a$ ) to escape the surface, particularly if they originated some distance within the surface. At short wavelength, the sensitivity of the detec-

\* For a discussion of the principles of nonphotoemissive detectors, refer to Appendix 4.

tor may be impaired by absorption by the envelope material. Most commercial tubes have  $\lambda_{th}$  between 600 and 1200 nm, and the short wavelength limit is about 350 nm with a glass envelope or 200 nm with silica. The shape of the spectral response curve (i.e., the plot of detector sensitivity versus wavelength) is thus a function of the cathode composition and envelope material and typically exhibits a broad maximum in the near-ultraviolet and visible region. There are a limited number of common combinations of cathode composition and envelope material; the corresponding response curves are denoted by "S" numbers such as S1, S5, and so on. A few are shown in Figure III-A-9.

A photoemissive detector is a "current source"; at a given radiant flux and wavelength, a given current is produced. This current flows through the load resistance  $R_L$ , developing the signal voltage  $e_s = i_a R_L$ . It is important to realize that the current is independent of the load resistance. Thus, for a given current, any desired signal voltage within reason may be obtained by

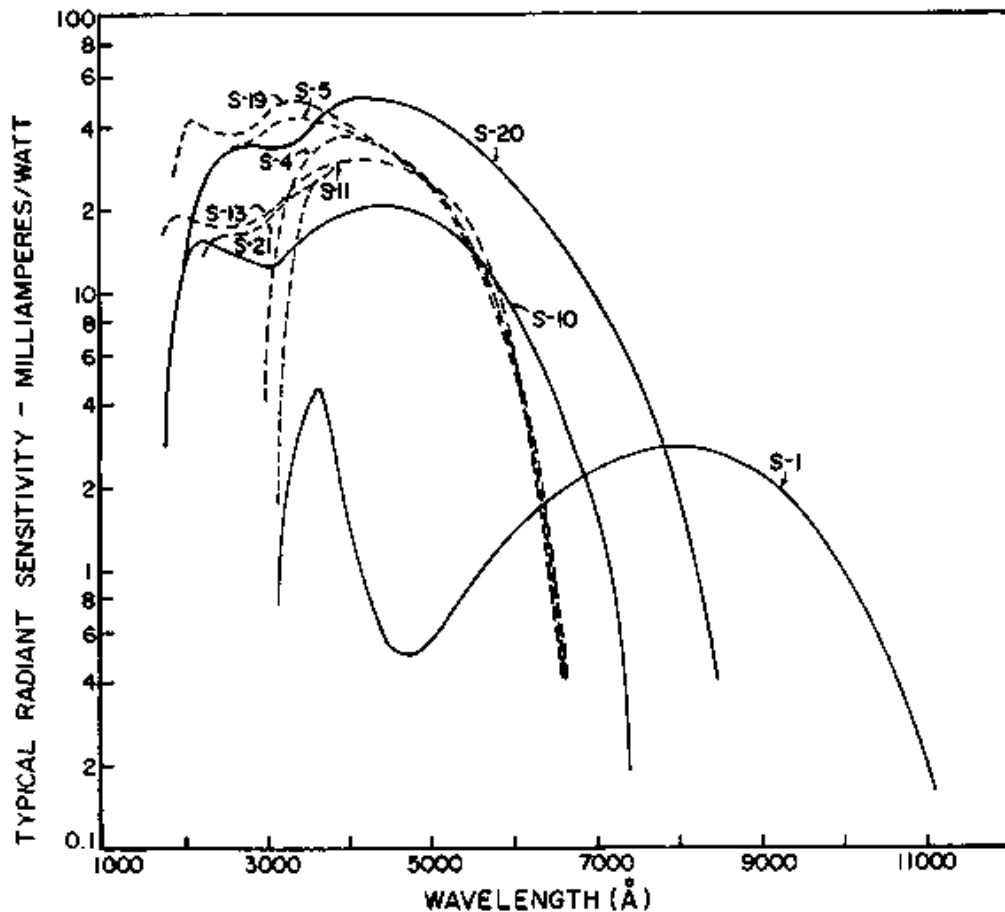


**Fig. III-A-9.** Typical spectral response curves for photoemissive surfaces taken from technical literature, Hamamatsu TV Co., Ltd., Hamamatsu, Japan. (With permission of Hamamatsu TV Co.)

selecting an appropriate load resistance. In general, a high value of  $R_L$  is desirable in order to reduce the required post detector electronic amplification. Two practical factors limit the magnitude of  $R_L$ : (a) the leakage resistance of the tube and associated circuit, which shunts the load resistance, and (b) the time constant  $R_L C_S$ , formed by the load resistance in parallel with stray capacitance  $C_S$  in the tube and wiring; this time constant degrades the effective response time of the detector. Values of  $R_L$  up to  $10^{10}$  ohms are commonly used. If long detector leads are used,  $C_S$  may be 100 pF\* or more, resulting in a time constant of up to 1 sec or more. Such a time constant would seriously degrade the accuracy of determination of the luminescence decay times (lifetimes) less than about 10 sec. Shorter leads, lower  $R_L$ , or combination of these would reduce the effect. In very high speed work, a miniature preamplifier is sometimes built right into the phototube base to minimize stray capacity.

All practical photoemissive detectors have a finite current output when no light is incident upon the cathode. This current, called the dark current  $i_d$  may interfere with the measurement of very low light intensities. The dark current may be the result of the following causes: (a) thermionic emission from the cathode or other internal parts of the device, (b) leakage currents over the envelope material or through tube base, socket, or circuit insulation, (c) positive ion current, and (d) field emission. The thermionic emission current  $i_{th}$  increases as  $\Phi_a$  decreases (i.e., as  $\lambda_{th}$  increases). For this reason, near-infrared-sensitive (S-1) phototubes, which have long threshold wavelengths, tend to have higher thermionic emission currents than other tubes. In general, the phototube with the lowest acceptable  $\lambda_{th}$  should be used, to minimize thermionic emission. The temperature of the cathode has a great effect on the thermionic emission. In fact, the most generally satisfactory method of reducing thermionic emission in a given phototube is to cool the tube.

Another way to reduce thermionic emission current is to reduce the area of the cathode. However, provision must be made to focus all the light to be measured onto the small cathode; otherwise the signal current will be reduced proportionately. Some commercial phototubes are fitted with very small cathodes to help reduce the thermionic emission current.

The leakage current over the surface of the phototube envelope may often be reduced by carefully cleaning and drying the surface to remove conducting contaminants. Low-leakage base and socket materials should be used. Phototubes are often mounted in air-tight enclosures containing a desiccant to reduce moisture on the insulating surfaces. One excellent method of eliminating the effect of leakage currents in the output is to apply a circular band of

\* 1 picofarad (pF) =  $10^{-12}$  farad.

electrically conductive paint (called a *guard ring*) surrounding but not touching the point at which the anode lead passes through the envelope. When this guard ring is connected to the circuit ground, any leakage currents will then flow between the cathode and guard ring without interfering with the anode current. Leakage from the guard ring to the anode can be neglected because the potential difference between them is usually very low.

Positive ion current is the result of the impact of positive ions onto the cathode surface. It is usually a small contribution to the total dark current. Positive ions are produced in the phototube by the ionization of residual gas molecules by collisions with thermionically emitted electrons from the cathode accelerated toward the anode, by the field gradient between the cathode and anode, and by background radiation. By reducing the supply voltage to reduce the field gradient or cooling the tube to reduce the thermionic emission, residual gas ionization and resulting positive ion current will be reduced.

Field emission is the emission of electrons from the cathode caused by the electric field gradient at the cathode. Like the positive ion current, it is generally a small contribution to the total dark current in properly operated tubes, and can be reduced by lowering the supply voltage.

The total dark current  $i_d$  is the sum of the above-mentioned contributions and may range from  $10^{-10}$  to  $10^{-6}$  A for various types of photoemissive detectors.

The ideal output current of a photodetector is a smooth DC current proportional to the incident light flux. In real detectors, however, an AC or noise component is superimposed on the DC signal. This noise limits the ability of the experimenter to make accurate measurements of low light levels or to determine small differences between similar light levels.

The primary source of noise in photoemissive detectors at room temperature is generally shot noise. Shot noise is due to the fundamentally discontinuous (quantized) nature of light energy and electrical current. Photons arrive at the cathode randomly even though the overall intensity of the light beam is constant.\* Thus photoelectrons are emitted from the cathode and arrive at the anode also randomly, and yet the long term rate of photoelectron pulses at the anode is constant and proportional to the light intensity. The same is true of thermionic electrons emitted from the cathode. Random, uncorrelated events like this are said to obey *Poisson statistics*, which has the fundamental property that the mean and the variance are identical; or in other words, the standard deviation is the square root of the mean. In terms

\* Photon shot noise is often called simply photon noise. Photon noise is ultimately the limiting noise when other noises are eliminated. In the discussion here, shot noise includes both dark current shot noise and photon shot noise.



of a photoemissive detector, this means that the standard deviation  $\sigma_N$  of the numbers of electrons arriving at the anode in each of a series of equal time intervals of time  $t$  is given by

$$\sigma_N = \sqrt{N} = \sqrt{nt} \quad (\text{III-A-36})$$

where  $N$  is the mean number of electrons arriving at the anode per time interval  $t$  and  $n$  is the average rate of arrival. Because each electron carries a charge of  $e$  coulombs, the average anode current  $i_a$  is  $ne$ , and the standard deviation of the averages of the currents flowing during each time interval  $t$  is\*

$$\sigma_i = \sqrt{ei_a/t} \quad (\text{III-A-37})$$

This  $\sigma_i$  is called the *rms shot noise current* and henceforth has the symbol  $\overline{\Delta i_s}$ . If the average current  $i_a$  is measured with a current meter which has an electrical noise bandwidth of  $\Delta f$ , in Hz, then the time interval  $t$  in the foregoing equation may be replaced by the effective averaging time of the current meter, which is

$$t = \frac{1}{2\Delta f} \quad (\text{III-A-38})$$

Thus

$$\overline{\Delta i_s} \equiv \sigma_i = \sqrt{2ei_a \Delta f} \quad (\text{III-A-39})$$

The average current  $i_a$  is the sum of the total photocurrent  $i_p$  and the thermionic current emission  $i_{th}$

$$i_a = i_p + i_{th} \quad (\text{III-A-40})$$

Leakage currents are not included in the shot noise because they do not flow internally through the tube.

The most seriously detrimental effect of thermionic emission is not so much its contribution to the average anode current, which can be eliminated electrically, but rather its contribution to the total shot noise, particularly at low light levels where  $i_p \leq i_{th}$ .

Another possible source of noise in the output signal from a photodetector is Johnson noise in the load resistor. Johnson noise is a randomly varying potential occurring across any finite resistance. It is caused by the thermal agitation of electrons in the resistor material. It is not a function of the

\* The reasoning is as follows: if  $\sigma_N$  is the standard deviation of the number of electrons, then  $e\sigma_N$  is the standard deviation of their charge and  $e\sigma_N/t$  is  $\sigma_i$ , the standard deviation of the average current in the time interval  $t$ . Combining this with equation III-A-36 and writing  $i_a$  for  $ne$  gives equation III-A-37.

current flowing through the resistance; thus Johnson noise in a phototube load resistance is constant at all signal levels. The rms Johnson noise current  $\overline{\Delta i_j}$  and voltage  $\overline{\Delta e_j}$  are given by

$$\overline{\Delta i_j} = \left( \frac{4kT \Delta f}{R_L} \right)^{1/2} \text{ A} \quad (\text{III-A-41})$$

$$\overline{\Delta e_j} = (4kT \Delta f R_L)^{1/2} \text{ V} \quad (\text{III-A-42})$$

where  $k$  is the Boltzmann constant,  $T$  is the temperature of the load resistance ( $^{\circ}\text{K}$ ),  $\Delta f$  is the electrical noise bandwidth of the circuit (Hz), and  $R_L$  is the load resistance (ohms). For instance, if  $R_L = 10^8$  ohms,  $T = 300^{\circ}\text{K}$ , and  $\Delta f = 1$  Hz,  $\overline{\Delta e_j} = 10^{-8}$  volt.

Since shot and Johnson noises are random and uncorrelated, they add quadratically. Thus the total rms noise current  $\overline{\Delta i_p}$ , due to shot and Johnson noise is

$$\overline{\Delta i_p} = (\overline{\Delta i_s}^2 + \overline{\Delta i_j}^2)^{1/2} = \left[ \frac{2e \Delta f}{R_L} \left( i R_L + \frac{2kT}{e} \right) \right]^{1/2} \quad (\text{III-A-43})$$

Because  $2kT/e$  equals about 0.05 volt at room temperature, Johnson noise is negligible as long as  $R_L$  is chosen high enough to make the signal voltage  $iR_L$  large compared to 0.05 volt.

#### b. CHARACTERISTICS OF SINGLE-STAGE PHOTOTUBES

Single-stage phototubes are not often used in luminescence instrumentation because of their low radiant sensitivities  $\gamma$  ( $10^{-3}$ – $10^{-1}$  A watt $^{-1}$ ). They are, however, quite stable, have a wide linear dynamic range, and have very fast response times (typically  $10^{-9}$  sec).

#### c. CHARACTERISTICS OF MULTIPLIER PHOTOTUBES

The most widely used photodetectors in luminescence spectrometry are the multiplier phototubes (called photomultiplier tubes by manufacturers), mainly because of their extremely high sensitivities.

A schematic diagram of a multiplier phototube and its circuitry is provided in Figure III-A-10. An evacuated tube of quartz or glass contains an anode  $A$ , a photocathode  $C$ , and a series of dynodes  $D_i$ . The resistor chain divides up the operating voltage  $V$  so that a potential difference of about 100 volts exists between adjacent electrodes. Photoelectrons emitted by the cathode are accelerated toward  $D_1$  by the potential across  $R_1$ . The kinetic energy gained in this acceleration is several times the binding energy of the electrons

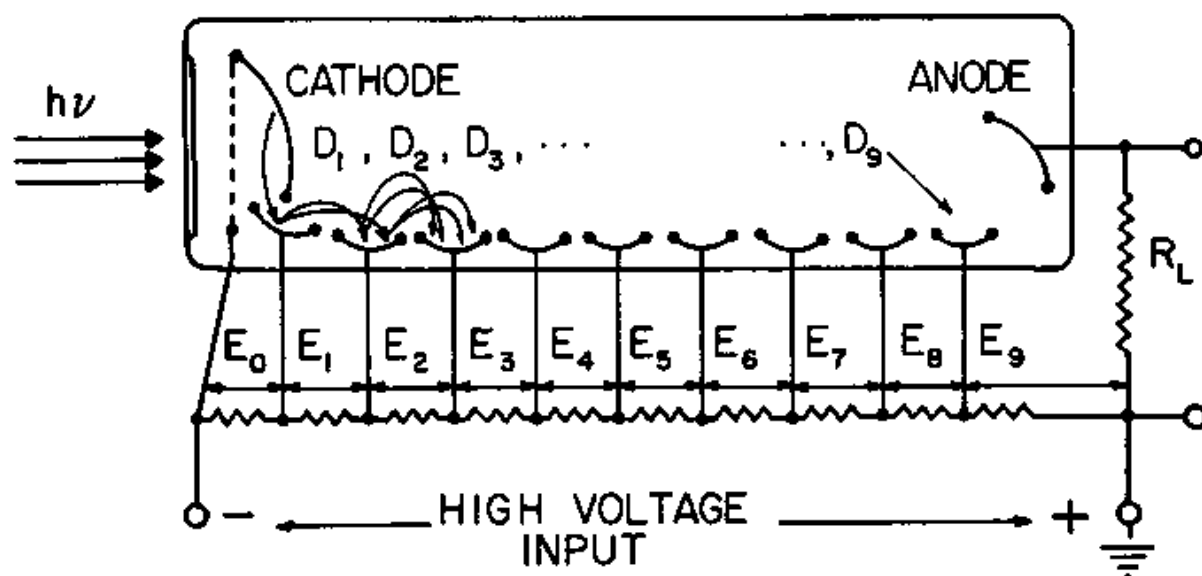


**Fig. III-A-10.** Schematic diagram of a multiplier phototube and its associated circuitry:  $D$ , dynodes;  $E$ , voltages applied to dynodes, and  $R_L$ , phototube load resistor.

on the surface of the dynodes. Each electron incident upon  $D_1$  causes the emission of several secondary electrons, which are subsequently accelerated toward  $D_2$  by the voltage across  $R_2$ . The same process is repeated for all the remaining electrodes. The resulting stream of electrons are collected by the anode. The anode current  $i_a$  flows through the load resistor  $R_L$ , generating the signal voltage  $i_a R_L$ , which is negative with respect to ground.

The *gain per stage*  $g$  is defined as the number of secondary electrons emitted by each dynode per incident electron and is typically 3 to 5. If  $z$  is the total number of dynode stages, the *total amplification* factor  $M$  is

$$M = g^z \quad (\text{III-A-44})$$

For example, a typical commercial multiplier phototube with 10 dynode stages and a gain per stage of 4 would have a total amplification of  $4^{10} = 10^6$ . Thus the anode current  $i_a$  would be  $10^6$  times the cathode current  $i_c$ . Such a phototube would have a sensitivity about  $10^6$  times that of a single-stage phototube with the same cathode type and envelope material. A similar tube with 13 stages would have a total amplification of  $10^8$ .

The gain per stage and amplification of a multiplier phototube depends very much on the operating voltage. Most commercial tubes with cesium-antimony dynode surfaces are operated at voltages from 80 to 120 volts per stage. It has been found experimentally that, in this range, the gain per stage is approximately proportional to the 0.7 power of the voltage.<sup>19</sup> The amplification of a 10-stage tube would then be proportional to the seventh

power of the voltage. Because of this very sensitive dependence of the amplification on the operating voltage, multiplier phototubes require a very stable high voltage power supply with a total drift and ripple at least  $\frac{1}{4}$  the maximum tolerable gain variation. A plot of the amplification of a typical 10-stage multiplier phototube versus the supply voltage  $V$  is shown in Figure III-A-11. The slope of the line on the logarithmic coordinate graph is about 7. The ability to change the sensitivity over such a wide range simply by changing the supply voltage is a significant and unique advantage of multiplier phototubes.

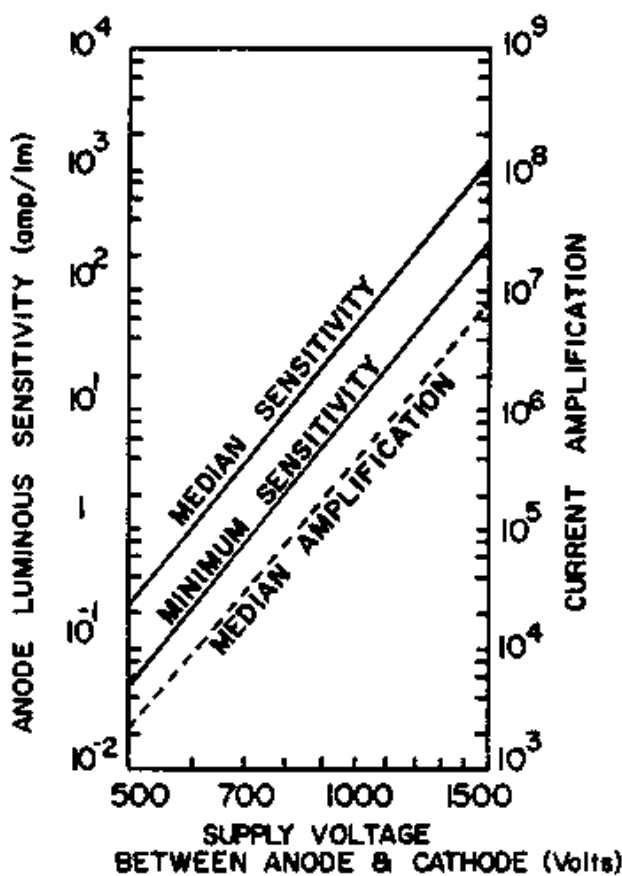


**Figure III-A-11.** Variation of amplification of a typical 10-stage multiplier phototube (photomultiplier). Curves taken from technical literature for a Hamamatsu R376 photomultiplier tube, Hamamatsu TV Co., Ltd., Hamamatsu, Japan. (With permission of Hamamatsu TV Co.)

The anode sensitivities  $\gamma_a$  of multiplier phototubes (i.e., sensitivities expressed in terms of the anode current) are much higher than those of single-stage tubes and vary over a wide range of values. Radiant sensitivities generally fall between 400 and 80,000 A watt<sup>-1</sup> at the wavelength of maximum response.

The spectral response of a multiplier phototube depends on the cathode type and envelope material and is not influenced by the multiplication process. Thus the response characteristics are similar to those of single-stage tubes and are catalogued by the same S number system.

At room temperature, the primary source of dark current in multiplier phototubes is almost always thermionic emission. Thermionic emission current from the cathode is amplified by the dynode secondary emission process in the same way as is the photoelectron current. (Any small differences between the average kinetic energies of thermal electrons and photoelectrons is easily swamped out by the large cathode-to-first-dynode potential). In addition, each of the dynodes exhibits some thermionic emission. Only the emission from the first few dynodes is significant, however, because that from latter dynodes is not sufficiently amplified. Leakage current, which is not amplified at all by the dynode multipliers, is much less important in multiplier phototubes than in single-stage tubes. Although the leakage current is directly proportional to the applied voltage, the thermionic emission current at the anode, like the photocurrent, is proportional to a high power of the voltage. At voltages below about 80 volts per stage, the gain may be so low that leakage current becomes significant. At 100 volts per stage, the operating voltage of most commercial photomultipliers, the thermionic emission current is always dominant, at least at room temperature. Above about 130 volts per stage, positive ion current and field emission may become significant. In addition, internal breakdown may occur at excessively high voltages, destroying the tube. It is therefore important never to operate a phototube above the manufacturer's recommended maximum voltage.

At room temperature the noise in multiplier phototubes is essentially all shot noise. Johnson noise in the load resistor is not amplified by the electron multiplier and hence is insignificant compared to the amplified shot noise. The equation for the shot noise  $\overline{\Delta i_s}$ , due to the total anodic current  $i_a$  (photocurrent plus thermionic current) must take into consideration the gain of the tube  $M$  as well as the shot noise contributed by the dynodes. This can be done by calculating the noise due to each electrode separately and then quadratically adding them to determine the total noise. The result is that the anodic shot noise  $\overline{\Delta i_s}$  is

$$\overline{\Delta i_s} = \sqrt{2eBM\Delta f i_a} \quad (\text{III-A-45})$$

where  $B$  is the symbol for

$$B = 1 + g^{-1} + g^{-2} + \cdots + g^{-z} = \sum_{\nu=0}^z g^{-\nu} \quad (\text{III-A-46})$$

and where the other symbols have been defined previously. In general,  $B$  is slightly greater than one. For instance, if  $g$  is 4, then  $B$  is about 1.3. By comparison with equation III-A-39, it is seen that  $B$  may be considered a "correction factor," which is multiplied by the amplified cathode noise to account for the small amount of extra noise (15% or so) introduced by the dynode multiplication process.

As mentioned before, the thermionic component of dark current and dark

current shot noise can be reduced greatly by cooling the tube. As a rule of thumb, each  $10^{\circ}\text{K}$  decrease in temperature halves the thermionic emission current. Liquid nitrogen and dry ice are commonly used coolants. In addition, thermoelectric cooling chambers are available which allow temperature adjustment. In many cases, it is possible to reduce the dark current by one or two orders of magnitude by cooling. Cooling may not, however, reduce the various other sources of noise significantly, so that these may become dominant at low temperatures. For each type of multiplier phototube, there is a minimum temperature below which it is not profitable to cool the tube. This occurs at about  $253^{\circ}\text{K}$  ( $-20^{\circ}\text{C}$ ) for most tubes with cesium-antimony cathodes. An additional noise source, which is important in some high grade multiplier phototubes operated at low temperatures, is cosmic ray scintillation noise.<sup>21</sup> This is the result of the passage of highly energetic cosmic particles (e.g.,  $\mu$  mesons) through the window of the tube, inducing Cherenkov radiation which may reach the cathode. Even though the average count rate of cosmic particles is low (ca.  $1$  or  $2 \text{ min}^{-1} \text{ cm}^{-2}$ ), each particle may produce hundreds of scintillation photons, resulting in a very large noise pulse at the anode. The effect is particularly evident in end-on tubes, because the cathode is so close to the window and because the window itself is relatively thick. Background radiation, as well as radiation from radioactive isotopes in the window material, may contribute to this source of noise.

The dynode voltages are usually obtained from a resistive voltage divider connected across a high voltage supply (as in Figure III-A-10). It is essential to observe polarity when connecting the phototube to the power supply; the *cathode must always be negative*. The current through the dynode resistor chain should be at least ten times the anode current so that the dynode potentials will not be reduced appreciably by the anode current. If the dynode chain current is excessively high, however, the heat dissipated by the resistors may warm the phototube, increasing the thermionic emission. For most applications, a dynode chain current of a few milliamperes is sufficient.

The most important interelectrode potential in a multiplier phototube is the cathode-to-first-dynode voltage, which should always be maintained at the value recommended by the manufacturer of the tube. This can be done by using a constant voltage (Zener) diode of the proper voltage in place of the cathode-to-first-dynode divider resistor. In this way, the voltage will remain constant even if the overall supply voltage or dynode chain current changes. The use of the recommended voltage ensures good collection efficiency and reduces the effect of stray magnetic fields.

Exposure of multiplier phototubes to high light levels may cause changes in the sensitivity of the tube (*fatigue*). Neither the cathode nor the anode currents should exceed their maximum ratings as specified by the manufacturer. A limitation on the cathode current density is set by the cathode resistivity. Photocurrent flowing through the cathode layer results in an electric

field across the cathode which opposes the cathode-to-first-dynode field, lowering the collection efficiency and gain of the first stage. This can result in a large change in the total gain of the tube. The customary cesium-antimony cathode material has a relatively high resistivity; the current density in a cathode of this material should not exceed about  $2 \times 10^{-8}$  A  $\text{cm}^{-2}$ . In a multiplier tube with an  $M$  of  $10^6$  and a cathode area of  $1.0 \text{ cm}^2$ , this would correspond to an anode current of 20 mA. In this connection, the effect of phototube refrigeration should be considered. Most cathode materials are semiconductors and, as such, exhibit higher resistivity at low temperatures. Thus cooling a tube will reduce its maximum cathode current tolerance. This effect influences the selection of an optimum operating temperature.

Anode current limitations are set by the maximum tolerable anode power dissipation, heating of the dynodes, and space charge effects (fatigue). The maximum anode power dissipation is usually quoted by the manufacturer and generally falls between 0.1 and 1 watt. Maximum recommended long-term anode currents generally fall between 0.1 and 1 mA. For best stability, the anode current should not exceed one-hundredth of the maximum rating. A fatigued phototube may often be rejuvenated if operated in the dark for some time at the normal operating voltage. Multiplier phototubes must never be exposed to room light, for irreversible damage may result.

The response time of a multiplier phototube is usually less than  $10^{-8}$  sec, sufficiently fast to allow the measurement of all but the fastest luminescence decay times.

## 5. AMPLIFIER-READOUT\* SYSTEMS<sup>22-24</sup>

The function of the amplifier-readout system in spectrophotometric instrumentation is to amplify and process the small electrical signal from the photodetector and display it in a convenient and readable form. In luminescence spectrometry, the information to be displayed is most commonly luminescence signal due to luminescence radiance as a function of analyte concentration (quantitative analysis), wavelength (spectra), or time (luminescence decay times).

The amplifier-readout system normally determines the electrical noise bandwidth  $\Delta f$  of the entire system, which in turn influences the amount of random noise on the readout signal and determines the response time of the system.

\* The reader is referred to Appendix 5 for a more detailed discussion on electronic signal processing.

## a. DC AMPLIFIER SYSTEMS

The simplest and least expensive type of amplifier, and the one most commonly found on commercial luminescence spectrometers, is the DC amplifier.<sup>25,26</sup> The output signal of this type of amplifier (the *readout signal*) is an amplified and filtered version of the DC component of the photodetector signal. The DC amplifier is called a *low-pass* system; it passes and amplifies DC signals and all AC frequency components in the photodetector signal output below a certain frequency (approximately equal to the bandwidth  $\Delta f$  of the system) while attenuating all frequency components above  $\Delta f$ . When the light level seen by the photodetector is constant (i.e., not chopped), the signal of interest appears at zero frequency (DC) and is passed by the DC amplifier. Noise (e.g., shot noise) appears at nonzero frequencies (AC) and some of it (the portion above  $\Delta f$ ) is attenuated. Thus the lower  $\Delta f$ , the lower the noise on the readout signal. The electrical noise bandwidth  $\Delta f_a$  of the amplifier is determined by the amplifier time constant  $\tau_a$ , which is determined by an RC filter somewhere in the circuit of the DC amplifier.

$$\Delta f_a = \frac{1}{4\tau_a} = \frac{1}{4RC} \quad (\text{III-A-47})$$

Direct-current amplifiers are simple, relatively inexpensive, and easy to understand and operate. The biggest single disadvantage is that they pass and amplify *undesirable* DC signals as well as the desired photocurrent signal. *Undesirable DC signals include phototube dark current, stray light that falls on the detector even in the absence of sample luminescence, and offset (bias) current or voltage in the amplifier itself.* These signals may be balanced out electrically by adding an artificial DC signal equal in magnitude but opposite in polarity to the total undesirable DC signal, thereby canceling it out. However, drift in the dark current, stray light, or amplifier offset will cause errors in the output signal until the circuit is rebalanced. Furthermore, since the random AC noise components of these signals (e.g., thermionic emission shot noise) cannot be balanced out, they remain in the signal.

When using current-source photodetectors such as multiplier phototubes, it is usual to pass the detector anode current  $i_a$  through a load resistor  $R_L$  to generate a voltage signal  $i_a R_L$  to be amplified by a voltage amplifier. The input impedance of the amplifier must be much larger than  $R_L$  in order to avoid a gain error. Electrometer amplifiers are commonly used. As mentioned previously, the effect of the input time constant  $R_L C_S$  must also be considered,  $C_S$  being the shunt capacity from the signal lead to ground due to cable capacity, amplifier input capacity, and so on. An alternate approach is to feed the detector anodic current directly to the summing point (negative input)



whose operation is dictated by the *polarity* of the signal (*polarity-sensitive*), is controlled by the *frequency* and *phase* of the signal (*phase-sensitive*). The simplest type is a full-wave inverter (rectifier) whose inversion depends on a *reference signal*, a *noise-free signal* whose frequency and phase are synchronized with the sample signal modulation. This is easily obtained from a small lamp and photocell placed so that the chopper disk passes between them. Because noise is random and not frequency or phase synchronized with the signal modulation, the noise offset is completely eliminated, even with a wide band preamplifier stage. Such systems are relatively expensive, complex, and difficult to operate, however. The system bandwidth is determined by the filter stage.

#### d. PHOTON COUNTING\* SYSTEMS<sup>28-30</sup>

Photon counting, a relatively new method for the measurement of low light intensities, is being used with increasing frequency in analytical spectrometry, particularly for Raman spectroscopy. Its use in luminescence spectrometry has thus far been limited to research applications.

In photon counting, a high speed electronic counter is used to count the photoelectron pulses at the anode of a multiplier phototube. Each photoelectron pulse contains, on the average,  $M$  electrons, for a total charge of  $eM$  coulomb. If  $M$  is of the order of  $10^6$ , then the resulting charge is of sufficient magnitude to cause a distinct and easily observable voltage (and current) pulse across the phototube load resistor  $R_L$ . One such pulse occurs for each photoelectron ejected at the cathode, and hence the average pulse count rate  $\bar{n}$  is proportional to the light level (under the condition that the cathode sensitivity is constant—which is a good assumption under normal conditions). Such photoelectron pulses are often of the order of several millivolts and are easily amplified by a wide band AC amplifier and counted by electronic counter circuits. This automatically provides a convenient, accurate, and easily read digital output. The technique is called *single-photoelectron counting*, or simply *photon counting* (even though not every photon is counted, of course).

The advantage of the photon counting system include the following:

1. A digital system is less subject to drift than an analog system.
2. Long counting times may be used at low light levels to accumulate the required number of total counts.
3. Many types of noise are discriminated against, particularly thermionic emission from the dynodes and leakage current.
4. The digital readout is easy to read and can be interfaced directly to computers.

\* The basic principles of photon counting are given in Appendix 6.

Disadvantages include greater cost and complexity. In recording spectra and luminescence decay times, the counter can be replaced by a rate meter with analog output for connection to a recorder. In fact, the counter may not be necessary at all if chart readout is satisfactory.

Fast amplifiers, discriminators, rate meters, and counters designed for nuclear counting are commercially available in convenient modular form. These are easily adapted for photon counting. In addition, there are several commercial photon counting systems. The method of photon counting is further discussed in Appendix 6.

#### e. STROBOSCOPIC SYSTEMS<sup>31</sup>

Many luminescence studies involve the use of pulsed sources to study fast fluorescence or phosphorescence decay times. The measurement of low intensity, short duration light flashes poses a particular problem in photo-detection. The simplest technique would be to amplify the signal from the phototube with a wide band amplifier and display the output on an oscilloscope. But the experimenter is faced with a dilemma. In order to preserve the waveform of a fast pulse, the bandwidth of the system must be high. For example, a 1- $\mu$ sec rectangular pulse would require at least a 3-MHz bandwidth. However, the large bandwidth usually reduces the signal-to-noise ratio, preventing accurate measurements of low intensity light pulses.

This problem can be solved very effectively by employing a photomultiplier in the pulsed mode. Because the tube is sensitive to light only when the proper dynode voltages are applied, it can be gated on and off as desired by applying a rectangular high voltage pulse to the dynode chain. This gate pulse, which defines the "on" time of the phototube, is made much shorter than the duration of the light pulse to be studied. By means of suitable delay circuits, the gate pulse can be made to occur at any desired time during the light flash to be studied. If the light flash and phototube gate pulse are repeated periodically at a rate of a few pulses per second or greater, the average DC component of the train of photocurrent pulses can be measured with an average-reading DC meter. The bandwidth of the meter circuit can be made as small as desired to reduce the noise to a satisfactory level. The time variation (waveform) of the light flash is easily determined by measuring the average DC signal in this way for different delay settings (i.e., with the gate pulse occurring at different times during the flash). The measured signals are then plotted against the corresponding delay times to reconstruct the pulse waveform. A more convenient procedure is to sweep the gate pulse slowly through the light flash while recording the measured intensity as a function of time on a pen recorder. This eliminates hand plotting of data. If desired, the time variation of the spectrum of the light flash can be determined by scanning the monochromator at various fixed delay times.

The type of stroboscopic operation just described has still another advantage; the performance of the multiplier phototube may be considerably improved by the use of pulsed DC dynode voltages. Much higher gains can be achieved in the pulsed mode, since higher voltages are permissible. For example, a 1P21, whose maximum DC voltage rating is 1230 volts may be operated at pulsed voltages in excess of 1500 volts, increasing the gain approximately tenfold. The primary limitation on the DC voltage is the appearance of destructive positive ion regeneration. However, the positive ions, being ionized atoms of the residual fill gas, are relatively heavy and slow compared with electrons. Thus the positive ion current requires a certain amount of time, perhaps several microseconds, to build up. If the gate pulse width is less than a microsecond or so, the positive ion current simply does not have enough time to build up before the end of the gate pulse, even at pulse voltages much higher than that permissible for DC operation. This not only reduces the positive ion component of dark current and dark current noise but also permits the use of higher voltages, which yield higher gains. Thus the signal-to-noise ratio of the tube is considerably enhanced in the pulsed mode.

#### f. READOUT SYSTEMS

The function of the readout system is to display the signal from the amplifier system in a convenient and readable form. The most common types of readout in luminescence spectrometry are analog, such as meters, recorders, and oscilloscopes, although digital systems are showing considerable promise.

*Meters* are simple and inexpensive, but they provide no permanent record and are difficult to read if the signal is noisy. Accuracy is limited to about 1 to 2%. The best types have mirrored scales to eliminate parallax errors.

*Pen recorders* are much more expensive than meters, but they provide a permanent record and they permit noise measurements and the averaging of noisy signals. Servomechanism (potentiometric) types are the most accurate (0.1–0.5%) and sensitive (1–10 mV full scale), but they are expensive and relatively slow. Recorder bandwidth is typically 1 or 2 Hz, and the slew rate—the maximum rate of change of the pen position (usually in. sec<sup>-1</sup>)—is also limited. This is important in the measurement of luminescence decay times. Galvanometric (millimeter) recorders are generally faster and less expensive but also less accurate and sensitive than servo recorders.

Most pen recorders record voltage (or current) as a function of time, but *x-y* servo recorders permit the recording of two electrical variables against each other.

*Oscilloscopes* offer the widest readout bandwidth (up to 10<sup>8</sup> Hz). Such large bandwidths may be required for the study of very fast luminescence decay

times. Accuracy is typically 1%. An oscilloscope camera can provide a permanent record if required. Storage oscilloscopes are also available.

*Digital readouts* usually involve the electronic conversion of the analog readout signal to digital form by means of a digital voltmeter. Photon counting systems provide a digital readout naturally. Digital displays are easy to read and very accurate (0.1–0.01%) but are more expensive than a simple meter. Printing of tapes or pages and interfacing to a computer is also possible.

#### g. SPECIAL SPECTROSCOPIC TECHNIQUES

Spectroscopic methods involving interferometry and Fourier spectrometry and correlation and multiplex spectrometry have not been utilized in analytical luminescence spectrometry. However, these methods should have considerable potential in future luminescence instrumentation, and so the reader is referred to Appendix 7 for a brief discussion of the principles and uses of these novel techniques.

### 6. GLOSSARY OF SYMBOLS

$a$	Linear aperture of monochromator, cm.
$A_l$	Lens area, cm <sup>2</sup> .
$b$	Thickness of prism base, cm.
$B_{B\lambda}$	Spectral radiance of black body, watt cm <sup>-2</sup> sr <sup>-1</sup> nm <sup>-1</sup> .
$B_{CA_0}^0$	Spectral radiance of continuum light source, watt cm <sup>-2</sup> sr <sup>-1</sup> nm <sup>-1</sup> .
$B_N^0$	Radiance of line light source, watt cm <sup>-2</sup> st <sup>-1</sup> .
$c$	Speed of light, cm sec <sup>-1</sup> .
$C$	Capacitance, farad.
$C_S$	Stray capacitance, farad.
$D$	Angular dispersion, angular degrees nm <sup>-1</sup> .
$D_c$	Collimator diameter, cm.
$e$	Charge on electron, coulomb.
$e_s$	Signal voltage, volt.
$f$	$f$ number of optical component, no units.
$F$	Frequency of measurement system, Hz.
$F_c$	Focal length of collimator lens, m.
$g$	Gain per stage of multiplier phototube, no units.
$H$	Monochromator slit height, cm.
$i$	Average power supply current, A.
$i_a$	Average anodic current of photoemissive detector, A.
$i_c$	Average cathode current of photoemissive detector, A.
$i_d$	Average dark current of photoemissive detector, A.
$i_p$	Average photoanodic current, A.

$i_{tb}$	Average thermionic emission anodic current of photoemissive detector, A.
$J$	Stored energy in condenser of flash tube current, joule.
$k$	Boltzmann constant, $8.0 \times 10^{-5}$ eV $^{\circ}\text{K}^{-1}$ .
$K_o$	Optics factor, $HT, \Omega$ , cm sr.
$m$	Grating diffraction order, no units.
$M$	Multiplier phototube multiplication factor, no units.
$n$	Refractive index, no units.
$n$	Rate of electron arrival at surface, $\text{sec}^{-1}$ .
$\bar{n}$	Average counting rate, $\text{sec}^{-1}$ .
$P_i$	Peak input power of flashtube, watt.
$\bar{P}_i$	Average input power of flashtube, watt.
$P_o$	Peak output power of flashtube, watt.
$r$	Radius of sphere for calculation of unit solid angle, cm.
$R$	Resistance of resistive device, ohm.
$R$	Resolving power, no units.
$R_d$	Reciprocal linear dispersion, $\text{nm cm}^{-1}$ .
$R_f$	Flashtube arc resistance, ohm.
$R_L$	Phototube load resistor, ohm.
$R_{\text{theor}}$	Theoretical resolving power.
$s$	Spectral bandpass, nm.
$s_a$	Aberration limited spectral bandpass, nm.
$s_{\text{min}}$	Minimum spectral bandpass corresponding to $W_{\text{min}}$ , nm.
$t$	Time interval, sec.
$T$	Temperature, $^{\circ}\text{K}$ .
$T_f$	Optical transmission factor, no units.
$V$	Power supply voltage, volt.
$W$	Monochromator slit width, cm.
$W_e$	Exit slit width, cm.
$W_{\text{min}}$	Minimum resolving power slit width, cm.
$W_s$	Entrance slit width, cm.
$x$	Linear distance at focal plane, cm.
$X$	Half width of diffraction pattern, cm.
$y$	Index for summations, no units.
$z$	Number of dynodes in multiplier phototubes, no units.
$\alpha$	Prism apex angle, angular degrees.
$\alpha_g$	Grating rotation angle, angular degrees.
$\beta$	Blaze angle of grating, angular degrees.
$\gamma_\lambda$	Phototube anodic sensitivity, A watt $^{-1}$ .
$\delta$	Number of grooves per centimeter for grating, $\text{cm}^{-1}$ .
$\Delta$	Grating constant, nm (or cm).
$\Delta f$	Electrical noise bandwidth, Hz.

$\overline{\Delta f_a}$	Amplifier noise bandwidth, Hz.
$\overline{\Delta i_a}$	Rms amplifier noise anodic current, A.
$\overline{\Delta i_j}$	Rms Johnson noise current, A.
$\overline{\Delta i_p}$	Rms phototube noise anodic current, A.
$\overline{\Delta i_s}$	Rms phototube shot noise anodic current, A.
$\Delta \lambda$	Base width of monochromator slit function, nm (or cm).
$\Delta \lambda_R$	Wavelength resolution, nm (or cm).
$\epsilon_\lambda$	Spectral emissivity of a black body, no units.
$\Phi$	Deviation angle (prism), angular degrees.
$\phi_a$	Work function of photoemissive surface, eV.
$\Theta_d$	Diffraction angle (grating), angular degrees.
$\Theta_i$	Incident angle on prism or grating surface, angular degrees.
$\Theta_m$	Angle between incident and diffracted rays on grating, angular degrees.
$\lambda$	Wavelength of radiation, nm (or cm).
$\lambda_{th}$	Threshold wavelength for photoemissive surface, nm (or cm).
$\nu$	Frequency of radiation, Hz.
$\pi$	3.1416 . . .
$\sigma_i$	Standard deviation of average current, appropriate units, a.
$\tau_a$	Amplifier time constant, sec.
$\Omega$	Solid angle of radiation collected by optical device, sr.

## 7. REFERENCES

1. D. W. Ellis, "Luminescence Instrumentation and Experimental Details," Chapter 2 in *Fluorescence and Phosphorescence Analysis*, D. M. Hercules, Ed., Wiley-Interscience, New York, 1966.
2. C. A. Parker, *Photoluminescence of Solutions*, Elsevier, Amsterdam, 1968.
3. L. R. Koller, *Ultraviolet Radiation*, 2nd ed., Wiley, New York, 1965.
4. L. A. Rosenthal, *Rev. Sci. Instr.*, **36**, 1329 (1965).
5. N. Z. Searle et al., *Appl. Opt.*, **3**, 923 (1964).
6. C. M. Doede and C. A. Walker, *Chem. Eng.*, **62**, 159 (1955).
7. W. A. Baum and L. Dunkelman, *J. Opt. Soc. Amer.*, **40**, 782 (1950).
8. Edgerton, Germeshausen, and Grier, Inc., *Xenon Flash Tube Handbook*, Boston, Mass.
9. D. E. Perlman, *Rev. Sci. Instr.*, **37**, 340 (1966).
10. R. A. Sawyer, *Practical Spectroscopy*, 3rd ed., Dover, New York, 1963.
11. E. J. Meehan, *Optical Methods of Analysis*, Wiley-Interscience, New York, 1964.
12. F. A. Jenkins and H. E. White, *Fundamentals of Optics*, McGraw-Hill, New York, 1957.
13. C. W. Sill, *Anal. Chem.*, **33**, 1584 (1961).
14. E. J. Bowen, *The Chemical Aspects of Light*, Clarendon Press, Oxford, 1946.
15. H. A. Strobel, *Chemical Instrumentation*, Addison-Wesley, Reading, Mass., 1960.

## C. MOLECULAR LUMINESCENCE INSTRUMENTATION<sup>1-3</sup>

### 1. SAMPLING DEVICES

The most common cell for condensed phase (solution) fluorimetry is similar to the 1-cm square cell that is standard for absorption spectrophotometry.<sup>2</sup> Usually all four faces of the cell are polished. Glass is suitable for excitation wavelength above 350 nm; quartz is used below 350 nm. Nonfluorescent synthetic silica is preferred to natural quartz in careful work. Larger cells are used for gas samples.

In fluorescence spectrometry, the design and geometry of the cell and cell holder greatly influence the amount of scattered excitation radiation seen by the detector, particularly if the wavelengths of excitation and emission are the same or very close. The excitation geometry is characterized by the angle between the axes of excitation and observation. (Section II-C-7 furnishes a consideration of the influence of angle between exciting and measuring beams and of the means of excitation in measurement, i.e., front surface versus right angle.) The common 90° angle is most suitable for dilute solutions or gaseous samples (fraction of radiation absorbed by analyte plus interferences is less than 5%) and is compatible with the square cell geometry. It is important that the detection system "see" only the fluorescing solution and not the cell walls through which the excitation light enters, but yet the entire sample should be illuminated and the entire luminescence emitted towards the detector should be measured. (See Section II-C-6 for an extensive theoretical treatment of the influence of incomplete illumination and/or incomplete measurement of the luminescence). For solid samples, or solutions that are very concentrated or turbid, the fluorescence may be viewed at an acute angle from the excitation axis. This is called the frontal or surface configuration.<sup>1,2</sup>

Sample cells for use in phosphorimetry and low temperature fluorescence studies are usually small (1-mm i.d.) tubes made of nonluminescent synthetic silica.<sup>3</sup> The tube is positioned in a silica Dewar flask filled with a liquid coolant (commonly liquid nitrogen). Right angle illumination is most common, although the frontal configuration is useful for solutions that form opaque "snows" at low temperature (cf, the rotating sample cell discussed later).

The small sample tubes are somewhat more difficult to fill, empty, and clean than fluorescence cells, but the smaller sample volume (typically 0.1 ml) means much lower absolute detection limits at a given concentration. The tubes can be emptied with a long, small diameter polyethylene tube connected to a water aspirator. They may be cleaned by successive rinses with

nitric acid, distilled water, and solvent or sample solution. Very dirty tubes can be stored under concentrated nitric acid to remove the last traces of organic matter.

Precision of measurements of low temperature luminescence of samples in small sample tubes is often limited by sample tube positioning errors. Hollifield and Winefordner<sup>4</sup> have described a sample tube spinning apparatus (see Figure III-C-1) that averages out optical inhomogeneities and minimizes the effect of variations in sampling position. They observed a ten-fold decrease in relative standard deviation when the spinning apparatus was used. A commercial nuclear magnetic resonance (NMR) sample tube spinner may also be used.<sup>5</sup>

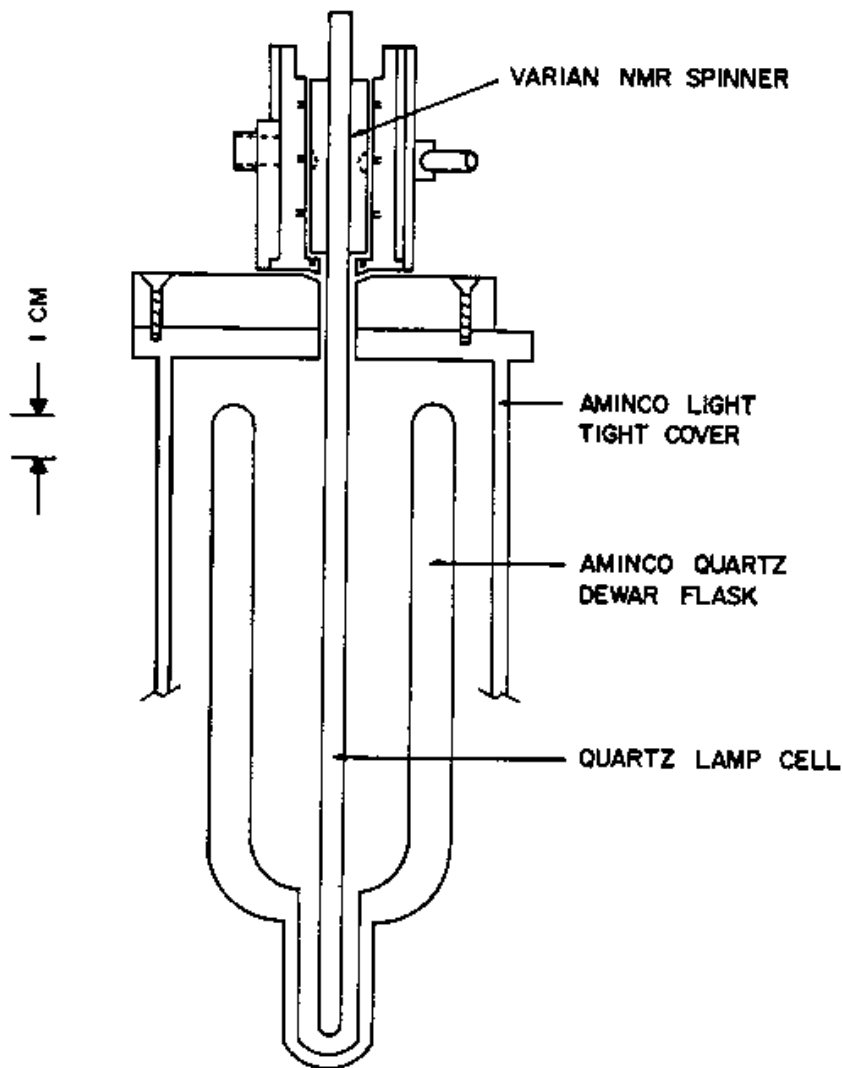


**Fig. III-C-1.** Representation of rotating sample cell immersion method of Refs. 4 and 5. (With permission of the authors.)



Parker<sup>2</sup> has described several elaborate specimen containers and compartments for variable temperature luminescence studies, including an apparatus for sample deaeration to reduce the quenching effect of oxygen and a frontal illumination system for low temperatures.

## 2. SAMPLE COOLING METHODS<sup>2,3</sup>

The simplest method of cooling a sample for low temperature studies is to immerse the sample tube directly into a transparent liquid coolant in a Dewar flask. A portion of the Dewar is left unsilvered to allow passage of the light. This system, illustrated in Figure III-C-2a, is the one most common in analytical applications. It has the advantage of rapid sample cooling and a stable, known sample temperature. However, there are several disadvantages:

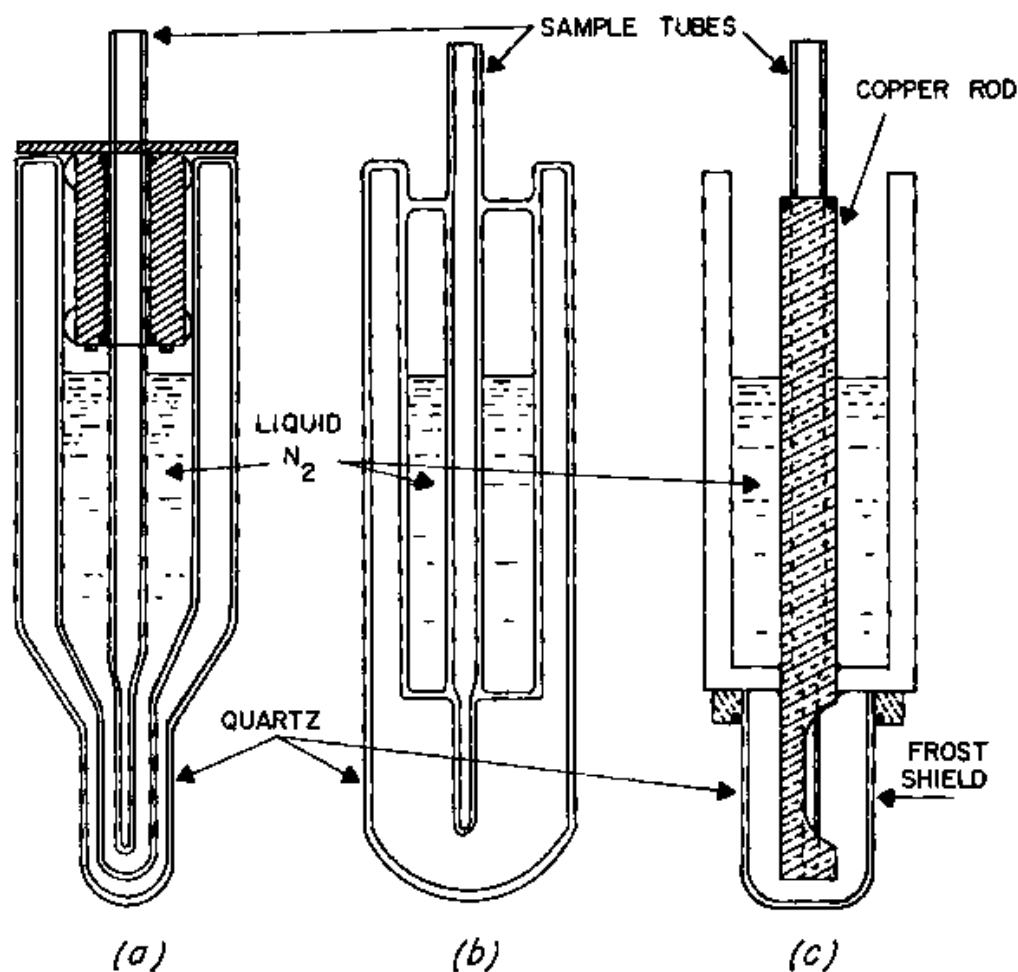


**Fig. III-C-2.** Types of cooling systems for low temperature luminescence spectrometry (predominantly phosphorimetry): (a) simple immersion method, (b) conduction cooling via quartz tube and sample, (c) conduction cooling via copper rod. (Drawings are reproductions of those found in Ref. 3—with permission of the authors.)

1. The excitation and emission light beams must each pass through three quartz layers. Even if the quartz is quite transparent, there are reflective losses at each of the twelve interfaces (typically 4% per interface), amounting to as much as 50% total light loss.

2. The coolant must be transparent and nonluminescent.

3. The convective motion and refractive index changes in the coolant cause flickering of both the incident and luminescence light beams; this effect may make a significant contribution to the total noise.

4. Occasional bubbling of the coolant may cause extremely unstable readings.

Other methods of sample cooling minimize these disadvantages by reducing the number of quartz layers through which the light beams must pass and by eliminating direct contact of the coolant with the end of the sample tube containing the sample. In Figure III-C-2*b* the sample tube is made an integral part of the Dewar flask. The reduction of reflective losses is only minor, but convection and bubbling noise are eliminated. The sample is cooled by conduction through the quartz sample tube walls and through the rigid solution itself. The disadvantages are the uncertainty and inhomogeneity in the sample temperature and the considerable inconvenience involved in changing samples. The system in Figure III-B-2*c* reduces thermal gradients by means of a highly conductive copper rod machined to fit the sample tube snugly. The frost shield reduces icing and fogging of the viewing area. However, the space inside the shield cannot be simply evacuated, and so condensation of air onto the sample tube and fogging of the shield itself by conductive cooling through the internal air space cannot be avoided. The copper rod conduction system has also been used for frontal illumination of solid samples.

Both conductive cooling systems can use solid-liquid coolants, but the immersion system is limited to boiling liquids. Liquid nitrogen, liquid air, and liquid nitrous oxide have been commonly used in phosphorimetry, although many other coolant systems could be used for other temperatures.<sup>3</sup> Minkoff<sup>6</sup> has given a helpful review of low temperature techniques.

### 3. MODULATION METHODS

The observation of long-lived ( $\bar{\tau} > 10^{-3}$  sec) luminescence without interference by prompt fluorescence and scattered light is most easily accomplished by the use of a mechanical phosphoroscope. The phosphoroscope is a rotating mechanical shutter that allows periodic out-of-phase excitation and observation of the sample. Two basic forms are in common use.

The rotating can phosphoroscope is shown in Figure III-C-3*a*. It consists of a hollow metal cylinder with two or more equally spaced apertures along

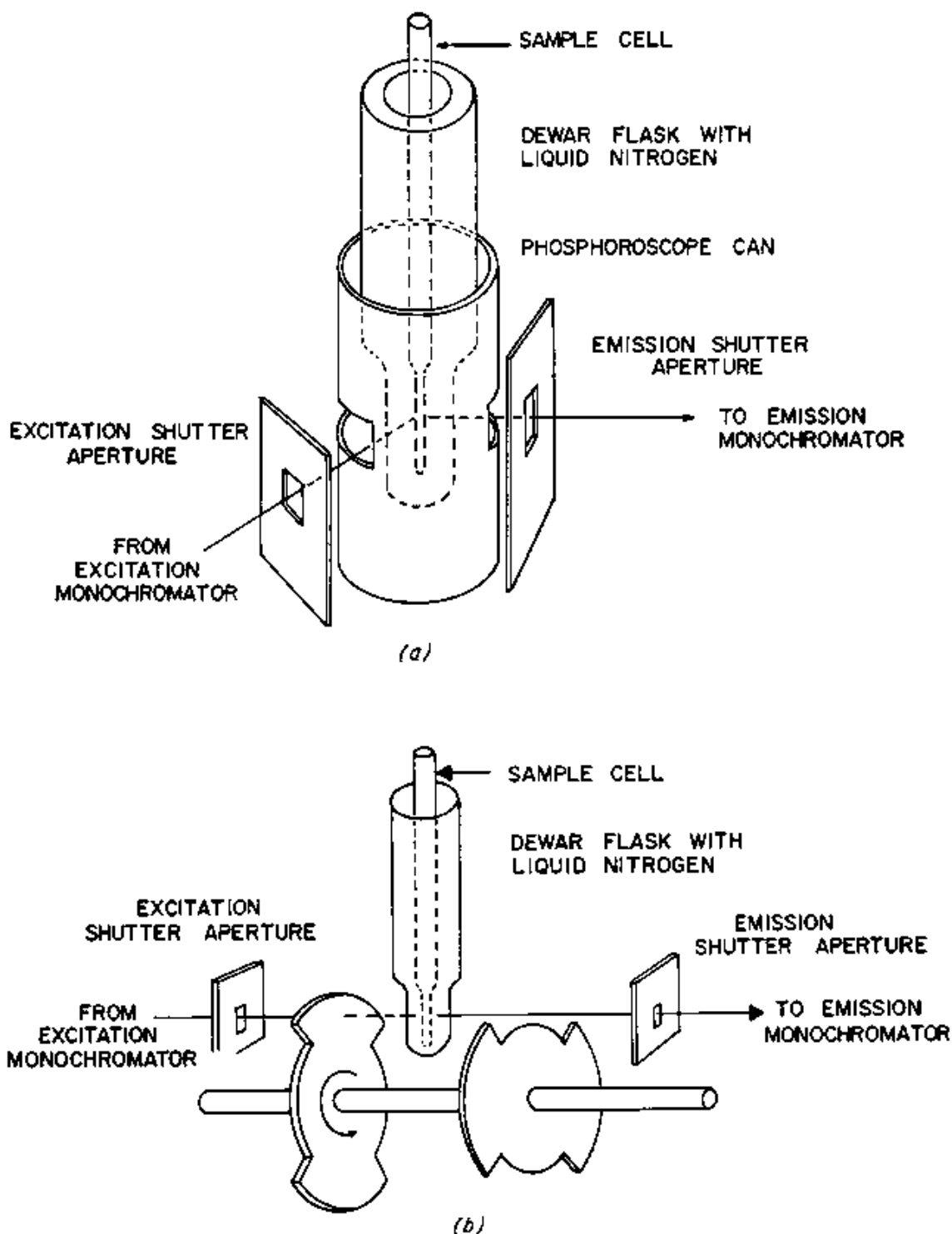


**Fig. III-C-3.** Schematic representation of phosphoroscope interaction with radiation: (a) rotating can device, (b) Becquerel-type device. (Drawings are reproductions of those found in Ref. 7—with permission of the authors.)

its circumference. The cylinder is rotated by a variable speed motor. The apertures allow the radiation from the excitation monochromator to strike the sample periodically and allow luminescence emission to reach the entrance slit of the emission monochromator between the excitation periods. The intensity of prompt fluorescence and scattered incident light decays very rapidly after termination of the excitation period, and so only long-lived luminescence (phosphorescence and delayed fluorescence) will remain when the phosphoroscope has turned from the point at which excitation is terminated to the point at which the observation period is initiated.

The Becquerel or rotating disk phosphoroscope (Figure III-B-3b) achieves the same effect with two sectorized disks mounted on a common motor-driven axle. This system is somewhat more versatile than the rotating can type because the phase relation between the two disks may be adjusted more easily.

Either type of phosphoroscopic system produces a train of approximately trapezoidal pulses of light. The resulting photocurrent pulses from the detector are usually measured with a DC readout system in commercial instruments. The response of the DC system is proportional to the average area under the current pulses. An AC or lock-in detection system could also be used, because the light is conveniently modulated by the phosphoroscope.

The operation<sup>7</sup> of both the can and disk phosphoroscopes is characterized by three time periods which are a function of the design and speed of the rotating components: the cycle time  $t_C$ , which is the period of one cycle of excitation and observation; the exposure time  $t_E$ , which is the time during which the sample is excited or observed (assumed equal); and the delay time  $t_D$ , which is the time between the end of the excitation period and the beginning of the observation period. The magnitudes of these time periods, relative to the lifetime  $\tau$  of the luminescent species, influences the measured radiant flux of luminescence. It is apparent that the presence of the phosphoroscope reduces the measured radiant flux because the sample is being excited (or observed) for only a fraction  $t_E/t_C$  of each measurement cycle. It can be shown<sup>7</sup> that the ratio  $\alpha$  of the average DC photocurrent observed using a phosphoroscope to that which would be observed without the phosphoroscope if prompt fluorescence and scattered light were not to interfere, is given by

$$\alpha = \frac{\tau(\exp - t_D/\tau)(1 - \exp (t_E/\tau))^2}{t_C[1 - \exp (-t_C/\tau)]} \quad (\text{III-B-1})$$

For long-lived luminescence ( $\tau \gg t_C$ ),  $\alpha$  is independent of  $\tau$  and of the speed of the phosphoroscope and is given by

$$\alpha = \left(\frac{t_E}{t_C}\right)^2 \quad (\text{III-B-2})$$

Because  $t_E$  must be less than one-half of  $t_C$ , this  $\alpha$  must be less than 0.25. For shorter decay times, or slower phosphoroscope speeds, where  $\tau < t_C$ ,  $\alpha$  begins to drop off. This occurs at about  $\tau = 10^{-3}$  sec for the Aminco phosphoroscope operating at maximum speed (7000 rpm).

It is usually desirable to operate the phosphoroscope fast enough so that  $\tau \gg t_C$ , because in that case undesirable changes in the phosphoroscope speed or changes in the sample luminescence lifetime (due to temperature variations, quenching by dissolved oxygen, etc.) will have little effect on the  $\alpha$  factor. On the other hand, some degree of resolution of a mixture of two spectrally similar compounds can be accomplished if their decay times are significantly different;  $t_C$  is made approximately equal to the larger decay time, therefore attenuating the response due to the shorter lived species. The degree of attenuation may be calculated using equation III-B-1.

Equation III-B-1 may be modified and generalized to apply to a stroboscopic system (see Section III-A-6-d) using a pulsed excitation source and a gated multiplier phototube.<sup>8-9</sup> If the half-intensity width  $t_F$  of the flash tube excitation source is much less than the lifetime  $\tau$  of the luminescent species then the corresponding  $\alpha$  value is

$$\alpha' = \frac{ft_F(\exp(-t_D/\tau)(1 - \exp(-t_P/\tau))}{1 - \exp(-1/f)} \quad (\text{III-B-3})$$

where  $\alpha'$  = ratio of average luminescence radiant flux observed per unit time to the hypothetical luminescence radiant flux per unit time produced by steady state luminescence.

$f$  = repetition frequency of light source and photomultiplier pulses  $\text{sec}^{-1}$ .

$t_D$  = delay time between end of excitation pulse and beginning of phototube pulse, sec.

$\tau$  = lifetime of luminescent species, sec.

$t_P$  = duration of phototube pulse, sec.

It may be shown that<sup>8</sup> the use of a pulsed system of this type would allow enhancement of the signal of one luminescent species with respect to other species of longer or shorter lifetime. The lifetime of maximum enhancement and the extent of relative enhancement is determined by the adjustable parameters  $t_D$ ,  $t_P$ , and  $f$ .

#### 4. COMMERCIAL INSTRUMENTS

Fluorescence spectrometers are manufactured by several firms. The Aminco-Bowman Spectrophotofluorometer (American Instrument Co., Silver Spring, Md.) contains two Czerny-Turner grating monochromators

Either may be scanned automatically for recording excitation and emission spectra. A high pressure xenon arc lamp is normally supplied as the excitation source. A 1P28 multiplier phototube and a DC amplifier system are used to detect the luminescence emission. Meter readout is supplied, although output connections for a recorder and oscilloscope are provided. Available accessories include adjustable slits, interchangeable gratings, photomultiplier cryostat, polarization accessory, multiple sample turret, and a phosphorescence attachment.

The Aminco SPF-125 is a smaller, simpler, less expensive spectrofluorometer intended primarily for quantitative clinical tests.

The Farrand Mark-1 Spectrofluorometer (Farrand Optical Co., Inc., Mount Vernon, N.Y.) is similar in principle to the Aminco-Bowman device. It also uses two grating monochromators. Electrically operated light shutters for decay time studies of phosphorescence are provided.

The Baird-Atomic Fluorispec (Baird-Atomic, Cambridge, Mass.) is unique in that it uses two double grating monochromators for high resolution and extremely low scattered light. A phosphoroscope attachment is available as an accessory.

None of the foregoing instruments gives "true" excitation or emission spectra corrected for variations in source radiance, monochromator transmission, and detector sensitivity with wavelength. Compensated or "corrected spectra" instruments include additional components to provide this correction. The Perkin-Elmer model 195 linear energy spectrofluorometer (Perkin-Elmer Corp., Norwalk, Conn.) uses two silica prism monochromators. A beam splitter samples a small portion of the light leaving the excitation monochromator and directs it onto a thermocouple detector\*. The thermocouple responds to the total energy striking it and is insensitive to the wavelength of the light (in contrast to the more sensitive photoemissive detectors). The thermocouple signal controls a slit servomechanism which keeps the energy emerging from the excitation monochromator constant. In this way, energy-corrected excitation spectra are obtained. Emission spectra are corrected by means of an adjustable electrical cam which controls a slit-servo in the emission monochromator.

The Turner Model 210 Absolute Spectrofluorometer (G. K. Turner Associates, Palo Alto, Calif.) records corrected excitation and emission spectra, as well as absorption spectra compensated for fluorescence errors. Excitation correction is accomplished by means of a time-shared bolometer detector, which compares the energy emerging from the excitation monochromator to that from a small reference lamp and adjusts the reference lamp to provide equal energy. The multiplier phototube is time-shared between a

\* Refer to Appendix 4.

beam from this reference lamp and the fluorescence radiant flux emerging from the emission monochromator. The ratio of the fluorescence signal to the reference signal is recorded. Emission correction is provided by a cam driven wedge attenuator in the reference beam. The cam is operated from the emission monochromator wavelength drive and is shaped to compensate for the spectral response of the multiplier phototube and emission monochromator.

The Aminco energy-corrected luminescence spectrometer uses a reference thermopile to obtain a wavelength-independent measure of the excitation intensity passing through the sample. Excitation spectra are corrected by dividing the uncorrected phototube signal by the thermopile signal. Emission spectra are corrected by means of an adjustable cam, linked to the emission monochromator wavelength drive, which drives a plunger on a potentiometer wired into an operational amplifier circuit.

Phosphoroscope attachments are available for the Aminco, Farrand, and Baird-Atomic instruments. These include a rotating mechanical shutter and a liquid nitrogen Dewar flask.

## 5. GLOSSARY OF SYMBOLS

- $f$  Frequency of pulsing, Hz.  
 $t_c$  Phosphoroscope period, sec.  
 $t_g$  Exposure time of analyte to exciting light per cycle, sec.  
 $t_D$  Delay time between end of excitation and beginning of observation, sec.  
 $t_F$  Duration of light flash, sec.  
 $t_P$  Phototube pulse (gate) width, sec.  
 $\alpha$  Phosphoroscope factor, ratio of average DC photocurrent observed using a phosphoroscope to the DC photocurrent observed with no phosphoroscope, no units.  
 $\alpha'$  Phosphoroscope factor with flash tube excitation, ratio of average luminescence radiant flux observed per unit time to hypothetical luminescence radiant flux produced by steady state luminescence, no units.  
 $\tau$  Luminescence decay time (lifetime), sec.

## 6. REFERENCES

1. D. W. Ellis, "Luminescence Instrumentation and Experimental Details," in *Fluorescence and Phosphorescence Analysis*, D. M. Hercules, Ed., Wiley Interscience, New York, 1966, Chapter 3.
2. C. A. Parker, *Photoluminescence of Solutions*, Elsevier, Amsterdam, 1968.
3. J. D. Winefordner, W. J. McCarthy, and P. A. St John, "Phosphorimetry as an Analytical Approach in Biochemistry," in *Methods of Biochemical Analysis*, Vol. 15, D. Glick, Ed., Wiley-Interscience, New York, 1967.

4. H. C. Hollifield and J. D. Winefordner, *Anal. Chem.*, **40**, 1759 (1968).
5. R. Zweidinger and J. D. Winefordner, *Anal. Chem.*, **42**, 639 (1970).
6. G. J. Minkoff, *Frozen Free Radicals*, Wiley-Interscience, New York, 1960.
7. T. C. O'Haver and J. D. Winefordner, *Anal. Chem.*, **38**, 602 (1966).
8. M. L. Bhaumik, *Rev. Sci. Instr.*, **36**, 37 (1965).
9. T. C. O'Haver and J. D. Winefordner, *Anal. Chem.*, **38**, 1258 (1966).

## D. SIGNAL-TO-NOISE RATIO THEORY

### 1. GENERAL ASPECTS

#### a. NOISE<sup>1-3</sup>

The readout (meter reading, pen position, scope deflection, digital number, etc.) of a spectrometric system consists of a desirable signal component, which is related in some way to the nature and concentration of the sample, and an undesirable signal component, which interferes with measurements of the sample. This undesirable component may consist of:

1. A *constant DC offset* or *bias* error, which might include background, dark current, amplifier offsets, zero-adjust errors, and so on. These signals are easily eliminated or compensated for.

2. A *drift* component, due perhaps to phototube fatigue, power supply drift, photodecomposition of a sample, or monochromator wavelength drift. Drift can be a serious source of error in many cases.

3. An *AC noise* component—it may be *periodic*, such as that due to pickup of 60-Hz power line frequency, 120-Hz power supply hum, or stray pickup of radio signals; or it may be *aperiodic* (random), such as shot or Johnson noise. Periodic noise is usually easy to eliminate by means of an electrical notch filter tuned to the proper frequency. Random noise, however, appears at not just one frequency but is distributed over a wide band of frequencies and is therefore much more difficult to filter out completely.

The frequency distribution of noise components is characterized by a power density spectrum, which is a plot of noise power per unit frequency interval ( $\text{watt Hz}^{-1}$ ) versus frequency, rather analogous to the spectrum of a light source. Noise whose power density is independent of frequency is called *white* noise (see Figure III-D-1). This is a very common type of noise; shot noise and Johnson noise are white under most conditions. *Nonwhite* noise may also be observed (see Figure III-D-1). One particularly common and troublesome type of nonwhite noise is called "pink" or  $1/f$  noise because its power density is inversely proportional to frequency.



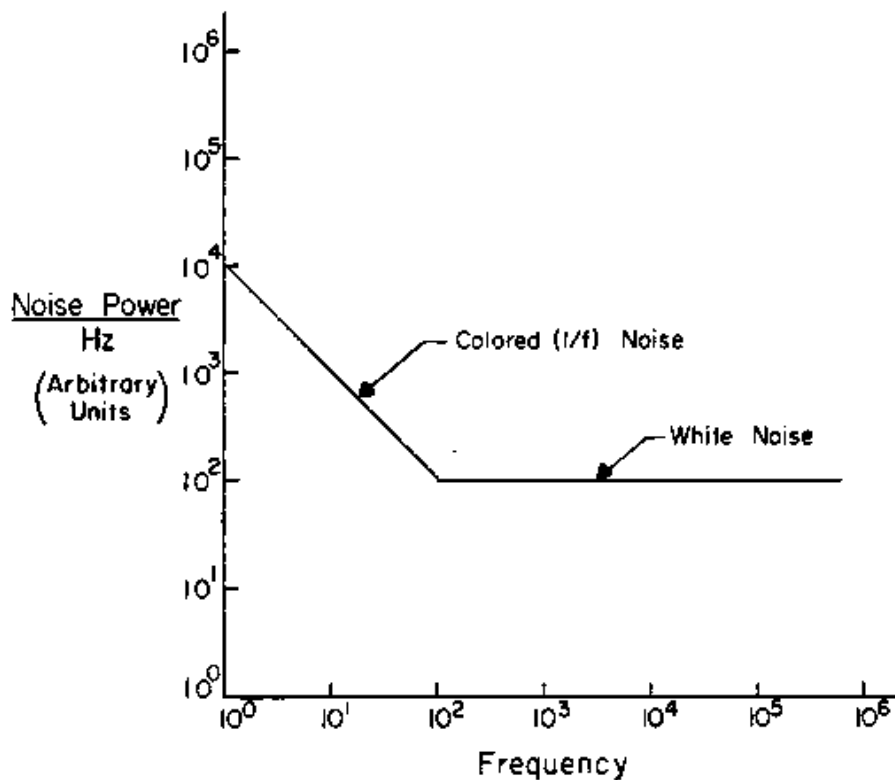


**Fig. III-D-1.** Representation of noise power spectrum.

#### b. ELECTRICAL BANDWIDTH

The *electrical bandwidth* of a system is a measure of how quickly the output (pen position, needle reading, oscilloscope trace, etc.) follows changes in the input signal (current or voltage). A system with high bandwidth (wide band) faithfully displays rapid changes in the input signal, whereas a system with low bandwidth (narrow band) smoothes out and/or attenuates input signal changes. As a result, systems with finite bandwidth exhibit a finite *response time*, an *averaging time*, and a *frequency response*.

(1) *Response Time*. If an input *step function* is applied to a system (i.e., an instantaneous change in the input signal), the output will not change instantly but will reach about 98% of its final reading in a time called the *response time*  $t_r$ , related to the electrical bandwidth  $\Delta f$  by<sup>2</sup>

$$t_r \approx \frac{1}{\Delta f} \quad (\text{III-D-1})$$

(2) *Averaging Time*. Any input signal changes are averaged over an effective time  $t_a$ :

$$t_a = \frac{1}{2\Delta f} \quad (\text{III-D-2})$$

Thus if a direct measurement of a white noise source is made with an rms AC voltmeter of electrical bandwidth  $\Delta f$ , then the observed rms voltage will be equal to the standard deviation of a number of successive time averages of the amplitude of the noise source, where each average is taken over a time period equal to  $1/2\Delta f$ .

(3) *Frequency Response.* If the input signal to the readout system is varied in amplitude sinusoidally at some frequency  $f$ , then the system response to that amplitude change will be a function of  $f$ . A plot of the system response to the sinusoidal variation in signal amplitude versus the frequency of the amplitude variation is called the *frequency response curve* of the system. The range of frequency  $\Delta f$  over which the system responds is called the *passband*, or more commonly, the *electrical bandwidth*, in frequency units. If the input signal is DC then a *low-pass* readout system can be used. A low-pass system responds equally to DC and to all AC frequencies up to approximately  $\Delta f$ , and it attenuates frequencies above  $\Delta f$ . If some form of modulation is used to produce an AC signal, then a *bandpass* system can be used. A bandpass system responds only to frequencies between certain frequency limits  $f_l$  and  $f_u$ , where  $f_l < f_u$ . The bandwidth  $\Delta f$  is given by  $f_u - f_l$ . In real systems, the rate of attenuation of response to frequencies outside of  $\Delta f$  is gradual, and this makes the determination of the exact bandwidth limits less direct.

Most readout systems are characterized by more than one bandwidth. For instance, AC systems have both a predetection bandwidth (the bandwidth of the AC amplifier before the demodulator) and a postdetection bandwidth (the bandwidth of the low-pass DC filter stage following the demodulator). Both AC and DC systems may use a chart recorder readout which is a low-pass system itself and has its own bandwidth. The total electrical bandwidth of the entire system  $\Delta f_t$  is given by

$$\Delta f_t = \left( \frac{1}{\Delta f_1^2} + \frac{1}{\Delta f_2^2} + \cdots + \frac{1}{\Delta f_j^2} \right)^{-1/2} \quad (\text{III-D-3})$$

where  $\Delta f_1 \cdots \Delta f_j$  are the bandwidths of each individual stage or component of the system. Obviously, if one  $\Delta f$  is much lower than the other, it will effectively determine the system bandwidth.

#### C. EFFECT OF ELECTRICAL BANDWIDTH ON NOISE

The response of a readout system to noise at the input depends on what portion of the noise spectrum is passed by the system. Noise frequency components beyond (above or below) the passband are attenuated. For white noise, the noise power per unit frequency interval (watt Hz<sup>-1</sup>) is constant. Therefore, the total noise power passed by a system is the product of the

input noise density (watt Hz<sup>-1</sup>) and the electrical noise bandwidth  $\Delta f$  of the system (Hz). Thus the measured noise voltage or current at the output is proportional to the square root of total noise power and thus to  $\sqrt{\Delta f}$ , which is why  $\sqrt{\Delta f}$  appears in the equations for shot and Johnson noise. If the noise is not white, the relation between noise and bandwidth is different; but in general reducing  $\Delta f$  reduces the noise at the output.

#### d. SIGNIFICANCE OF RESPONSE TIME

As a rule, random noise in the output signal of an analytical system may be reduced by reducing the electrical bandwidth of the system. However, the response time  $t_r$  increases as  $\Delta f$  decreases. In many cases, the increase in response time will introduce systematic errors or other undesirable side effects which effectively limit the extent to which  $\Delta f$  may be profitably reduced.

(1) *Analysis Time.* After changing a sample, it is necessary to wait at least one response time, and preferably longer, before taking a reading, so that no systematic error will occur because of incomplete response of the instrument to the change. If  $\Delta f$  is reduced to reduce noise, the response time  $t_r$  increases, so each reading takes longer. If multiple readings are desired for a statistical check, the total analysis time may become excessive if the response time is too long ( $\Delta f$  is too low). The proper balance between  $\Delta f$  and  $t_r$  must be judged for the particular application.

(2) *Sample Consumption.* In the flame techniques, such as atomic fluorescence spectrometry, the sample is consumed at some rate\* continuously during the analysis. If we attempt to increase the signal-to-noise ratio, the increase in response time that is produced will require the consumption of more sample for each reading, with the result that the absolute (weight) detection limit may be increased.

(3) *Drift Errors.* Instrumental drifts resulting from source spectral radiance drift, photomultiplier fatigue, amplifier drift, and so on, have a greater effect on analytical accuracy the longer it takes to get a reading. Decreasing  $\Delta f$  to reduce noise errors may increase drift errors.

(4) *Sample Stability.* Some samples in molecular luminescence work are photolyzed by the high excitation radiance or are otherwise unstable. Excessively long readout response time may lead to cumulative errors and irreversible damage to the sample.

\*Actually one of the authors (JDW) has recently utilized discrete sampling (1  $\mu$  l) in atomic fluorescence flame spectrometry. With discrete sampling, a large  $\Delta f$  and a smaller  $t_r$  are required.

(5) *Spectrum Scanning*.<sup>4,5</sup> Excitation and emission spectra are usually obtained by scanning the appropriate monochromator wavelength drive at a constant rate and recording the emission signal versus time. Excessively long  $t_r$ , fast scan speeds, or both may distort spectral peaks and blur out important details and fine structure. The optimum scan speed depends on  $\Delta f$  and on the structure of the spectrum.

For recording line spectra, the monochromator scan speed  $r$  ( $\text{nm sec}^{-1}$ ) should be approximately

$$r \leq \frac{s'}{t_r} = s'(\Delta f) \quad (\text{III-D-4})$$

where  $s'$  is the spectral bandpass of the monochromator,  $t_r$  is the system response time (sec), and  $\Delta f$  is the electrical noise bandwidth ( $\text{sec}^{-1}$ ). For recording band spectra,  $r$  should be

$$r \leq \frac{\Delta\lambda'}{t_r} = (\Delta\lambda')(\Delta f) \quad (\text{III-D-5})$$

where  $\Delta\lambda'$  is the half width (nm) of the most narrow band or spectral feature to be observed. If the electrical bandwidth  $\Delta f$  is adjustable, rather than the scan speed, then the foregoing relations may be used to determine the smallest permissible value of  $\Delta f$ .

(6) *Luminescence Decay Time Measurements*. There is a conflict between random noise errors at large  $\Delta f$  and systematic errors at small  $\Delta f$  due to the long response time in luminescence decay time measurements, also. The response time must be much smaller than the decay time to be measured.

In many of the previously described situations, an optimum value of electrical bandwidth may exist for a particular set of experimental conditions. This optimum value must usually be determined experimentally. In those cases in which excessively long response time introduces systematic errors, a series of measurements made at various values of  $\Delta f$  and extrapolated to  $\Delta f = \infty$  ( $t_r = 0$ ) will give an indication of the significance of  $t_r$ . However, those readings taken at high  $\Delta f$  may be imprecise because of the increased noise.

#### e. NOISE SOURCES IN SPECTROMETRIC INSTRUMENTATION

The most important sources of random noise in luminescence spectrometry include the following ones.

(1) *Source of Excitation*. Drift and random fluctuations\* in source radiance may be due to line voltage variations, lamp aging, arc wander, sputtering and

\*A  $1/f$  noise component also exists in source fluctuation.

evaporation of electrode material onto lamp walls, thermal turbulence and convection in the arc gases, and so on. The noise is a constant fraction of total source radiance and thus increases linearly as the measured photosignal is increased by, for example, opening the monochromator slits or increasing detector or amplifier gain.

(2) *Sample and Sample Cell.* The sample and the sample cell constitute a noise source highly dependent on the particular model. It includes such factors as flame noise in flame fluorescence work and coolant convection and bubbling in low temperature luminescence spectrometry of molecules in the condensed phase.

(3) *Photodetector.*<sup>6-10</sup> Detector noise, mainly dark current shot noise in multiplier phototubes, is attributable to the fundamental quantum nature of electrons and photons and is often the fundamental limiting noise when other noise sources have been reduced or eliminated.

(4) *Amplifier-Readout System.*<sup>3</sup> Electronic noise in the amplifier and readout system is usually insignificant with modern instrumentation. However, some types of noise may still cause trouble, particularly stray pickup of 60-Hz hum, radio and TV signals, radar, and so on. Drift in DC systems may be significant.

#### f. ADDITION OF NOISE SOURCES

In analytical applications we are usually interested in the total effect of the various noise sources on the readout signal. It is convenient to express noise amplitudes in terms of rms current noise at the output of the photodetector. Each noise source is evaluated in terms of its contribution to the total noise  $\overline{\Delta i_t}$  in the photodetector output current. The way in which the various noise sources combine is important. Offsets and drifts add linearly and algebraically (i.e., with regard to sign). On the other hand, independent random noises add quadratically:

$$\overline{\Delta i_t} = \left( \sum_n \overline{\Delta i_n^2} \right)^{1/2} \quad (\text{III-D-6})$$

where  $\overline{\Delta i_t}$  is the total rms current noise in the photodetector output current and the  $\overline{\Delta i_n}$  are the individual rms current noises due to each of the various noise sources. In some cases the relative contribution of the various noise sources to the total noise may be determined by investigating the dependence of total noise at the output on the detector current; this may be accomplished by varying the monochromator slit width or height to change the radiant flux reaching the detector. Source noise is a constant fraction of the total source radiance (spectral radiance), and thus its noise contribution to the output noise increases linearly with the radiant flux reaching the detector

(and thus with the detector current). Shot noise increases as the square root of detector current. Electronic noise is constant, independent of any variable before the electronics. It may be possible to determine, for instance, whether any one noise source is dominant.

g. SIGNAL-TO-NOISE RATIO AND THE OPTIMIZATION OF EXPERIMENTAL CONDITIONS<sup>11-15</sup>

The signal-to-noise ratio\*  $i_L/\overline{\Delta i_T}$ , must be considered when experimental conditions for any spectrochemical method are being optimized. It is generally desirable to obtain the largest possible signal-to-noise ratio in order to obtain the most precise results and the lowest limit of detection. If analytical expressions for  $i_L$  and  $\overline{\Delta i_T}$  could be obtained, then the optimum value of any experimental parameter  $X$  could be found by differentiating  $i_L/\overline{\Delta i_T}$  with respect to  $X$ , setting the resulting derivative equal to zero, and solving for  $X_{opt}$ . It is usually necessary to do this graphically, however. A plot of  $i_L/\overline{\Delta i_T}$  versus each parameter  $X$ , obtained experimentally, will reveal which parameters do in fact exhibit maxima.

h. EFFECT OF RANDOM NOISE ON ANALYTICAL PRECISION AND DETECTION LIMITS<sup>16,17</sup>

In many instances the precision of analytical measurements is limited by random noise. This is particularly true in trace analysis near the limit of detection. In such cases, statistical methods may be used to evaluate the effect of random noise on analytical *precision*.

Analytical determinations invariably involve the measurement of at least two signals, one or both of which may be noisy. Most commonly, the *difference* between two signal levels is sought (e.g., the difference between a sample signal and a blank signal). It is necessary to consider separately the noise on the blank signal  $\overline{\Delta i_b}$  and the noise on the sample signal  $\overline{\Delta i_s}$ . Consider two noisy current signals  $i_s$  and  $i_b$  having rms noises  $\overline{\Delta i_s}$  and  $\overline{\Delta i_b}$ , respectively, such that  $i_s > i_b$  (these are sample and blank signals, respectively). Let us define the difference  $i_s - i_b$  as the analytical signal  $S$  (i.e.,  $S = i_L$ )

$$S = i_s - i_b \quad (\text{III-D-7})$$

The respective rms noise  $\sigma_s$  is the standard deviation of the difference; that is,  $\sigma_{i_s - i_b}$ , and can be shown to be

$$\sigma_s = \sqrt{\overline{\Delta i_s^2}/n_s + \overline{\Delta i_b^2}/n_b} \quad (\text{III-D-8a})$$

\* The  $i_L$  represents the detector photocurrent due to analyte luminescence.

where  $n_s$  and  $n_b$  are the number of measurements of  $i_s$  and  $i_b$ , respectively, which constitute each measurement of  $S$ . In practical work  $n_s$  and  $n_b$  are made equal. Thus if  $n_s = n_b = n$ :

$$\sigma_s = \sqrt{(\overline{\Delta i_s^2} + \overline{\Delta i_b^2})/n} \quad (\text{III-D-8b})$$

The magnitude of  $\sigma_s$  has an effect on several important specifications of analytical measurements.

(1) *Relative Standard Deviation*<sup>15</sup> In a random-noise-limited system, the relative standard deviation  $RSD$  of a series of successive readings of  $S$  is given by

$$RSD = \frac{100\sigma_s}{S} = \frac{100}{S} \sqrt{(\overline{\Delta i_s^2} + \overline{\Delta i_b^2})/n} \quad (\text{III-D-9})$$

There are two useful limiting cases for this equation. For large sample concentrations,  $i_s \gg i_b$ . In luminescence spectrometry the most important sources of noise increase in amplitude with the analytical signal, and thus  $\overline{\Delta i_s} \gg \overline{\Delta i_b}$  at large sample concentrations; therefore,

$$RSD \cong \frac{100 \overline{\Delta i_s}}{\sqrt{n} S} \quad (\text{III-D-10})$$

At low sample concentrations,  $i_s \approx i_b$  and  $\overline{\Delta i_s} = \overline{\Delta i_b} = \overline{\Delta i}$ . Thus

$$RSD \cong \frac{100\sqrt{2} \overline{\Delta i}}{\sqrt{n} S} = \frac{141 \overline{\Delta i}}{\sqrt{n} S} \quad (\text{III-D-11})$$

(2) *The Limit of Determination.* Often we want to know the smallest analytical signal  $S_l$  that can be measured with a given maximum acceptable  $RSD$ . This is easily found from equation III-D-9 or its two limiting cases:

$$S_l = \frac{100}{RSD} \sqrt{(\overline{\Delta i_s^2} + \overline{\Delta i_b^2})/n} \quad (\text{III-D-12})$$

The sample concentration corresponding to this value of  $S$  is called the *limit of determination*.

(3) *Limiting Detectable Sample Concentration.*<sup>16, 17</sup> In some cases it may be useful to know the smallest analytical  $S_m$  that can be detected with a given level of confidence. This is derived from small sample statistical theory by the use of the "Student  $t$ " statistic. The Student  $t$  is defined as the ratio of the

smallest detectable difference between two means to the standard deviation of those differences, or in our terms:

$$t = \frac{(i_s - i_b)_m}{\sigma_s} = \frac{S_m}{\sigma_s} \quad (\text{III-D-13})$$

where  $S_m$  is the minimum detectable  $S$ . The value of  $t$  (no units) is available in tables and is a function of the number of degrees of freedom and the confidence level desired. The number of degrees of freedom is equal to  $2n - 2$ , where  $n$  is the number of measurement pairs, each measurement pair consisting of one measurement each of  $i_s$  and  $i_b$ . Combining equations III-D-8 and III-D-13, we have

$$S_m = t\sigma_s = \frac{t\sqrt{\overline{\Delta i_s^2} + \overline{\Delta i_b^2}}}{\sqrt{n}} \quad (\text{III-D-14})$$

In general,  $S_m$  is small, so that  $i_s \simeq i_b$  and  $\overline{\Delta i_s} \simeq \overline{\Delta i_b} = \overline{\Delta i}$ . In that case

$$S_m = \frac{\sqrt{2t} \overline{\Delta i}}{\sqrt{n}} \quad (\text{III-D-15})$$

The sample concentration giving a signal equal to  $S_m$  is called the *limiting detectable sample concentration*, sometimes shortened to *limit of detection* or *detection limit*.

## 2. ATOMIC FLUORESCENCE FLAME SPECTROMETRY

### a. SIGNAL AND SHAPE OF ANALYTICAL CURVES<sup>18,19</sup>

The average photodetector signal current  $i_L$  due to atomic fluorescence of the analyte (assuming the atomic fluorescence line half width is considerably less than the spectral bandpass of the measuring monochromator) is given by

$$i_L = mW'K'_o\gamma B_L \quad (\text{III-D-16})$$

where  $m$  is a factor that accounts for the light loss when a mechanical source intensity chopper is used ( $m$  equals 0.5 for most choppers and 1.0 if no chopper is used),  $W'$  is the monochromator\* slit width (cm),  $K'_o$  is the optics factor\* (cm sr) discussed in Section III-A-4-h,  $\gamma$  is the radiant sensitivity of the photodetector (A watt<sup>-1</sup>), and  $B_L$  is the radiance (watt cm<sup>-2</sup> sr<sup>-1</sup>) of fluorescence (cf. Section II-C-10). The magnitude of  $B_L$  was seen to depend on the atomic concentration of  $n_o$  atoms in the flame gases, according to

\* The primes designate emission monochromator. Actually in atomic fluorescence studies only an emission monochromator is used (i.e., no excitation monochromator).



APPENDIX

III

**GENERAL EXPRESSIONS FOR THE MEASURED LUMINESCENCE SIGNAL OF A SPECTROMETRIC SYSTEM\***

A. THE OPTICAL SYSTEM UNDER CONSIDERATION

The arrangement of the optical system schematically shown in Figure A3-1 is used to represent any spectrometric system. Even if more than one lens or mirror is used in the entrance optics or in the spectrometer, the following general treatment will still apply, except that certain factors must be changed to account for the additional optical components (e.g., the transmission of the optical components).

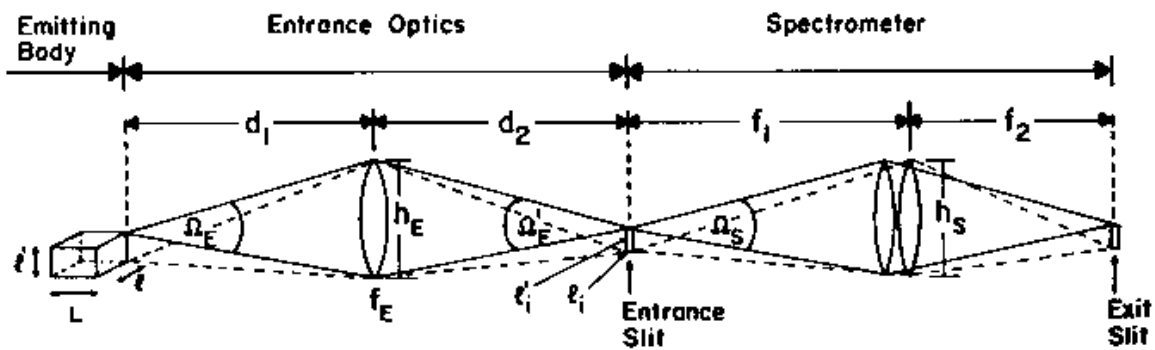


**Fig. A-3-1** Arrangement of optical system for measurement of luminescence (or any source of radiation).

Assumptions and conditions necessary for luminescence signal expressions to be valid are:

1. The solid angle of the entrance beam  $\Omega'_E$  must exceed or at least be equal to the solid angle collected by the spectrometer  $\Omega_s$ ; that is,

$$\Omega'_E \geq \Omega_s \quad (\text{A3-1})$$

In other words, the spectrometer optics (lens, mirror, or dispersing device) *determines* the linear aperture (the size of the light beam transmitted through the spectrometer).

\* The contents of this section are a result of informal discussion with V. Svoboda during his stay at the University of Florida. (V. Svoboda is now at Dvorakova 10, Praha 4-Modrany, Czechoslovakia.)

2. The height of the source image  $l_i$  on the entrance slit of the spectrometer must be equal to or greater than the slit height  $H_s$ ; that is,

326

## LUMINESCENCE SIGNAL OF A SPECTROMETRIC SYSTEM

Using the foregoing conditions, assumptions, and relationships, the following equations can be derived.\* From condition 1, it can be shown that

$$h_E \geq \frac{h_s d_1 f_E}{f_1} \sqrt{1/(d_1^2 - 2d_1 f_E + f_E^2)} \quad (\text{A3-11})$$

and from conditions 2 and 3 it can be shown that

$$l' \geq H_s \frac{d_1}{d^2} = H_s \left( \frac{f_E}{d_1 - f_E} \right) \quad (\text{A3-12})$$

$$l \geq W_s \frac{d_1}{d_2} = W_s \left( \frac{f_E}{d_1 - f_E} \right) \quad (\text{A3-13})$$

As long as these expressions are valid, then the general treatment to follow is valid. It should be stressed, however, that the experimental conditions needed for validity of the expressions used are almost always experimentally attainable for analytical spectrometric systems (luminescence as well as absorption spectrometers). Finally, it should be pointed out that the expressions to be derived are valid for the measurement of radiation from any (line or continuum) source of radiation (source of excitation such as a hollow cathode lamp or a xenon arc lamp or an emitting or luminescing media).

### B. GENERAL EXPRESSION FOR RADIANT FLUX EMERGING FROM EXIT SLIT OF SPECTROMETER SET AT A FIXED WAVELENGTH

The radiant flux  $\Phi_D$  (watt) emerging from the exit slit of a spectrometer and striking a detector is given, for a luminescent sample and a spectrometric system as shown in Figure A3-1, by

$$\Phi_D = t_E t_s \Omega_s H_s \int_{\lambda_l}^{\lambda_u} B_{L\lambda} F_{\lambda_s}(\lambda) d\lambda \quad (\text{A3-14})$$

where  $t_E$  is the transmittance of the entrance optics and  $t_s$  is the transmittance of the spectrometric system between the limiting wavelengths of  $\lambda_l$  and  $\lambda_u$ ;  $H_s$  is the spectrometer\* entrance slit height (cm);  $F_{\lambda_s}(\lambda)$  is the spectrometric or apparatus function,† in (cm), which depends on the wavelength setting of the monochromator  $\lambda_s$  and the wavelength range (essentially the spectral bandpass  $s$  of the monochromator) when the spectrometer is *not* being wavelength scanned; and  $B_{L\lambda}$  is the spectral radiance‡

\* The thin lens approximation is used:  $1/d_1 + 1/d_2 = 1/f_E$ , where  $f_E$  is the focal length of the entrance optics lens.

\* It is also assumed in this treatment that the entrance and exit slit widths are identical, for this is the case in most analytical spectrometers.

† Also called the slit function of the spectrometer. This function should have a triangular distribution if it is true that the entrance and exit slits are identical (except for spectrometer slit widths near the diffraction limited slit width).

‡ In this section  $\lambda$  rather than  $\lambda'$  as in the text is used to denote emission wavelength.

of luminescence being emitted by the sample (see Section II-C-1). The product of the terms  $B_{L\lambda}$  and  $F_{\lambda_s}(\lambda)$  is said to be folded (convoluted). The wavelength range  $\lambda_i$  to  $\lambda_u$  designates the range over which  $F_{\lambda_s}(\lambda)$  is greater than zero; because  $F_{\lambda_s}(\lambda) \rightarrow 0$  for wavelengths outside this range, the integration limits can be changed to zero to infinity (more convenient to handle). Nevertheless, the integral in equation A-314 can only be readily solved by numerical methods.

It is important to point out that the value of  $\Phi_D$  depends on the product of  $B_{L\lambda}$  and  $F_{\lambda_s}(\lambda)$  integrated from  $\lambda_i$  to  $\lambda_u$ . For the limiting cases in which the spectral line from the emitter is much narrower than the spectral bandpass of the spectrometer or for the limiting case in which spectral radiance of the emitter is constant over the spectral bandwidth of the spectrometer, the simplified expressions given in Chapter III can be used with good accuracy. However, such expressions as in Chapter III are limiting cases and give only an approximation of the measured signal. Fortunately, the expressions in Chapter III are analytically useful for most real experimental cases and can be used in most real cases for estimating the influence of variables on the luminescence signal. The general expressions provided here are useful for all cases and give useful results for intermediate cases, but the expressions in this appendix are more unwieldy and of less interest to the analyst.

To convert the radiant flux  $\Phi_D$  (watt) passing through the spectrometer exit slit and striking the photocathode of a multiplier phototube into an electrical signal  $S_L$ , in the following expression is used:

$$S_L = \gamma_L G \Phi_D R_L \quad (\text{A3-15})$$

where  $R_L$  is the load resistance, in ohm,  $\gamma_L$  is the photoanodic sensitivity of the multiplier phototube [A (at anode) watt<sup>-1</sup> (radiant flux at cathode)] and  $G$  is the overall gain of the measurement circuit [A (at readout) to A (at anode of phototube)].

### C. TOTAL RADIANT ENERGY EMERGING FROM EXIT SLIT OF SPECTROMETER WHEN WAVELENGTH SCANNING THE SPECTRAL LINE OR BAND

In the scanning mode, the total amount of radiant energy  $Q_D$  (watt sec) corresponding to some luminescence line or band that emerges from the spectrometer exit slit and reaches the photocathode of the multiplier phototube is given by

$$Q_D = \int_{t_1}^{t_2} \Phi_D dt = t_E t_s \Omega_s H_s \int_{t_1}^{t_2} \int_{\lambda_i}^{\lambda_u} B_{L\lambda} F_{\lambda_s}(\lambda) dt d\lambda \quad (\text{A3-16})$$

where  $F_{\lambda_s}(\lambda)$  is a function of the spectral bandwidth of the monochromator  $s$ , the wavelength limits  $\lambda_u$  and  $\lambda_i$ , and the wavelength setting of the spectrometer  $\lambda_s$ , which is a function of time. All terms before the integral are assumed to be constant with time between the initiation time  $t_1$  and the final time  $t_2$  of the wavelength scan and constant with wavelength.

If it is now assumed that the scanning speed is constant, then

$$\lambda_s = a + bt \quad (\text{A3-17})$$

where  $a$  and  $b$  are constants for the scanning system. Therefore

$$\frac{d\lambda_s}{dt} = b \quad (\text{A3-18})$$

Assuming a triangular slit (apparatus) function,\*  $F_{\lambda_s}(\lambda)$  is given† by

$$F_{\lambda_s}(\lambda) = F_{\lambda_s}(\lambda_s) \left[ 1 - \frac{|\Delta\lambda|}{s} \right] \quad (\text{A3-19})$$

where  $\Delta\lambda = |\lambda - \lambda_s|$ , where  $\lambda$  is any wavelength between the limits of  $\lambda_i$  and  $\lambda_u$  which are imposed by the scanning limits and  $s$  is the spectral bandpass of the spectrometer.

To convert  $Q_D$  into a measured readout signal, it is necessary to use an integrating system and to measure stored charge (coulomb). If the photoanodic sensitivity of the multiplier phototube is  $\gamma_{\lambda_s}$  A watt<sup>-1</sup>, then the charge  $q_D$  (coulomb), stored in a capacitor connected to the photoanode is

$$q_D = Q_D \gamma_{\lambda_s} \quad (\text{A3-20})$$

It was assumed that  $\gamma_{\lambda_s}$  was a constant\* over the wavelength limits ( $\lambda_u$  to  $\lambda_i$ ) of the

\* We assume that the spectrometer has equal entrance and exit slit widths (and heights) and that the slit widths are greater than the diffraction-limited slit width; that is,

$$W_s \quad \text{or} \quad W_e \gg \frac{2\lambda_s f_1}{H_s}$$

where  $\lambda_s$  is the spectrometer wavelength setting (cm),  $f_1$  is the collimator focal length (cm), and  $H_s$  is the slit height (cm). If this condition is *not* valid, see K. D. Mielenz, *J. Opt. Soc. Amer.*, **57**, 66 (1967).

† If  $W_s \neq W_e$ , then the apparatus function will be trapezoidal rather than triangular, and the wavelength width of the top  $\Delta\lambda_{\text{top}}$  and base  $\Delta\lambda_{\text{base}}$  of the trapezoid will be

$$\Delta\lambda_{\text{top}} = \left[ W_s \left( \frac{f_2}{f_1} \right) - W_e \right] R_d$$

$$\Delta\lambda_{\text{base}} = \left[ W_s \left( \frac{f_2}{f_1} \right) + W_e \right] R_d$$

where  $R_d$  is the reciprocal linear dispersion of the spectrometer (nm cm<sup>-1</sup>). For this case, the peak value of  $F_{\lambda_s}$  at  $\lambda_s$ , which is designated  $F_{\lambda_s}(\lambda_s)$ , is a constant for the wavelength range over  $\Delta\lambda_{\text{top}}$ . For  $\lambda - \lambda_s > \Delta\lambda_{\text{top}}$  or  $\lambda - \lambda_s < -\Delta\lambda_{\text{top}}$ ,  $F_{\lambda_s}(\lambda)$  drops off in the same manner as for the triangular slit function. Also, for the limiting case of a triangular slit function—that is,  $W_s = W_e$  and  $f_2 = f_1$ ;  $\Delta\lambda_{\text{top}} = 0$  and  $\Delta\lambda_{\text{base}} = 2R_d W_s = 2s$  (twice the spectral bandpass of the spectrometer).

\* The value of  $\gamma_{\lambda_s}$  is approximately a constant over the wavelength range of  $\lambda_p + 1000 \text{ \AA}$  to  $\lambda_p - 1000 \text{ \AA}$ , where  $\lambda_p$  is the peak response wavelength for the specific multiplier phototube being used. For some phototubes, the range is even greater. Outside of this range, especially at the low wavelength end,  $\gamma_{\lambda_s}$  varies rapidly with  $\lambda_s$ , and so the wavelength dependence of  $\gamma_{\lambda_s}$  must be accounted for.

scan; if  $\gamma_{\lambda_s}$  varies over the wavelength range, then it would be necessary to account for the wavelength sensitivity by including  $\gamma_{\lambda_s}$  within the integral in equations A3-20 and A3-16 (i.e., convolution of the photoanodic sensitivity factor with the luminescence spectral radiance and the apparatus function). The luminescence spectral radiance function  $B_{L\lambda}$  is known or can be estimated for most atomic lines—it can be approximated by the expressions in Section II-C—but is known much less accurately for molecular bands. The expressions in Section II-C are useful for obtaining the integrated spectral luminescence radiance; that is,  $B_L$  ( $\text{erg sec}^{-1} \text{cm}^{-2} \text{sr}^{-1}$ ) but the spectral luminescence radiance  $B_{L\lambda}$  ( $\text{erg sec}^{-1} \text{cm}^{-2} \text{sr}^{-1} \text{nm}^{-1}$ ) can only be obtained if the spectral distribution of molecular luminescence is known in detail.

## IV

**PRINCIPLES OF OPERATION OF  
NONPHOTOEMISSIVE DETECTORS****A. PHOTOVOLTAIC OR BARRIER-LAYER CELLS**

One of the simplest types of photodetectors is the photovoltaic cell; it is self-generating and requires no auxiliary power supply. However, it is one of the least satisfactory photodetectors for luminescence work because of its limited sensitivity and relatively narrow linear dynamic range. A description is included here mainly for completeness.

The usual type of photovoltaic cell consists of a thin layer of crystalline selenium deposited on a metal base plate. The selenium layer is covered with a very thin, semi-transparent layer of metal (usually silver) which forms the other electrode. Photons passing through the semitransparent metal layer are absorbed at the "barrier layer" between the selenium and the thin metal layer and produce electron-hole pairs. The migration and resulting separation of these holes and electrons cause a small difference in potential to develop between the base plate and the thin metal layer.

Either the open-circuit voltage or the short-circuit current from the photovoltaic cell may be measured and used as a gauge of light intensity. Only the short-circuit current, however, increases linearly with increasing illumination; the open-circuit voltage increases approximately as the logarithm of the incident intensity.

The short-circuit current can be measured accurately only with a low resistance current meter (milliammeter or microammeter); that is, the input resistance of the current meter must be very small compared with the internal resistance of the photovoltaic cell. Unfortunately, the internal resistance is quite low (of the order of 100 ohm) and this requires that the meter input resistance be of the order of an ohm. Such a low value is difficult to obtain in a sensitive meter. A sensitive meter is required because the sensitivity of the photocell is low—of the order of  $0.1 \text{ mA watt}^{-1}$  of incident radiation in the visible and near-ultraviolet regions. The useful spectral range extends from 250 to about 750 nm.

The logarithmic characteristic of the open-circuit voltage is useful for some applications: certainly the voltage would be easier to measure, because high resistance voltmeters are commonly available. The output voltage is typically of the order of several millivolts. Unfortunately, the logarithmic characteristic is limited in dynamic range, and the large capacitance of the cell increases the response time seriously when loaded by a high resistance.

Photovoltaic cells are occasionally found on simple colorimeters. Their dynamic range is too restricted for use in most fluorescence instruments. Spectral ranges of several cells are given in Figure A4-1.

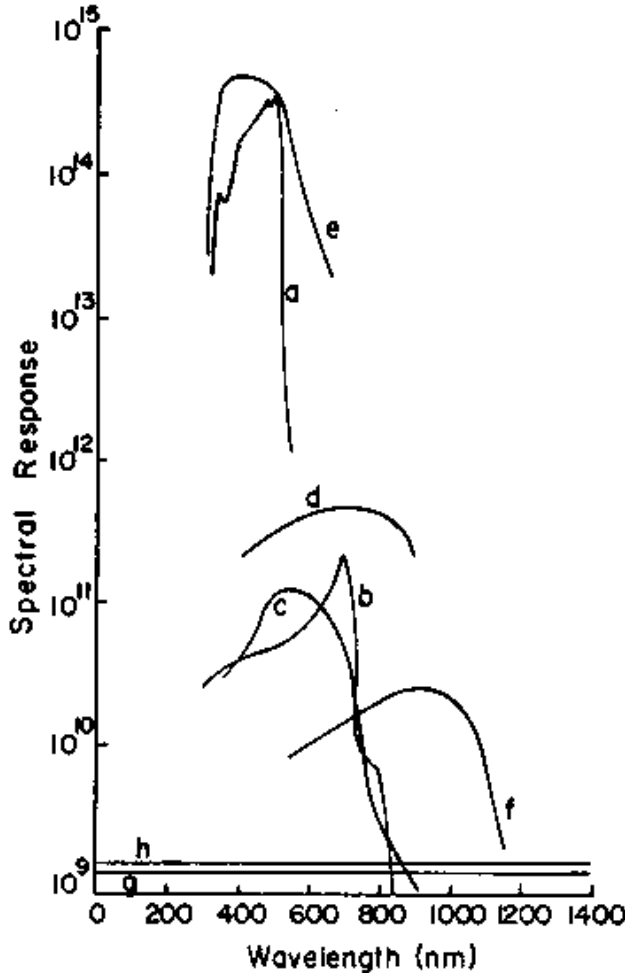


**Fig. A-4-1** Spectral ranges of photo-detectors; plots are of spectral detectivity (called response here)  $D_\lambda^*$  versus wavelength  $\lambda$ . Spectral detectivity is a figure of merit of the phototube and is defined as the reciprocal of the noise equivalent power,  $P_N$ , (watts  $\text{Hz}^{-1}$ ) times the square root of the detector area  $A_D$  ( $\text{cm}^2$ ) onto which radiation falls. Thus spectral detectivity has units of  $\text{cm Hz}^{1/2} \text{watt}^{-1}$ . It is related to spectral responsivity  $R_\lambda$  (volt  $\text{watt}^{-1}$ ) by  $D_\lambda^* = R_\lambda A_D \Delta f / V_N$ , where  $\Delta f$  is the noise bandwidth of the measurement system and  $V_N$  is the rms noise voltage. Plots are: (a) CdS photoconductivity cell modulated at 90 Hz, (b) CdSe photoconductivity cell modulated at 90 Hz, (c) Se-SeO photovoltaic cell modulated at 90 Hz, (d) GaAs photovoltaic cell modulated at 90 Hz, (e) 1P21 multiplier tube (for reference), (f) 1N217 silicon photo-duodiode photovoltaic cell modulated at 400 Hz, (g) radiation thermocouple modulated at 5 Hz, (h) Golay cell modulated at 10 Hz. Curves from P. W. Kruse, L. N. McGlauchlin, and R. B. Quistan, *Elements of Infrared Technology*, Wiley, New York, 1962, with permission of the authors.

## B. PHOTOCONDUCTIVE CELLS

Photoconductive cells are essentially light-variable resistors. They are not self-generating and so they require an auxiliary voltage supply. Nevertheless, they are much more sensitive than barrier-layer cells and have a wider dynamic range.

Photoconductive cells may be constructed of almost any crystalline semiconductive material. Selenium, silicon, germanium, and some metal oxides, sulfides, and halides are commonly used. Electrical connections are made to each end of a bar or plate of semiconductor material, and a small potential is applied across these electrodes by means of an external battery or power supply. When light strikes the semiconductor material, its resistance decreases and a current flows that is proportional to the incident light intensity. In the dark, the resistance of the cell is very high, and only a small "dark" current flows.

Photoconductivity is caused by the excitation of valence-band electrons to the conduction band by the absorption of incident photons. The energy of the photon  $h\nu$  must be greater than the energy gap  $\Delta E$  between the valence and conduction

bands. This sets a lower limit on the energy (and an upper limit on the wavelength) of an incident photon. Semiconductors, whose values of  $\Delta E$  are comparatively small, are used as photoconductors in order to obtain good response to reasonably long wavelengths.

The transfer function of a photoconductive detector (i.e., the characteristic of photocurrent  $i$  versus incident light flux  $\Phi$ ) is sometimes linear, as in the case of lead sulfide, silicon, and germanium photoconductors. But the current  $i$  often varies with  $\Phi^n$ , where  $n$  may be either less than or greater than unity. In grey selenium, for example,  $n$  is about 0.5. In cadmium sulfide and selenide detectors,  $n$  decreases with increasing light flux. An additional source of nonlinearity may arise because as the current  $i$  increases, the voltage  $V$  across the element is reduced by the drop across the resistance of the current meter. This effect can be reduced by using a very low resistance meter, as for the photovoltaic cells.

Photoconductive detectors may be used over a spectral range extending from the infrared into the ultraviolet. Some types even respond to X-rays, gamma rays, and to  $\alpha$  and  $\beta$  particles. The sensitivity usually drops off sharply at long wavelengths, when the energy of the photons drops below the gap energy  $\Delta E$ . The long wavelength response can often be improved by cooling the detector. The spectral ranges of a variety of photoconductors are summarized in Figure A4-1.

Radiant sensitivities of commercial photoconductive detectors are generally of the order of a few hundred amperes per watt at the wavelength of maximum sensitivity. The sensitivity can be increased by increasing the voltage across the cell; however, a limitation is imposed by the maximum power which the element can dissipate without damage, which is typically less than 1 watt  $\text{cm}^{-2}$ .

If an appreciable amount of power is dissipated, the resulting temperature increase will increase the dark current. In general, the photocurrent increases linearly with the applied voltage unless polarization or barrier-layer formation occurs.

The dark resistance of photoconductors varies widely with the type of material. Typical values range from about  $10^5$  ohms for selenium and lead sulfide cells to greater than  $10^{10}$  ohms for cadmium sulfide cells. In general, materials with small gap energies  $\Delta E$  have relatively low dark resistances, since room temperature thermal excitation can promote more electrons to the conduction band across a narrow energy gap. Cooling the detector with dry ice or liquid nitrogen will reduce the thermal excitation and thus increase the dark resistance.

The electrical properties of photoconductors are affected greatly by extremely small amounts of impurities, whether accidentally or intentionally added. Certain types of impurities provide current carriers at an energy level only very slightly below the conduction bands, thereby increasing the infrared response and the dark current. Pure germanium, for instance, which has a gap energy of 0.7 eV, responds out to about  $2 \mu$ ; whereas in gold-doped germanium the energy gap is reduced to about 0.01 eV and the infrared response extended to about  $40 \mu$ .

The response time of a photoconductive detector may range from microseconds to many seconds, depending on the particular material.

Noise currents in photoconductors consist primarily of Johnson (thermal agitation) noise, photocurrent noise,\* and dark current noise. The last-named noise increases with decreasing gap energy and increasing temperature and can be reduced by cooling the detector. An additional noise source may arise from the formation of bar-



rier surfaces at the point of contact between the photoconductive material and the two electrodes. This noise,<sup>†</sup> which exhibits a  $1/f$  frequency characteristic, may be reduced by the use of special electrode materials.

Although photoconductive cells cannot compare for sensitivity, linearity, and response time with photomultiplier detectors, they do find some service as source intensity monitors in ratio fluorometers. They have the advantage of small size, low cost, and low voltage requirements.

### C. THERMAL DETECTORS<sup>‡</sup>

A disadvantage of many types of detectors (the so-called photon detectors) is that their sensitivity varies strongly with the wavelength of the incident light. This is not the case for the various types of thermal detectors. Thermal detectors operate by first converting the light energy into an equivalent amount of heat and then measuring the resulting temperature rise by means of a voltage change, resistance change, or expansion of a gas. Thus thermal detectors respond to the total energy absorbed by the detector. Fortunately, it is possible to construct very effective and wavelength-insensitive black body absorbers simply by coating the absorbing surfaces with special coatings of high blackness. Commonly used coatings include platinum black and evaporated gold, bismuth, antimony, and aluminum.

*Thermocouple detectors* convert heat produced by incident light into a small voltage. They are made by attaching a small blackened piece of metal foil, usually gold, to a small thermocouple junction. All the parts are made quite small in order to reduce the heat capacity and thermal inertia of the system. As a consequence, the incident radiation must be carefully condensed and focused onto the tiny element.

The output voltage of a single thermojunction is of the order of  $0.1 \text{ volt watt}^{-1}$  of incident flux over a wide range of incident powers and wavelengths. In a device called a thermopile several thermojunctions can be connected in series in order to increase the sensitivity. However, since this arrangement increases the size, heat capacity, and radiation losses, and increases the response time compared with a single junction, the overall performance is not necessarily improved.

Heat losses by the thermocouple detector and by conduction, convection, or re-radiation, limit the maximum temperature to which a given detector will rise under irradiation by light of a given intensity. These losses can be reduced, and the sensitivity consequently increased, in several ways. Conduction losses are lessened by making the external electrical connections to the junction by means of very thin wires. Convection losses are reduced by enclosing the thermojunction in an evacuated housing at a pressure of the order of  $10^{-4}$  torr. A disadvantage, however, is that absorption in the window may compromise the wide spectral response unless the window is made of a very thin piece of some relatively transparent material (e.g., silica). Radiation losses are proportional to the temperature of the junction and are therefore reduced by cooling the detector (in liquid nitrogen, e.g.). This is rarely done in practice, however.

Thermocouple detectors are most effectively used in AC detection systems; the

\* Also called generation-recombination noise.

† Also called contact noise.

‡ Spectral response curves of several thermal detectors appear in Figure A4-1.

incident radiation is chopped, and the AC component of the output voltage is measured. In this way, the effects of slow changes in the ambient temperature are reduced. The response time of most thermocouple detectors is poor, however, so the chopping frequency is limited to a few hertz at most. Because the resulting signal is AC, it can be coupled to the amplifier electronics by means of a step-up input transformer which increases the signal voltage and matches the low junction resistance (a few tens of ohms) to the relatively higher amplifier input impedance (a few thousand ohms). The transformer must be carefully shielded and must be capable of responding to the low chopping frequency.

*Bolometers* are essentially temperature-sensitive resistors. They may be made of any material whose temperature coefficient of resistivity is sufficiently high. Examples are platinum and various semiconductor materials ("thermistors"). As for the thermocouple detector, the bolometer resistance element must be small and light, and it must be blackened to absorb efficiently. The bolometer usually forms one arm of a resistance (Wheatstone) bridge. The bridge imbalance voltage is used as a measure of light flux. The relation between resistance and light flux is essentially linear for metal bolometers, which simplifies calibration. Bolometers typically have response times of the order of milliseconds—much faster than thermocouples. The sensitivity of a bolometer is of the same order as that of a thermocouple detector.

Neither the thermocouple detector nor the bolometer is used to measure luminescence intensities in quantitative analytical work. The photomultiplier is preferred because of its much greater sensitivity. However, the wavelength-independent response of thermal detectors is very valuable, and the instruments find much use in the calibration of light sources and more sensitive photodetectors and in monitoring excitation source radiances.

Thermal detectors are also an important component of corrected-spectra *luminescence spectrometers*, where they are used to measure the absolute radiant flux of the excitation beam emerging from the exit slit of the excitation monochromator. In some cases, the thermal detector is used in a servo loop controlling the monochromator slit width in order to maintain a constant excitation radiant flux at all wavelengths.

Thermal detectors themselves may be calibrated by comparison with a calibrated light source (such as a black body radiator) or to another calibrated detector. Alternately, they may be calibrated more or less directly by attaching the sensitive element to an electrically heated resistance and calculating the sensitivity from the known Joule heat (voltage times current) dissipated in the resistor and the output of the detector.

#### D. CHEMICAL DETECTORS: THE FERRIOXALATE ACTINOMETER

A chemical actinometer is a light detector system consisting of a solution of a photo-reactive substance (photolyte) capable of undergoing an irreversible photoreaction of known and reproducible quantum efficiency (the yield of products for a given photon flux) upon exposure to light. After exposure, the products of the reaction are determined by an appropriate quantitative analytical method and the photon flux of the light is calculated from the known quantum efficiency and stoichiometry of the reaction. A satisfactory photolyte should have the following characteristics:

1. The photolyte solution should absorb strongly over the wavelength region of interest; but the photolysis products should absorb weakly or not at all, to prevent interference with the linearity of the system.

2. Both photolyte and photolysis products should be stable in the dark and the photoreaction must be irreversible.

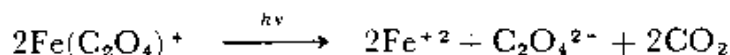
3. The quantum efficiency should be high and reasonably constant over the wavelength range of interest.

4. The photolysis products should be easily measurable with speed and precision by a convenient method.

5. The photolyte should be readily available in a pure form.

The advantages which an actinometer would be expected to have over a conventional electrical detector include: improved interlaboratory reproducibility, the fact that the integrating system acts as a dosimeter, and flexibility—the physical size and shape of the solution vessel may be chosen to suit the dimensions of the light beam.

Parker\* has recommended a 0.006 to 0.15*M* solution of potassium ferrioxalate  $K_3Fe(C_2O_4)_3 \cdot 3H_2O$  in 0.05*M* sulfuric acid. Upon exposure to light of the appropriate wavelength region (approximately 200–580 nm), the following overall reaction occurs:



After irradiation, the ferrous ion is determined spectrophotometrically following conversion to the *o*-phenanthroline complex. The quantum efficiency of the foregoing photoreaction remains constant over a very wide range of incident quantum fluxes† ( $5 \times 10^{-12}$  to  $2 \times 10^{-4}$  einstein  $cm^{-2} sec^{-1}$ ) and total radiation doses (up to  $5 \times 10^{-6}$  einstein  $ml^{-1}$ ). The minimum detectable dose is about  $2 \times 10^{-10}$  einstein  $ml^{-1}$ . The quantum efficiency varies smoothly with wavelength and remains within  $1.0 \pm 0.25$  from 250 to about 500 nm. Several workers have independently determined the quantum efficiency of this system at various wavelengths by reference to calibrated thermocouples or other standards; the results have indicated a remarkable degree of interlaboratory consistency. Thus the ferrioxalate actinometer would seem to be a valuable and highly versatile tool for absolute light-level measurements.

## E. QUANTUM COUNTERS

A quantum counter is a detector whose response is directly proportional to the *quantum irradiance* of a light beam (e.g., photon  $sec^{-1} cm^{-2}$  or einstein  $sec^{-1} cm^{-2}$ ) independent of the wavelength of the light. We can contrast this to a thermal detector, whose response is proportional to irradiance (e.g., watt  $cm^{-2}$ ). A chemical quantum counter may be made by utilizing the following data: that the spectral distribution of the fluorescence emission of all known pure fluorescent compounds (in the condensed phase) is independent of the wavelength of excitation, and that the fluorescence

\* C. A. Parker, *Photoluminescence of Solutions*, Elsevier, Amsterdam, 1968.

† An einstein is equal to  $6 \times 10^{23} h\nu$  erg or 1 einstein is equivalent to  $(1.196 \times 10^9)/\lambda$  watt, where  $\lambda$  is the wavelength (nm).

quantum yield of some fluorescent species is also independent of the wavelength of excitation. A sufficiently concentrated solution so such a substance will absorb all the radiant flux of an incident light beam and convert it into a proportional number of quanta of fluorescence radiation whose spectral distribution is independent of the wavelength of the incident beam (at least over the spectral region in which the substance absorbs appreciably). Any convenient photodetector (e.g., a photomultiplier tube) may then be used to measure the radiance of the resulting fluorescence emission; the wavelength dependence of the sensitivity of this detector is unimportant, since the spectral distribution of the light it views does not change.

In luminescence spectrometry, quantum counters are sometimes used to monitor the relative quantum irradiance of the excitation beam, thereby allowing the direct measurement of corrected excitation spectra and the compensation for uncontrolled fluctuations in the source intensity. A portion of the excitation beam is sampled by means of a quartz plate beam splitter and monitored by the quantum counter. The quantum counter phototube is best positioned slightly off-axis from the direction of the sampled beam in order to avoid obtaining an erroneous response due to any stray light in the beam that is not absorbed by the quantum counter solution.

Some of the solutions that have been used as quantum counters include a 1 g liter<sup>-1</sup> solution of esculin in water, a 3 g liter<sup>-1</sup> solution of rhodamine B in ethylene glycol, and a 0.004*M* solution of fluorescein in water. The concentration of these solutions must be sufficiently high that all the incident radiation is absorbed in a relatively thin layer at the front part of the cell. In this way, the fluorescence radiation passes through a relatively constant depth of remaining solution before reaching the phototube. Thus the filtering effect of this solution is relatively independent of the depth of penetration of the incident beam into the solution, which varies with the incident wavelength and with the molar extinction of the solution. Very pure materials must be used in quantum counter solutions; even small amounts of absorbing impurities may have significant effect in spectral regions in which the molar extinction of the quantum counter substance is low.

## F. PHOTODIODES AND PHOTOTRANSISTORS

An ordinary semiconductor "*pn*" junction, of the type found in transistors and diodes, can also be used as a photosensitive element. The reverse leakage current (i.e., the current flowing through a *pn* junction when it is reverse biased) is generally quite small in the dark but increases when the junction is illuminated. The principle of operation is similar to that of the photoconductive or photovoltaic detector, except that *doped* semiconductor materials are used in a photodiode, the junction being between an *n*-doped region and a *p*-doped region of the same semiconductor (e.g., germanium or silicon). An external voltage supply is required.

Photodiodes have several important advantages over photoconductive and photovoltaic cells. They are more sensitive and have better long wavelength response than photovoltaic cells. The response time is also much shorter, since the junction area and capacitance are small. Photodiodes are physically very small.

A phototransistor is essentially a photodiode with built-in current amplification. It is typically several times more sensitive than, but otherwise similar to, a photodiode.

## APPENDIX

### V

## ELECTRONIC SIGNAL PROCESSING INSTRUMENTS

### A. SINGLE-SECTION LOW-PASS FILTER

A single-section RC low-pass filter has a signal bandwidth of  $(2\pi RC)^{-1}$  and a noise bandwidth of  $(4RC)^{-1}$ . It is the simplest and cheapest noise-reduction device, but it is also quite limited in some respects. The 1% response time of a low-pass filter is relatively long, about  $4.6RC$ , and thus no signal components occurring in a time faster than about  $4.6RC$  will be recorded with fidelity (see the discussion of the effects of response time in Section III-D-1-d).

### B. DC INTEGRATOR

A DC integrator is a circuit whose output voltage  $e_o$  is proportional to the time integral of the input voltage  $e_i$

$$e_o = k \int_0^{t_i} e_i dt \quad (\text{A5-1})$$

where  $k$  is a circuit constant and  $e_o = 0$  at  $t = 0$ . If  $t_i$  is made equal to  $k^{-1}$ , then

$$e_o = \frac{1}{t_i} \int_0^{t_i} e_i dt = \bar{e}_i \quad (\text{A5-2})$$

that is,  $e_o$  is the mean value of  $e_i$  during the interval  $t = 0$  to  $t = t_i$ . Such a circuit is easily constructed from an operational amplifier with a capacitor in the feedback loop. The response time of a DC integrator is simply the integration time  $t_i$ . The effective noise bandwidth is  $(2t_i)^{-1}$ . The main advantage of a DC integrator over a low-pass filter is that the response time of the integrator is less than half that of the filter for the same noise bandwidth. For example, compare a low-pass filter with a time constant of 2.5 sec to a DC integrator with an integration time of 5.0 sec. Both devices have noise bandwidths of 0.1 Hz and thus would result in equal signal-to-noise ratios; but the filter has a response time of 11.5 sec, whereas the integrator may be read after only 5 sec. A disadvantage of the integrator, however, is that its output signal is inherently discontinuous and is thus unsuitable for continuous recording of spectra and other time-variant signals.

### C. HIGHER ORDER FILTERS

Although the DC integrator is more efficient than a simple single-section (first-order) low-pass filter, higher order filters are often more efficient than integrators. High-order filters of several types are available commercially, but they are relatively expensive and their bandwidths may not be changed easily.

## D. AC SYSTEMS

We discussed AC detection and modulation methods in Section III-A-5-b. In terms of noise reduction capability, AC systems have the advantage that the signal frequency is transformed by modulation from DC to some convenient AC frequency high enough to avoid low frequency noise sources such as drift and "1/f noise." However, it should be realized that this is effective only for drift and noise components that *add to* but do not *modulate* (multiply by) the AC signal waveform. For example, variations (drift and noise) in phototube dark current, amplifier offset, and background radiation reaching the photodetector (e.g., flame background emission in atomic fluorescence) are all additive type noises; that is, they affect only the DC level of the AC signal waveform and not its amplitude. Thus any drift and 1/f characteristics of these noise sources will be reduced by an AC detection system. However, variations in phototube supply voltage, amplifier gain, excitation-source radiance, sample introduction rate into the cell in atomic fluorescence spectrometry, or scattering signals (in all types of luminescence spectrometry) are multiplicative in nature when source intensity modulation (chopping) is used; that is, these factors influence the amplitude of the AC signal waveform. Drift and 1/f noise in these factors are reduced no more by AC detection systems than by DC systems of the same noise bandwidth. Other modulation methods may have specific advantages in this respect. For example, wavelength modulation used in continuum-source atomic fluorescence should reduce drift and 1/f noise caused by scattering of incident radiation by droplets in the flame.

## E. BOXCAR INTEGRATOR

A boxcar integrator is essentially a gated amplifier followed by a low-pass filter or integrator. It is useful when only a small interval of a repetitive signal waveform is of interest. The boxcar is gated *on* only during the interval of interest and thus will ignore all the noise components outside that interval. Normally the gate width and delay time are adjustable. By slowly varying the delay time between the initiation of the signal waveform and the generation of the gate pulse, a complex repetitive waveform can be extracted from a great deal of random noise. The effective signal bandwidth, which determines the ability to resolve small time elements in the signal waveform, is inversely proportional to the gate width, whereas the noise bandwidth is simply that of the low-pass filter or integrator following the gated amplifier. Since these two factors are unrelated in a boxcar circuit, it is possible to have a large signal bandwidth and a small noise bandwidth simultaneously, thus preserving the signal waveform as well as filtering out noise. In nongated DC or AC systems, on the other hand, low noise bandwidth and poor time resolution (long response time) are inseparable. A boxcar integrator is useful in luminescence decay studies as well as in stroboscopic flash spectroscopy.

A disadvantage of using the boxcar circuit in the sweep-delay mode to extract a waveform is that all the signal information falling outside the gate interval in any one instant is wasted. The efficiency of information collection is essentially the gate width divided by the total delay sweep time; thus this efficiency becomes very small if an

attempt is made to achieve good time resolution (necessitating short gate widths) and low noise bandwidth (resulting in long output response time and long sweep times).

## F. MULTICHANNEL SIGNAL AVERAGERS

The last-mentioned disadvantage of boxcar circuits is eliminated in the multichannel signal averager, which is in effect a collection of boxcar integrators gated sequentially in synchronization with the signal waveform. Each boxcar is "assigned" a particular time segment of the signal waveform and is gated *on* only during that particular segment. In this way, the signal is "sliced up" into many time segments, and each segment is averaged over many repetitions of the signal waveform. Thus none of the signal information is wasted. Random noise in the signal waveform will be averaged out toward zero as the number of repetitions is increased; only the net signal waveform accumulates point by point in each channel. Multichannel signal averagers have the same kinds of applications as boxcar integrators, but their superior efficiency permits shorter measuring times and, consequently, much less trouble from long term drifts in the instrumental system.

## G. SUMMARY

The relation between the various types of sample signal processing systems may be seen in the following summary, based on the frequency components of the signal of interest.

1. If the sample signal of interest occurs within a frequency region centered about DC (zero frequency), a low-pass filter or DC integrating system may be used. If the dependence of the sample signal on time or some other time-related variable is of interest (e.g., spectrum scanning, phosphorescence decays), then the response time of the system must be faster than the shortest time interval to be resolved in the sample signal.

2. If the sample signal of interest occurs or can be made to occur within a frequency region centered about some nonzero frequency and if only the amplitude, not the waveform, or the sample signal is of interest (e.g., luminescence spectrometry with chopped source, derivative spectroscopy, sample introduction modulation in flame methods), then an AC detection system may be used to convert the AC signal to DC, whereupon it may be processed by a DC filter or integrator system as previously. If a reference signal of high signal-to-noise ratio and definite frequency and phase relation to the sample signal can be obtained, then a lock-in system may be used. The response time of an AC system, which is determined by *both* the pre- and the post detector bandwidths, must satisfy the same requirements as the DC systems discussed earlier.

3. If the sample signal is a repetitive transient occurring over a relatively wide band of frequencies and if the detailed waveform of the sample signal is of interest, then a gated signal averager, either single-channel (boxcar) or multichannel, can be used. A reference (trigger) signal related in frequency and phase to the sample signal is required. In contrast to linear AC and DC systems, the time resolution of gated signal averagers is independent of and can be made much shorter than the total averaging time (which determines the effective noise bandwidth).

## APPENDIX

### VI

## PRINCIPLES OF SINGLE PHOTON COUNTING (SPC)

If the average anode current of a multiplier phototube is  $i_a$ , then the average count rate of anode pulses  $\bar{n}$  is given by

$$\bar{n} = \frac{i_a}{Me} = \frac{\gamma_a \Phi}{Me} = \frac{\gamma_c \Phi}{e} \quad (\text{A6-1})$$

where  $\Phi$  is the light flux on the cathode (watt),  $\gamma_a$  and  $\gamma_c$  are the anodic and cathodic sensitivities of the phototube, respectively ( $\text{A watt}^{-1}$ ),  $M$  is the multiplication factor of the phototube, and  $e$  is the charge on the electron. Thus we see that  $\bar{n}$  is directly proportional to  $\Phi$  but is not a function of  $M$ . Therefore,  $\bar{n}$  is not a function of the phototube supply voltage, which is an advantage over the analog methods.

As an illustration of the range of count rates to be expected, consider the following example. A typical photomultiplier with a multiplication factor of  $10^6$  is used as a detector in a luminescence spectrometer at a wavelength at which its anodic radiant sensitivity is  $10^4 \text{ A watt}^{-1}$ . In luminescence spectrometry, it is reasonable to expect values of incident light flux from about  $10^{-14}$  watt near the limit of detection to about  $10^{-9}$  watt near the upper end of the analytical curve. This would correspond to average count rates of 100 to  $10^6 \text{ sec}^{-1}$ . Because these count rates are within the range of modern electronic counters, the SPC technique is well suited to applications in luminescence spectrometry.

It is important to realize that equation A6-1 gives only the *average* count rate of photoelectron pulses. Because photoemission is a statistical process, the instantaneous count rate over a short period of time varies statistically above and below the average value  $\bar{n}$ . This, of course, is ultimately the cause of shot noise as observed in the analog methods. The effect in photon counting is quite analogous; the standard deviation of the number of photoelectron counts accumulated in a series of equal time intervals  $t_c$  from a light source of constant intensity is

$$\sigma_c = \sqrt{C_t} = \sqrt{\bar{n}t_c} \quad (\text{A6-2})$$

where  $C_t$  is the total counts accumulated per time interval  $t_c$ . The signal-to-noise ratio  $S/N$  is therefore

$$\frac{S}{N} = \frac{C_t}{\sqrt{C_t}} = \sqrt{C_t} = \sqrt{\bar{n}t_c} \quad (\text{A6-3})$$

This puts a lower limit on the total number of photoelectrons to be counted and, therefore, on the minimum count rate measurable in order to obtain sufficient accuracy in a given observation time. For example, if a relative standard deviation of



10% is tolerable, at least 100 pulses must be totaled; and if the observation time is not to exceed 100 sec, the lowest count rate measurable is  $1 \text{ sec}^{-1}$ . The signal-to-noise ratio increases with  $\bar{n}$  for a given counting time, but the maximum allowable count rate is limited by the speed of the electronics. One other result of the statistical variation of instantaneous count rate is that the *maximum count rate of the counter must exceed  $\bar{n}$  by at least 20-fold* in order to avoid losing an appreciable number of counts during those instants when the instantaneous count rate exceeds the counter capability. The bandwidth of the phototube amplifier should also exceed the maximum expected count rate by at least 20-fold.

Furthermore, the effect of the input time constant  $R_L C_S$  must be considered. The input time constant  $R_L C_S$  (formed by the phototube load resistance  $R_L$  and the shunt capacitance  $C_S$ ) influences both the *height* and the *width* of the *photoelectron pulses*. This in turn affects the amount of required amplification, the setting of the pulse height discriminator, and the maximum count rate. Usually  $C_S$  is determined by the available equipment, and  $R_L$  is the only convenient variable. If  $R_L$  is too large, the pulse width will be too large, increasing the danger of pulse overlap and loss of counts. If  $R_L$  is too small, the pulse height may be too low, requiring excessive amplification before counting. Usually  $R_L C_S$  is much greater than the transit time spread of the phototube, and in this case, the pulse height  $V_p$  (volt) and the pulse width  $t_p$  (sec) are given by

$$V_p \cong \frac{Me}{C_S} \quad (\text{A6-4})$$

and

$$t_p \cong 0.7 R_L C_S \quad (\text{A6-5})$$

For this case, the maximum count rate  $R_M$  (Hz) must never exceed

$$R_M \cong \frac{1}{20 R_L C_S} \quad (\text{A6-6})$$

For a typical luminescence spectrometer, the phototube might have a multiplication factor  $M$  of  $10^6$ , a transit time spread of  $2 \times 10^{-9}$  sec, and the stray capacitance of the system might be 100 pF ( $10^{-10}$  farad). For this case, an  $R_L$  of  $10^3$  ohms would result in pulses of height of  $1.6 \times 10^{-19} \times 10^6 / 10^{-10}$  or 1.6 mV and of width of  $0.7 \times 10^3 \times 10^{-10}$  or  $0.07 \mu\text{sec}$ . The maximum counting rate would be  $1/20 \times 10^9 \times 10^{-10} = 5 \times 10^5$  Hz.

It is desirable that only photoelectron pulses be counted in a photon counting experiment. In order to reject pulses with heights other than that expected for photoelectron pulses (i.e., approximately  $Me/C_S$  volt), a *pulse-height discriminator* is often inserted between the amplifier and the counter. This is an electronic device that passes only those pulses whose heights fall within a certain voltage range (the "window"). The window is adjustable in both position and width to suit the particular phototube; in practice, it is usually centered on the single photoelectron pulse height. Unfortunately, not every photoelectron pulse has exactly the same pulse height, as calculated previously, because of the statistical variations in  $M$  from pulse to pulse. Thus the discriminator window must be wide enough to avoid losing an appreciable number of photoelectron pulses, yet not so wide that stray pulses and noise are picked up. The optimum conditions must usually be determined experimentally.

## APPENDIX

### VII

## SPECIAL SPECTRAL TECHNIQUES

### A. FOURIER TRANSFORM SPECTROMETRY

Fourier transform spectrometry (FTS) is a technique of measuring visible and infrared spectra that is fundamentally different in concept and instrumentation from conventional dispersive spectrometry. The principal advantages of FTS are greatly increased signal-to-noise ratio, optical speed, resolution, and analysis time.

A Fourier transform spectrometer is based on the familiar Michelson interferometer. The entering light beam is collimated and falls on a  $45^\circ$  beam splitter. The two resulting perpendicular beams strike two plane mirrors at normal incidence and are reflected back to the beam splitter, where the two beams are recombined into one beam which leaves the instrument at  $90^\circ$  to the incident beam. The emerging beam passes through the sample cell (in absorption studies) and on to the detector. One of the plane mirrors is fixed and the other is made movable in order to change the path difference between the two beams. So far this is just a conventional Michelson interferometer. In an FTS, the movable mirror is caused to move smoothly in one direction with constant velocity by means of an electromechanical drive mechanism.

The operation of the FTS system is best understood by considering first the special case in which the incident radiation is a *monochromatic* beam of wavelength  $\lambda$ . In this case, destructive interference (zero detector signal) will occur for all those positions of the movable mirror for which the beam path difference is an odd multiple of  $\lambda/2$ . The mirror positions for which this condition is satisfied are separated evenly by a distance of  $\lambda/2$ . Thus, if the mirror is moved at a constant velocity  $V$ , destructive interference will occur  $2V/\lambda$  times per second. Similarly, constructive interference (maximum signal) will occur at path differences that are even multiples of  $\lambda/2$ , and partial interference will occur for all intermediate positions. In fact, it is not difficult to see that the detector output will be a sine (or cosine) wave of frequency  $2V/\lambda \text{ sec}^{-1}$ . In this way, the wavelength or frequency of the incoming light could be continuously measured by simply measuring the detector output frequency by means of a frequency meter or similar instrument. If the incident light is polychromatic (i.e., a mixture of monochromatic lines of various frequencies and intensities), then the detector output will be a more complex waveform consisting of the sum of sinusoidal components, each one having a frequency and intensity corresponding to one of the spectral components of the incident light. Such a waveform could be analyzed with a spectrum analyzer in order to separate the various frequency components.

If a *polychromatic* (white) light source is used, the detector output will contain a single burst at the instant the beam path difference is zero. In general, the detector output is a very complex waveform; it does not appear at all like a conventional spec-

trum but does nevertheless contain the same frequency and intensity information. It is, in fact, the Fourier transform of the intensity-path difference information which can be converted to the more recognizable form by means of a well-known but unfortunately very tedious mathematical transformation. In recent years, however, it has become feasible to perform the required computations by means of a small, relatively low-cost digital computer. The computer is connected on-line and is, in fact, considered an integral part of the instrument. In addition, multichannel signal averaging can be done in the computer memory in order to increase the signal-to-noise ratio. Furthermore, the computer is capable of correcting, ratioing, and subtracting spectra, computing absorbances, and performing other desired operations.

In order for an FTS system to be useful, the mirror position must be known to a fraction of a wavelength of the light to be studied. This can cause considerable experimental problems, particularly at short wavelengths. The most successful commercial systems use the "fringe-reference" system. In these systems, another mirror is attached to the moving mirror drive so that the two mirrors move exactly together. This additional mirror forms part of a separate "reference" interferometer which accepts monochromatic light from a laser source. The sinusoidal interference "fringe" signals from the reference interferometer detector are counted and serve as a very precise measure of the mirror velocity. A beam of white light from a small incandescent lamp is also passed through the reference interferometer and produces a burst at a precisely reproducible point on the sample interferogram. This burst serves as a trigger signal for the signal averaging.

The resolution of an FTS instrument is determined by the quality of the optics, by the degree of collimation of the incident light, and, most important, by the length of the mirror sweep. In fact, resolution is inversely proportional to the mirror excursion. Fortunately, the fringe-reference system allows long mirror excursions to be measured with precision, and so resolutions of  $0.1 \text{ cm}^{-1}$  can be obtained.

The advantages of FTS over conventional spectrometry are several:

1. *Higher throughput.* An interferometer has an aperture of at least several square centimeters, much larger than the area of even the largest slits used in dispersive spectrometry. Thus much more light can be put into the FTS system, which is a considerable advantage at low light levels.

2. *Fellgett's advantage.* The so-called Fellgett's advantage arises from the fact that the entire spectrum is measured continuously, whereas in a dispersive instrument only that portion of the spectrum falling on the exit slit is measured at any one time. If there are  $M$  resolution elements in the spectrum (i.e.,  $M$  equals the ratio of spectral range covered in a given spectrum with a dispersive spectrometer to spectral bandwidth), then the FTS system can achieve a signal-to-noise ratio  $\sqrt{M}$  higher than a dispersive instrument under the same conditions of resolution and measurement time, simply because a dispersive instrument wastes most of the light that enters its exit slit. This is quite significant;  $\sqrt{M}$  is often of the order of 10 to 100.

3. *Rapid response.* The signal-to-noise advantage of an FTS system may be traded off for greatly increased speed. That is, an FTS instrument can obtain a spectrum approximately  $M$  times faster than an equivalent dispersive spectrometer. It is routinely possible to obtain a good spectrum in only 1 sec. This opens up tremendous

possibilities; for example, in gas or liquid column chromatography systems, the complete infrared spectrum of each component can be measured "on the fly" as it comes off the column.

At the present time, FTS systems are limited to the visible through far-infrared regions ( $40,000\text{--}10\text{ cm}^{-1}$ ) and a resolution of  $0.1\text{ cm}^{-1}$ . The possibilities of application of FTS to luminescence spectrometry are numerous but yet largely unexplored.

## B. HADAMARD SPECTROMETRY

Hadamard spectrometry involves the use of a multiplexed dispersive spectrometer. The system consists of a dispersive spectrometer (generally a grating instrument) with a mask containing numerous open and closed slots (slits) in place of the normal exit slit. The size of the slots is equal to or a multiple of the spectral bandpass of the dispersive spectrometer. Actually the mask is cyclic with  $2n - 1$  total spectral elements. (A spectral element consists of either an opaque or an open slot equal to the spectral bandpass of the instrument.) The mask is then moved (by a stepping motor) across the exit slit plane in front of the photomultiplier tube. At each position of the mask, the detector "sees" a linear combination of radiant fluxes corresponding to each spectral component allowed to reach the detector surface. By making a total of  $n$  measurements\* ( $n$  different positions of the mask) and performing a Hadamard transformation with a digital computer, the spectral information (radiant flux versus wavelength) can be obtained.

Hadamard spectrometry (HS) has less precise mechanical and alignment problems than Fourier transform spectrometry (FTS). Nor does HS exhibit the intense zero-order spike characteristic of FTS. Finally, HS involves a simpler mathematical computation than FTS. On the other hand, both the optical throughput (speed) and the signal-to-noise ratio of FTS are greater than HS with one Hadamard mask. However, if in addition to the exit plane Hadamard mask an additional mask is placed at the entrance focal plane in place of the entrance slit and if these two masks are independently stepped, then the doubly multiplexed Hadamard spectrometer approaches the FTS system in optical throughput and in signal-to-noise ratio. The doubly multiplexed Hadamard system is rather mechanically complex. The greatest advantage of FTS over HS is certainly the much greater wavelength range in the former; for example, FTS can cover 1 to  $1000\ \mu$  in one measurement period, whereas HS covers a much smaller range as 1 to  $3\ \mu$ .

At the time of writing this book, neither FTS nor HS had been utilized for luminescence spectrometry. However, because of the mechanical difficulties of maintaining plate parallelism and of measuring path differences at small optical path difference, measurements below about  $0.8\ \mu$  have not been made with FTS. No such limitations seem to exist for HS, and so HS may find considerable use in luminescence spectrometry—particularly for atomic fluorescence spectrometry.

\* The grating angle is constant during any given series of measurements. Thus the Hadamard spectrometer covers a range determined by the width of the detector (sensitive area) and the reciprocal linear dispersion of the grating monochromator.

### C. OTHER SYSTEMS

Fabry-Perot spectrometers will probably find little use in luminescence spectrometry because of their small wavelength ranges—typically a few nanometers. Such spectrometers, however, because of their great resolving powers, will certainly be used for studies related to luminescence spectrometry, such as measurement of the structure of spectral lines from various sources (electrodeless discharge lamps, hollow cathode discharge lamps, flames, lasers, etc.).

Rapid-scan spectrometers involve dispersive spectrometers in which one of the spectral elements (a mirror, a dispersive element, or a slit) is moved rapidly (rotated, oscillated, vibrated, etc.). Rapid-scan spectrometers are capable of covering a fairly wide wavelength range—for example, 2000 to 6000 Å in time periods less than one second (e.g., milliseconds). Such devices are useful for studying plasmas, flash photolysis, explosions, gas chromatographic effluents, and so on. Because of the vast store of spectral information in the infrared region, most rapid-scan spectrometers have been utilized in the infrared wavelength region. Nevertheless, it would seem that rapid-scan dispersive luminescence spectrometers could serve for investigating some rapid kinetic processes. Of course, if either FTS or HS instrumentation becomes available for luminescence spectrometry, rapid-scan spectrometers with their inferior resolution, optical speed, and mechanical complications would probably find little use even for kinetic studies.